ASSOCIATION INTERNATIONALE DE GÉODÉSIE

BUREAU GRAVIMETRIQUE INTERNATIONAL

BULLETIN D'INFORMATION

N° 58

Juin 1986

18, avenue Edouard-Belin
31055 TOULOUSE CEDEX
FRANCE

Informations for Contributors

Contributors should follow as closely as possible the rules below :

Manuscripts should be typed (double-spaced) in Prestige-Elite characters (IBM-type), on one side of plain paper 21 cm x 29.7 cm, with a 2 cm margin on the left and right hand sides as well as on the bottom, and with a 3 cm margin at the top (as indicated by the frame drawn on this page).

Title of paper. Titles should be carefully worded to include only key words.

Abstract. The abstract of a paper should be informative rather than descriptive. It is not a table of contents. The abstract should be suitable for separate publication and should include all words useful for indexing. Its length should be limited to one typescript page.

Table of contents. Long papers may include a table of contents following the abstract.

Footnotes. Because footnotes are distracting, they should be avoided as much as possible.

Mathematics. For papers with complicated notation, a list of symbols and their definitions should be provided as an appendix. All characters that are available on standard typewriters should be typed in equations as well as test. Symbols that must be handwritten should be identified by notes in the margin. Ample space (1.9 cm above and below) should be allowed around equations so that type can be marked for the printer. Where an accent or underscore has been used to designate a special type face (e.g., boldface for vectors, script for transforms, sans serif for tensors), the type should be specified by a note in the margin. Bars cannot be set over superscripts or extended over more than one character. Therefore angle brackets are preferable to overbars to denote averages, and superscript symbols (such as *, $'$, and $^{+}$) are preferable to accents over characters. Care should be taken to distinguish between the letter O and zero, the letter l and the number one, kappa and k, mu and the letter u, nu and v, eta and n, also subscripts and superscripts should be clearly noted and easily distinguished. Unusual symbols should be avoided.

Acknowledgments. Only significant contributions by professional colleagues, financial support, or institutional sponsorship should be included in acknowledgments.

References. A complete and accurate list of references is of major importance in review papers. All listed references should be cited in text. A complete reference to a periodical gives author (s), title of article, name of journal, volume number, initial and final page numbers (or statement "in press"), and year published. A reference to an article in a book, pages cited, publisher, publisher's location, and year published. When a paper presented at a meeting is referenced, the location, dates, and sponsor of the meeting should be given. References to foreign works should indicate whether the original or a translation is cited. Unpublished communications can be referred to in text but should not be listed. Page numbers should be included in reference citations following direct quotations in text. If the same information has been published in more than one place, give the most accessible reference ; e.g. a textbook is preferable to a journal, a journal is preferable to a technical report.

Tables. Tables are numbered serially with Arabic numerals, in the order of their citation in text. Each table should have a title, and each column, including the first, should have a heading. Column headings should be arranged to that their relation to the data is clear.

Footnotes for the tables should appear below the final double rule and should be indicated by a, b, c, etc. Each table should be referred to in the text.

Illustrations. Original drawings of sharply focused glossy prints should be supplied, with two clear Xerox copies of each for the reviewers. Maximum size for figure copy is (25.4 x 40.6 cm). After reduction to printed page size, the smallest lettering or symbol on a figure should not be less than 0.1 cm high ; the largest should not exceed 0.3 cm. All figures should be cited in text and numbered in the order of citation. Figure legends should be submitted together on one or more sheets, not separately with the figures.

Mailing. Typescripts should be packaged in stout padded or stiff containers ; figure copy should be protected with stiff cardboard.

BUREAU GRAVIMETRIQUE INTERNATIONAL

Toulouse

BULLETIN D'INFORMATION

Juin 1986

N° 58

Publié pour le Conseil International des
Unions Scientifiques avec l'aide financière
de l'UNESCO
Subvention UNESCO 1986 DG/2.1/414/50

Address :

BUREAU GRAVIMETRIQUE INTERNATIONAL

18, Avenue Edouard Belin

31055 TOULOUSE CEDEX

FRANCE

Phone :

61.27.44.27
61.27.40.72

Telex :

CNEST B 531081 F

TABLE OF CONTENTS

Bull. d'Inf. n° 58

Pages

PART I : *INTERNAL MATTERS*

PART II : *CONTRIBUTING PAPERS*

PART I

INTERNAL MATTERS

LAST ANNOUNCEMENT

This is the last announcement of the next (12th.) meeting of the INTERNATIONAL GRAVITY COMMISSION.

It will be held in Toulouse, France, from September 22 to 26, 1986.

It was first announced in the Bulletin d'Information n° 56, then more precisely in the following issue (B.I. n° 57) in which necessary participation forms and hotel forms were enclosed.

By this time those who had not yet responded by June 1st should have received the last circular. We really urge you to send immediately the forms back if you intend to participate.

Looking forward to seeing you all in Toulouse.

Have a pleasant summer !

INFORMATIONS

I. The BGI Gravity Data Base

Due to the quick and unexpected leave of J.F. I-Isaac-Grieux who was responsible for the data base and its management system, the data base has been frozen in its state as of August 1985 due to a lack of precise information on various critical pieces of software.

M. Sarrailh took it over could only finish the complete understanding phase of the system a month and a half ago. He is presently upgrading some software which still suffered from uncorrected bugs.

We hope to be able to present to the community an updated data base system and contents (comprising the data collected in the last twelve months) at the next meeting of IGC in September.

II. Bibliographie

For the same reason as above, the software for managing and editing the bibliographical references at BGI was partly lost and not usable anymore.

We were able to get a student working on this task in the last two months (Miss M. Laliat) and we will resume the publication of our references in the next issue of the Bulletin.

PART II

CONTRIBUTING PAPERS

GRAVIMETRIC WORK IN CHINA

(1983-1986)

H.T. HSU

I. Absolute Gravimetry

The Chinese Academy of Metrology has successfully developed the second generation movable absolute gravimeter (model NIM-II) and took part in international absolute gravimeter comparison observation from June to July, 1985 in Paris. Five countries (USA, USSR, France, Italy and China) and six sets of instruments joined this comparison, and Pr. Groten, Chairman of SSG 3.87, IAG, is in charge of handling the result, according to Boulanger's private communication on Nov. 25, 1985 the result obtained by Chinese instrument NIM-II after reducing to serves A_3 point is (2) :

$$g = 980925944.5 \ \mu gal$$

the difference between it and average value obtained from six sets of instruments is + 6 μgal.

II. Establishment of Gravity Fundamental Network (85) in China (1)

During the period of 1983-1985, the State Bureau of Surveying and Mapping in China organized the Institute of State Bureau of Surveying and Mapping and Institute of Geodesy and Geophysics, Chinese Academy of Sciences and so on, to establish gravity fundamental network (85) of China, there are 57 points altogether, including 6 datum points, 46 fundamental points and 5 initial points. Absolute gravimetry was carried out for all datum points in network, its accuracy is about ± 20 μgal. The instruments we used come from Torino Institute of Metrology, Italy and Chinese Academy of Metrology respectively, in several datum points, both results are utilized simultaneously. The relative connection for every point in the network was measured by using 9 sets of LaCoste gravimeters (model G), its accuracy is about ± 20 μgal. To improve and check up the reliability of network (85), the relative connection with international gravity points in Paris, Tokyo and Hong Kong and so on is made respectively.

Least square adjustment was used for processing the network (85), absolute and relative observations are combined together by use of different weight. In error equation of relative observation segment the mathematical model with linear, quadratic and periodic term scale correction is used before adjustment, the drift, height, tide and atmospheric pressure corrections are taken into consideration. Besides, we utilized the results of international connection to check the absolute gravity observation and determine its weight.

The result shows that MSE of gravity value in each point of network after adjustment is ± 7.8 μgal, the maximum error is ± 13 μgal, MSE of each segment after the adjustment is ± 15 μgal.

III. Development and Test of Dynamic Gravimetric Instrument (3-11)

In recent years, Institute of Geodesy and Geophysics, Chinese Academy of Sciences, has developed a new sea-gravimeter, model CHZ. The new design of this meter is to use linear sensor system so that C-C effect is eliminated. Besides, zero length spring suspension, silicon-oil damping, high accuracy capacitive transducer, digital filter and data acquisition and processing system are its characters.

Gravimeter (model CHZ), through the test in laboratory and at sea, can withstand the perturbation in case of 500 gal in vertical acceleration and 200 gal in horizontal acceleration. In 1985, the comparison observation between CHZ meter (China) and KSS-30 meter (West Germany) on the same ship at the South China Sea was made. The mean square discorrespondency of both instruments is ± 2 μgal.

IV. Geophysical Explanation for Gravity Data

In recent years, the progress has been made by using the gravity data to inverse Earth crust-mantle structure. Liu Yuanlong et al. have developed original two-dimension surface-mass method to three-dimension (12) ; Pan Zuoshu (13), Gao Jinyao (14) et al. have calculated the thickness of earth crust from gravity data with FFT method. Liu Zuhui (15), Gao Jinyao (16) et al. have made calculation and interpretation for deep structure of the South China Sea and Qinghai-Xizang plateau respectively according to the linear experimental isostasy. Hong Rui (17), on the basis of Paker's potential-field formula, has inversed the Earth crust thickness and upper mantle density by utilizing a lot of seismic measurement as control ; Zhang Chijun (18) et al. have calculated the Earth crust thickness of Qing-Xizang plateau from geoid undulation and so on the basis of integral equation of single layer potential, determined the density distribution of inside lithosphere by means of high order portion of satellite gravity field (19).

V. Theoretical Research on Gravity Field

In aspect of classical Stokes' theory the approximation method with constraint is proposed in order to improve the convergence of Stokes' series. A optimum approximation of both the height anomaly and vertical deflection are suggested by using set of approximation coefficients (20, 21, 22, 23, 24). Furthermore, this new concept is applied to Stokes'problem in case of ellipsoid earth so that a solution of considering ellipsoid flattening is obtained (25), and the convergence about this problem is improved in comparison with Rapp's solution. In addition, the determination of geoid and its error estimation by use of the least square spectrum combination is under test (26).

With respect to the modern approximation theory of gravity field and its representation, the embedded masses approximation method of discrete geodetic boundary value problem and choice of density and embedded depth of perturbation mass points are studied (27, 28). In view of defect of this method, the approximation behaviour for embedded mass point has been judged, it is pointed out that this solution is not optimum, simultaneously, we suggested so-called semi-collocation (29, 30) form of discrete geodetic boundary value problem. On the other side, a method by setting up the fictitious single layer density to express the gravity field outside the Earth is discussed (30, 31, 32). The kernel of solution is a fundamental solution of Laplace equation, like the embedded mass point solution, its structure is the simplest, and the equivalent principle shows that this theory is a variant of Bjerhammar's solution, the practical calculation indicates that it is better than Bjerhammar's solution due to simplicity of computation, quick convergence and high accuracy.

In respect of the gravity field at high altitude, the valuation model of outer attraction field including fictitious single layer method and continuation of Molodensky's surface solution (34) is discussed. As to the gravity field expression at lower altitude a translocation in case of ellipsoid is suggested (35). The given solution not only contains Euclid effect of topography, but also the effect of Earth flattening. And the Bjerhammar's translocation solution can be considered as a special case of it.

In the determination of geoid in China, we try to use a combined technique of the determination of the Earth's disturbing potential (36), and the accuracy of height anomaly obtained from Doppler observation is analyzed too (37).

References

1. Chen Junyong, "A new stage of gravimetric technique progress in China", Cehui Tongbao, n° 5, 1985.

2. Guo Youguang, "International Comparison in Paris", Private communication.

3. Zhang Shanyan, Li Xiqi, "A new developed sea-gravimeter (model CHZ). A paper presented at 18th FIG, Canada, 1986.

4. Liang Chujian, "Application of locking amplifier to relative gravimeter", Acta Geodaetica et Geophysica, n° 5, 1984.

5. Pan Xianzhang, "Electron-constant temperature system design of sea-gravimeter (model CHZ)", Acta Geodaetica et Geophysica, n° 4, 1983.

6. Zhang Xianlin, "Data collection and processing system of sea-gravimeter (model CHZ)", Automatization and Instrumentation", n° 1, 1986.

7. Ye Bing, "Sea-gravimeter (model CHZ) constant through design", Acta Geodaetica et Geophysica, n° 5, 1984.

8. Liu Ruozhen, "Sea-gravimeter (model CHZ) spring system design", Acta Geodaetica et Geophysica, n° 8, 1986.

9. Liu Ruozhen, "Spring system liquid damping of sea-gravimeter (model CHZ)",

Acta Geodaetica et Geophysica", n° 8, 1986.

10. Liang Chujian, "Calibration of inside scale value of sea-gravimeter (model CHZ)", Acta Geodaetica et Geophysica, n° 7, 1985.

11. Zhang Xianlin, "Ultra-low frequency digital filter of sea-gravimeter (model CHZ)", Acta Geodaetica et Geophysica, n° 8, 1986.

12. Private communication.

13. Physical and chemical exploration, n° 4, 1982.

14. Acta Geodaetica et Geophysica, n° 8, 1986.

15. Acta Geodaetica et Geophysica, n° 8, 1985.

16. Master postgraduate's thesis, Institute of Geodesy and Geophysics, Chinese Academy of Sciences, 1985.

17. Acta Seismologica Sinica, Vol. 7, n° 2, 1985.

18. Acta Geophysica Sinica, Vol. 28, (Supplement), 1985.

19. Private communication.

20. Hsu, H.T., Zhu, Z., 1979, "The approximation of Stokes'function and estimation of truncation error", paper presented at 17th IUGG General Assembly, Canberra, Australia.

21. Hsu, H.T., Zhu, Z., 1981, "The approximation of Stokes'function and estimation of truncation error", Acta Geophys. Sinica, vol. 24-39.

22. Hsu, H.T., Yang, H.B., "Some remarks on the estimation of truncation error in calculation of height anomalies", Acta Geod. et Cartogr. Sinica, 12, 95-102.

23. Hsu, H.T., 1984, "Kernel function approximation of Stokes'integral", Proceedings, Local Gravity Field Approximation, Beijing International Summer School, Aug. 21-Sept. 4, 1984. Reprint by Division of Surveying Engineering, The University of Calgary, Canada.

24. Hsu, H.T., Zhu, Z., 1985, "Kernel function approximation of Stokes' integral", IGG Special Publication, Chinese Academy of Sciences, n° 8, 10-40.

25. Zhu, Z., 1981, "The Stokes'problem for the ellipsoid using ellipsoidal kernel", Dept. of Geod. Sci. and Sur., Rep. n° 319, OSU, Columbus.

26. Cao, H., 1986, "Determination of geoid by using least square spectrum combination", Awaiting publication.

27. Xuerong, C., 1984, "A discrete method of geodetic boundary value problem", Acta Geod. et Cartogr. Sinica, Vol. 13, 122-130.

28. Wu, X., 1983, "Point mass model principle of Earth local perturbation

gravity field, its formation method and accuracy researches" (Master's thesis).

29. Zhu, Z., Hsu, H.T., 1985, "Discrete exterior boundary value problem in consideration of local topographic effect". Scientia sinica, (Series B), Vol. XXVIII, n° 6, 662-671.

30. Hsu, H.T., 1984, "Two notes on gravity field approximation", Proceedings, Local Gravity Field Approximation, Beijing International Summer School, Aug. 21-Sept. 4, 1984.

31. Hsu, H.T., Zhu, Z., 1984, "Representation of gravity field outside the Earth using fictitious single layer density", Scientia Sinica (Series B), vol. XXVII, n° 9, 985-992.

32. Hsu, H.T., Zhu, Z., "A model of gravity field outside the Earth developed by using a fictitious single layer", IGG Special Publication, The Chinese Academy of Sciences, n° 8, 41-50.

33. Cao, H., Zhu, Z. et al., "Digital realization of the theory of representing the Earth gravity field by fictitious single layer density", Acta Geod. et Cartogr. Sinica, vol. 14, n° 4, 262-273.

34. Hsu, H.T., Zhu, Z. et al., 1986, "The valuation model of Earth outer attraction field" (awaiting publication).

35. Zhu, Z., 1986, "Translocation in case of ellipsoid, Scientia Sinica (series B), n° 3, 328-336.

36. Luo Shiming, 1985, "Calculation geoid method by using satellite Doppler positioning results", Cehui Tongbao, n° 4.

37. P. Shi, 1984, "Combined determination of the Earth's disturbing potential, Acta Geod. et Cartogr. Sinica, vol. 13, n° 4, 241-248.

METHODS OF IMPROVING THE CONVERGENCE OF THE EARTH'S POTENTIAL EXPANSION

M.S.Petrovskaya, K.V.Pishchukhina
Institute of Theoretical Astronomy
of the USSR Academy of Sciences, Leningrad

Summary

Two methods of improvement of convergence of the earth's disturbing potential expansion in terms of spherical functions have been suggested. In one of these, a series in Chebyshev polynomials is used, as an intermediate one. Then its partial sums are converted into linear combinations of spherocal functions. The other method is based on employment of a power series, as an intervening one, and the subsequent application of Lanczos' method of economization to it. Finally, the transfer to spherical functions has been performed, as well. As a result, the earth's potential is approximated by the sequences of linear combinations of spherical functions which converge more rapidly than the partial sums of the standard series. Practically, each new approximating polynomial is derived from the original one only by multi-

plying its coefficients, that is Stokes' constants C_{nm}, by certain numerical factors. Thus, the new approximants are constructed on the same basis of coefficients of spherical functions as the ordinary earth's potential expansion. The results can be utilized in two ways, for improving the approximation of the global gravitational field. Let a set of Stokes' constants C_{nm} be known for $n \le N$ and $|m| \le n$. Then the initial approximating polynomial of degree N can be "contracted" to a polynomial of a lower degree $N_0 < N$, without increasing the error of approximation. If the degree N of an approximating polynomial is fixed then the corresponding new approximant of the same degree has a lesser error than the initial one. Numerical experiments have been performed for estimating the efficiency of both methods.

1. Formulation of the problem

The earth's disturbing potential T is generally presented as a series of solid spherical functions

$$T = \sum_{n=2}^{\infty} T_n \,, \quad T_n = R^n \sum_{m=-n}^{n} C_{nm} \Phi_{nm}(r, \varphi, \lambda), \tag{1.1}$$

$$\Phi_{nm} = r^{-n-1} Y_{nm}(\varphi, \lambda),$$

$$Y_{nm} = P_{n|m|}(\sin\varphi) \begin{cases} \cos m\lambda \,, & m \ge 0 \\ \sin |m|\lambda \,, & m < 0 \,. \end{cases}$$

Here (r, φ, λ) are spherical coordinates of a point x of exterior space, Φ_{nm} = solid spherical functions,

C_{nm} = Stokes' constants (corresponding to the disturbing potential), P_{nm} = adjoint Legendre functions, $P_{no} = P_n$ = Legendre polynomials, R = radius of thc sphere σ enveloping the earth. The zero and first degree harmonics in the expansion of T are absent due to a certain choice of parameters of the normal earth /8/.

The series (1.1) converges uniformly outside and on the sphere σ (the domain Σ) as well as its partial derivatives of the first order. We intend to improve convergence of this series in the domain $\bar{\Sigma} = \Sigma \cup \sigma$ of its validity.

The earth's disturbing potential can be presented as a surface layer potential /6/ or in form of some generalized potentials /1/, /2/, /7/. Since we confine ourselves to the domain $\bar{\Sigma}$, the surface layer potential may be referred to the boundary surface σ :

$$T = \int_\sigma \nu \ell^{-1} d\sigma \quad , \quad x \in \bar{\Sigma} \, , \tag{1.2}$$

where

$$\ell^2 = R^2 + r^2 - 2Rr\cos\psi,$$

$$\ell^{-1} = r^{-1} \sum_{n=0}^{\infty} \left(\frac{R}{r}\right)^n P_n(\cos\psi), \tag{1.3}$$

$$\cos\psi = \sin\varphi \sin\varphi_1 + \cos\varphi \cos\varphi_1 \cos(\lambda - \lambda_1) \, , \quad x_1(\varphi_1, \lambda_1) \in \sigma$$

The density ν is determined from the integral equation which results from substituting (1.2) into the boundary con-

dition

$$\lim_{x \to \sigma} \left(\frac{\partial T}{\partial r} + \frac{2}{r} T \right) = -\Delta g \qquad (1.4)$$

where $\Delta g = \sum_{n=2}^{\infty} \Delta g_n$ is the gravity anomaly on σ.
On this sphere, (1.2) converts into the Stokes' formula

$$T = \frac{R}{4\pi} \int_{\omega} \Delta g \, S(\psi) \, d\omega , \quad x \in \sigma, \qquad (1.5)$$

where $S(\psi)$ is the Stokes' function and ω means the unit sphere.
In the domain Σ any generalized potential can be presented as

$$T = \frac{1}{4\pi} \int_{\sigma} \mu \, K(r, \psi) \, d\sigma , \quad x \in \Sigma . \qquad (1.6)$$

The kernel K depends on the coordinates of a current point $x_1 (\varphi_1, \lambda_1) \in \sigma$ and, for a fixed values of φ_1 and λ_1, it represents a harmonic function in Σ, regular at infinity. The generalized density μ is derived from the boundary condition (1.4). By choosing different harmonic functions $K(r, \psi)$ one can obtain different generalized potentials. On the sphere σ all of these will be reduced to the Stokes' formula. We choose such a kernel $K(r, \psi)$ in (1.6) which is best suited for performing transformations, leading to improvement of convergence of the series (1.1). Herewith, we are guided by the following requirements, with respect to the kernel in (1.6). First of

all, the series of solid spherical functions for $K(r,\Psi)$ should converge more rapidly than the expansion (1.3) of the kernel ℓ^{-1} in the expression for the surface layer potential (1.2). The second demand consists in choosing from a variety of harmonic functions with the same rate of convergence of their expansions (e.g. their terms may decrease as $\frac{1}{n}$, $\frac{1}{n-1}$ or $\frac{1}{n+1}$) such a function $K(r,\Psi)$ which has the most simple form. These conditions are best satisfied, from our point of view, for the kernel

$$K = r^{-1}F , \qquad F = -\ell n \frac{r - R\cos\Psi + \ell}{2r} . \tag{1.7}$$

The corresponding generalized potential is

$$T = \frac{R^2}{4\pi r} \int_0^{2\pi}\int_0^{\pi} \sigma F(r,\Psi) \sin\Theta_1 \, d\Theta_1 \, d\lambda_1 , \tag{1.8}$$

where Θ_1 means the polar angle. The function F can be expanded in a series of solid spherical functions /12/

$$F = \sum_{n=1}^{\infty} \frac{1}{n} \left(\frac{R}{r}\right)^n P_n(\cos\Psi) . \tag{1.9}$$

It may be easily seen that the terms of this series are n times less than the ones in (1.3) for the kernel ℓ^{-1} in (1.2). From (1.4), (1.8) and (1.9) we determine the generalized density :

$$\sigma = 2\sum_{n=2}^{\infty} (n+2)\Delta g_n - \Delta g + 3\sum_{n=2}^{\infty} \frac{\Delta g_n}{n-1} ,$$

or

$$\mathcal{M} = -2R\frac{\partial \Delta g}{\partial r} - \Delta g + \frac{3}{4\pi}\int_{\omega} \Delta g\, S(\psi)\, d\omega. \qquad (1.10)$$

The formulas (1.7)-(1.10) define the basic expression for the potential T which will be used for improving convergence of the series (1.1).

The Stokes' constants are expressed in terms of $\mathcal{M}$ as

$$c_{nm} = \frac{2}{\delta_m}\,\frac{1}{n}\,\frac{(n-|m|)!}{(n+|m|)!}\,\frac{R^2}{4\pi}\int_0^{2\pi}\int_0^{\pi} \mathcal{M}\, Y_{nm} \sin\theta_1\, d\theta_1\, d\lambda_1,$$

$$\delta_0 = 2\,;\ \delta_m = 1\,,\ m \neq 0.$$

Now we shall estimate the order of decreasing the general term of (1.1). On the sphere σ one has

$$T\big|_{\sigma} = \sum_{n=2}^{\infty} T_n\big|_{\sigma}\,. \qquad (1.11)$$

Let us perform the change of variables of integration in (1.8) by transferring the pole to the computation point :

$$\theta \to 0\,,\ \lambda \to 0 \quad \Rightarrow \quad \theta_1 \to \psi\,,\ \lambda_1 \to \bar{\lambda}_1\,. \qquad (1.12)$$

As a result, (1.8), (1.9) and (1.11) give

$$T_n\big|_{\sigma} = \frac{R}{4\pi n}\int_0^{2\pi}\int_{-1}^{1} \mathcal{M}(z,\bar{\lambda}_1)\, P_n(z)\, dz\, d\bar{\lambda}_1\,, \qquad (1.13)$$

$$n = 2, 3, \ldots$$

Let us denote

$$\Delta g_{max} = \max |\Delta g| , \quad x \in \sigma ,$$

$$\Delta g^*(z) = \frac{1}{2\pi} \int_0^{2\pi} \Delta g(z, \bar{\lambda}_1) \, d\bar{\lambda}_1 , \quad -1 \le z \le 1 ,$$

and by Δg_{var} we shall assume the total variation of $\Delta g^*(z)$ over the interval $/ -1,1 /$. Making use of the estimates /15/

$$\int_{-1}^{1} |P_n(z)| \, dz < \sqrt{2} \, n^{-1/2} ,$$

$$\left| \int_{-1}^{1} \Delta g^* P_n(z) \, dz \right| < \frac{4}{\sqrt{\pi}} \left(\Delta g_{var} + \Delta g_{max} \right) n^{-3/2} ,$$

we derive from (1.13)

$$\left| \frac{1}{R} T_n |_\sigma \right| < \Delta g_{max} \, n^{-3/2} , \qquad (1.14)$$

$$\left| \frac{1}{R} T_n |_\sigma \right| < 2 \left(\Delta g_{var} + \Delta g_{max} \right) n^{-5/2} . \qquad (1.15)$$

It should be noted that the constant Δg_{var}, depending on the total variation of the gravity anomaly and its radial derivative, according to (1.10), can greatly exceed the constant Δg_{max}. Therefore, the right-hand side of (1.15) may be smaller than that of (1.14) only for very large values of n. In any case, for the number of terms of the series (1.1) which are currently taken into account, the estimate (1.15) is too overstated.

Basing on (1.14) and (1.15), one can readily estimate the general term of (1.1) by relation

$$T_n = \frac{R^{n+1}}{r^{n+1}} T_n|_\sigma \quad , \quad x \in \Sigma \, . \qquad (1.16)$$

The expansion (1.1) defines the sequence of approximants

$$T^{(N)} = \sum_{n=2}^{N} T_n \quad , \quad N = 2,3,\ldots \qquad (1.17)$$

which converges to the potential T in both the mean square and uniform metrics. Using certain methods of the theory of approximation, some other sequences of linear combinations of solid harmonics $\Phi_{nm}(r,\varphi,\lambda)$ can be constructed differing from (1.17) and converging more rapidly (in the uniform metric) to the potential T , than the sequence $\{T^{(N)}\}$. Two such methods will be applied below. In one of these we proceed from the expansion of F (see (1.7)) with respect to the Chebyshev polynomials $T_n(\cos\psi)$, rather than the Legendre ones, $P_n(\cos\psi)$, in distinction to (1.3) and (1.9). This is done because in the class of ultraspherical polynomials, the Chebyshev polynomials yield expansions which display the strongest possible convergence /17/. The second approach is based on development of F in powers of $x = \cos\psi$ and subsequent application of Lanczos' method of telescopic shift /5/ or, by another terminology, the method of economization /17/. In both cases the partial sums of the above mentioned series are finally transformed into linear combinations of solid spherical functions $\Phi_{nm}(r,\varphi,\lambda)$.

2. Application of the expansion in Chebyshev polynomials

We begin with the method employing an expansion in Chebyshev polynomials. Consider a function $f(x)$ and its expansion in Legendre polynomials in the range / -1,1 / :

$$f(x) = \sum_{n=0}^{\infty} a_n P_n(x) .$$

Thus, $f(x)$ is approximated by members of the sequence $\{f^{(N)}(x)\}$:

$$f^{(N)}(x) = \sum_{n=0}^{N} a_n P_n(x) , \qquad N = 0,1,\ldots$$

In the same interval for x , the function $f(x)$ can be presented as a series of Chebyshev polynomials :

$$f(x) = \sum_{n=0}^{\infty} b_n T_n(x) .$$

The corresponding sequence of approximants is

$$\tilde{f}^{(N)}(x) = \sum_{n=0}^{N} b_n T_n(x) , \qquad N = 0,1,\ldots$$

Suppose that the series of Chebyshev polynomials converges more rapidly than the Legendre series, which usually occurs. Then, for a fixed N , the function $\tilde{f}^{(N)}$ provides better approximation to f than $f^{(N)}$. If, however, one prefers to deal with Legendre polynomials, instead of Chebyshev ones, then $\tilde{f}^{(N)}$ can be expressed in terms of $P_n(x)$:

$$\tilde{\zeta}^{(N)}(\tau) = \sum_{n=0}^{N} c_n^{(N)} P_n(\tau) \quad , \qquad N = 0,1,\dots$$

where $c_n^{(N)} \neq a_n$ and depend on the degree N of the polynomial.

We shall apply this procedure to the function F defined in (1.7), with $\tau = \cos\Psi$. First, the transformations will be performed at the boundary surface σ and then the results will be converted to exterior space Σ, by using (1.16). On the sphere σ, we have from (1.8) and (1.9)

$$T|_\sigma = \frac{R}{4\pi} \int_0^{2\pi}\int_0^{\pi} S(\psi)\, f \sin\theta_1 \, d\theta_1 \, d\lambda_1 \,, \qquad (2.1)$$

where

$$f \equiv F|_\sigma \quad , \quad f = \sum_{n=1}^{\infty} \frac{1}{n} P_n(\cos\Psi) . \qquad (2.2)$$

These formulas define a sequence of functions converging to $T|_\sigma$:

$$T^{(N)}|_\sigma = \frac{R}{4\pi} \int_0^{2\pi}\int_0^{\pi} S(\psi)\, f^{(N)} \sin\theta_1 \, d\theta_1 \, d\lambda_1 \,, \qquad (2.3)$$
$$N = 2,3,\dots$$

with

$$f^{(N)} = \sum_{n=1}^{N} \frac{1}{n} P_n(\cos\Psi) . \qquad (2.4)$$

Each of the functions (2.3) is a linear combination of spherical functions of degree $n \leq N$ and represents the restric-

tion of (1.17) to σ :

$$T^{(N)}|_{\sigma} = \sum_{n=2}^{N} T_n|_{\sigma} \quad , \qquad N = 2,3,\ldots \tag{2.5}$$

We present F (see (1.7)) as

$$F = F_1 + F_2 \quad , \quad x \in \bar{\Sigma} \, ,$$

$$F_1 = -\ln \frac{\ell}{2r} \quad , \qquad F_2 = -\ln \frac{r - R\cos\Psi + \ell}{\ell} \, .$$

Then for f defined in (2.2) it follows, respectively,

$$f = f_1 + f_2 \quad , \quad x \in \sigma, \tag{2.6}$$

$$f_1 \equiv F_1|_{\sigma} = -\ln \sin\frac{\Psi}{2} \quad , \tag{2.7}$$

$$f_2 \equiv F_2|_{\sigma} = -\ln\left(1 + \sin\frac{\Psi}{2}\right) . \tag{2.8}$$

Consider f_1 and f_2 in the open interval $0 < \Psi < \pi$. One has /12/

$$f_1 = \frac{1}{2} + \frac{1}{2}\sum_{n=1}^{\infty} \frac{2n+1}{n(n+1)} P_n(\cos\Psi) \tag{2.9}$$

$$f_2 = -\frac{1}{2} + \frac{1}{2}\sum_{n=1}^{\infty} \frac{1}{n(n+1)} P_n(\cos\Psi) \, . \tag{2.10}$$

The general term of the first series decreases (approximately) n times slower than that of the second one. As a result, the rate of convergence of the series in (2.2) is de-

fined by the expansion (2.9) of (2.7). Below, we shall derive for ζ_1 (and for ζ , respectively) another series, converging more rapidly than the expansion (2.9). It can be seen that the factor $\sin\theta_1$ contained in (2.1) improves the analytical properties of the integrand, on the whole. This can be easily established if the transformation (1.12) is performed in (2.1), which gives

$$T|_\sigma = \frac{R}{4\pi}\int_0^{2\pi}\int_0^{\pi} \mathcal{M}\,\zeta(\psi)\sin\psi\,d\psi\,d\bar{\lambda}_1 .$$

For $\psi \to 0$ we obtain from (2.6)-(2.8) : $\zeta\sin\psi \to 0$ while $\zeta \to \infty$. This circumstance was not taken into account when expanding the integrand in (2.1) by the use of (2.2). We shall take advantage of the factor $\sin\theta_1$ in (2.1), for constructing a new expansion of $T|_\sigma$. Consider an auxiliary function ζ_3 on the interval $0 < \psi < \pi$:

$$\zeta_3 \equiv \sin\psi\,\zeta_1(\psi) = -\sin\psi\,\ln\sin\frac{\psi}{2} .$$

For (2.7) we have an expansion /11/ :

$$\zeta_1 = \sum_{n=1}^{\infty}\frac{1}{n}\cos n\psi + \ln 2 .$$

It can be treated as a series in Chebyshev polynomials $T_n(\cos\psi) = \cos n\psi$. The last two formulas give

$$\zeta_3 = \sum_{n=2}^{\infty}\frac{1}{n^2-1}\sin n\psi + (\ln 2 - 1/4)\sin\psi$$

and, correspondingly, the new expansion $\tilde{\zeta}_1$ of (2.7) is

$$\tilde{\zeta}_1 = \ln 2 - \frac{1}{4} + \frac{2}{3}\cos\psi + \sum_{n=2}^{\infty} \frac{\sin(n+1)\psi}{n(n+2)\sin\psi}\,, \qquad 0 < \psi < \pi\,. \tag{2.11}$$

We put

$$\tilde{\zeta} = \tilde{\zeta}_1 + \zeta_2 \tag{2.12}$$

where ζ_2 is the series (2.10). After transferring $\zeta \to \tilde{\zeta}$ in (2.1), a new expression $\tilde{T}|_\sigma$ of the potential $T|_\sigma$ follows :

$$\tilde{T}|_\sigma = \frac{R}{4\pi}\int_0^{2\pi}\int_0^{\pi} \rho\mu\, \tilde{\zeta} \sin\theta_1\, d\theta_1\, d\lambda_1\,. \tag{2.13}$$

Application of (1.12) leads to

$$\tilde{T}|_\sigma = \frac{R}{4\pi}\int_0^{2\pi}\int_0^{\pi} \rho\mu\, \tilde{\zeta} \sin\psi\, d\psi\, d\bar{\lambda}_1\,. \tag{2.14}$$

It can be easily seen that the factor $\sin\psi$, entering the denominator in (2.11), vanishes after substituting this series into (2.12) and, then, into (2.14). Thus, it does not "prevent" the expansion of the integrand to converge along the whole closed interval $0 \le \psi \le \pi$.
After adding term by term the series (2.10) and (2.11), we get from (2.12) and (2.13)

$$\tilde{T}|_\sigma = \sum_{n=2}^{\infty} \tilde{T}_n|_\sigma\,, \tag{2.15}$$

where

$$\widetilde{T}_n|_\sigma = \widetilde{T}_{n1} + \widetilde{T}_{n2} \quad , \tag{2.16}$$

$$\widetilde{T}_{n1} = \frac{R}{4\pi n(n+2)} \int_0^{2\pi}\int_0^{\pi} \mathcal{M} \frac{\sin(n+1)\Psi}{\sin\Psi} \sin\Theta_1 \, d\Theta_1 \, d\lambda_1 \, , \tag{2.17}$$

$$\widetilde{T}_{n2} = \frac{R}{8\pi n(n+1)} \int_0^{2\pi}\int_0^{\pi} \mathcal{M} P_n(\cos\Psi) \sin\Theta_1 \, d\Theta_1 \, d\lambda_1 \, . \tag{2.18}$$

By using the substitution (1.12), the following estimate can be derived

$$\left| \frac{1}{R} \widetilde{T}_n|_\sigma \right| < 2 \frac{\mathcal{M}_{max}}{n(n+1)} \, , \quad n = 2, 3, \ldots \tag{2.19}$$

and also

$$\left| \frac{1}{R} \widetilde{T}_n|_\sigma \right| = O(n^{-3}) \, , \quad n = 2, 3, \ldots ,$$

the latter depending on $\mathcal{M}_{var}$ and $\mathcal{M}_{max}$. Comparing the last two formulas with the estimates (1.14) and (1.15), we may conclude that (without taking into account the constant factors) the general term of the new expansion (2.15) of $T|_\sigma$ is $\sqrt{n}$ times less than that of the original series (1.11).

The formulas (2.15)-(2.18) define the following sequence of functions $\widetilde{T}^{(N)}|_\sigma$ approximating $T|_\sigma$:

$$\tilde{T}^{(N)}\Big|_\sigma = \frac{R}{4\pi}\int_0^{2\pi}\int_0^{\pi} M\,\tilde{\xi}^{(N)} \sin\theta_1\, d\theta_1\, d\lambda_1\,, \qquad (2.20)$$

$$N = 2, 3, \ldots$$

where

$$\tilde{\xi}^{(N)} = \tilde{\xi}_1^{(N)} + \xi_2^{(N)}\,,$$

$$\tilde{\xi}_1^{(N)} \equiv \sum_{n=2}^{N} \frac{1}{n(n+2)} \frac{\sin(n+1)\psi}{\sin\psi}\,,$$

$$\tilde{\xi}_2^{(N)} \equiv \sum_{n=2}^{N} \frac{1}{n(n+1)} P_n(\cos\psi).$$

Presentation of $\tilde{\xi}_1^{(N)}$ as a linear combination of Legendre polynomials $P_n(\cos\psi)$ gives

$$\tilde{\xi}^{(N)} = \sum_{n=2}^{N} \frac{1}{n} d_n^{(N)} P_n(\cos\psi)\,, \qquad (2.21)$$

with

$$d_n^{(N)} = \frac{1}{2(n+1)} + \frac{(1)_n}{\left(\frac{1}{2}\right)_n (n+2)} \sum_{k=0}^{(\tilde{N}-n-1)/2} \frac{(n+1)_k \left(\frac{n}{2}\right)_k \left(\frac{1}{2}\right)_k}{(1)_k \left(n+\frac{3}{2}\right)_k \left(\frac{n}{2}+2\right)_k}\,, \qquad (2.22)$$

where

$$\tilde{N} = \begin{cases} N\,, & \text{if } (n+N) \text{ is odd,} \\ N+1\,, & \text{if } (n+N) \text{ is even,} \end{cases}$$

$$(a)_k = a(a+1)\ldots(a+k-1).$$

Expressions (2.20)-(2.22) allow to present $\widetilde{T}^{(N)}|_\sigma$ as a linear combination of spherical functions $\Phi_{nm}(R, \varphi, \lambda)$ of degree $n \leq N$ (with $|m| \leq n$) :

$$\widetilde{T}^{(N)}|_\sigma = \sum_{n=2}^{N} T_n^{*(N)}|_\sigma \quad , \quad N = 2,3,\ldots \qquad (2.23)$$

Comparison of (2.20) and (2.21) with (2.3) and (2.4) leads to the conclusion that the terms of (2.23) and (2.5) are connected by the relation

$$T_n^{*(N)}|_\sigma = d_n^{(N)} T_n|_\sigma \quad , \quad n = 2,3,\ldots,N, \quad N = 2,3,\ldots$$

Consequently,

$$\widetilde{T}^{(N)}|_\sigma = \sum_{n=2}^{N} d_n^{(N)} T_n|_\sigma \quad , \quad N = 2,3,\ldots \qquad (2.24)$$

Now we may state that for improving convergence of the sequence $\{T^{(N)}|_\sigma\}$ it is sufficient to multiply the terms of the polynomials (2.5) by positive constants $d_n^{(N)}$, which are defined in (2.22).

It can be established from (2.22) that

$$d_N^{(N)} = O(N^{-1/2}) . \qquad (2.25)$$

In other words, the last term in (2.24) is $\sqrt{N}$ times less than in (2.5).

The estimate (2.19) and the following one show that when $N \to \infty$ the sequence $\{\widetilde{T}^{(N)}|_\sigma\}$ converges uniformly to the

potential $T|_\sigma$. It means that, by tending N to infinity in (2.24), we must obtain (1.11). Let us check this directly. By limiting transfer $N \to \infty$ in (2.22) for a fixed n , we have

$$\alpha_n^{(\infty)} = \frac{1}{2(n+1)} + \frac{(1)_n}{(1/2)_n (n+2)} \, {}_3F_2\left(n+1, \frac{n}{2}, \frac{1}{2}; n+\frac{3}{2}, \frac{n}{2}+2; 1\right),$$

where ${}_3F_2$ is the generalized hypergeometric Gauss' function /16/. Its numerical value can be estimated with the aid of Dixon's theorem (ibid.), which results in

$$\alpha_n^{(\infty)} = 1 \quad , \qquad n = 2, 3, \ldots$$

Thus, the limit of (2.24) for $N \to \infty$ is really the series (1.11). We should like to note, however, that the identity of the original expansion and the new one, in the limit, does not mean that, with increasing N , all the factors $\alpha_n^{(N)}$ in (2.21) tend to unit. The estimate (2.25) holds true for any finite N , while for small fixed n (e.g. for $n=2$) we have indeed : $\alpha_n^{(N)} \to 1$ when N increases. We also draw attention to the following fact. It may be inferred from formula (2.20) and the next three ones that polynomials $\widetilde{T}^{(N)}|_\sigma$ are the partial sums of a certain series, that is (2.15), which is not yet a series of spherical functions. From (1.11) and (2.24) it can be seen that the partial sums of (2.15) are linear combinations of $\Phi_{nm}(R, \varphi, \lambda)$ for $n \le N$, $|m| \le n$. At the same time, the coefficient of a fixed function Φ_{nm} in (2.24) varies with increasing N .

Thus, we have constructed a new sequence $\{\widetilde{T}^{(N)}|_\sigma\}$ such that

$$\lim_{N \to \infty} \widetilde{T}^{(N)}|_\sigma = T|_\sigma \ .$$

The factors $\alpha_n^{(N)}$ in (2.24) provide more rapid convergence of this sequence, as compared to the partial sums of the spherical harmonic series (1.11) for the function $T|_\sigma$. Considering the functions (2.24) as boundary conditions on the sphere σ , the polynomials $\widetilde{T}^{(N)}$ can be constructed, by relation (1.16), as harmonic functions in Σ :

$$\widetilde{T}^{(N)} = \sum_{n=2}^{N} \alpha_n^{(N)} T_n \quad , \qquad N = 2,3,\ldots, \qquad (2.26)$$

their restrictions to σ being represented by (2.24). Since the sequence (2.26) consists of functions which are continious in the closed domain $\bar{\Sigma}$ and converge uniformly on its boundary, then the Harnack's first theorem of the theory of harmonic functions /4/ assures uniform convergence of this sequence, over the whole domain $\bar{\Sigma}$. The limiting function should be harmonic in Σ and in any closed subset of the domain Σ the derivatives of $\widetilde{T}^{(N)}$ of any order converge uniformly to the corresponding derivatives of the limiting function. According to the maximum principle of harmonic functions (ibid.), we have

$$\varepsilon_\Sigma^{(N)} \equiv \sup_{\forall x \in \Sigma} |T - \widetilde{T}^{(N)}| < \sup_{\forall x \in \sigma} |T - T^{(N)}| \equiv \varepsilon_\sigma^{(N)}$$

and, consequently, for $N \to \infty$

$$\varepsilon_{\sigma}^{(N)} \to 0 \quad \Rightarrow \quad \varepsilon_{\Sigma}^{(N)} \to 0 .$$

Thus

$$\lim_{N \to \infty} \widetilde{T}^{(N)} = T \quad , \qquad \widetilde{T}^{(N)} = \sum_{n=2}^{N} a_n^{(N)} T_n ,$$

where T_n is the general term of (1.1).

On the boundary surface σ , the expansion (2.15) of the potential converges more rapidly than the traditional series of spherical functions (1.11), that is the general term of the new series is $\sqrt{n}$ times less than that of the original one. Then the maximum principle of harmonic functions allows to establish stronger convergence of the sequence of polynomials $\widetilde{T}^{(N)}$ in Σ to the potential T , as compared to the sequence of partial sums of (1.1). From comparison of (2.26) and (1.1) it follows that, in order to provide a higher precision approximation of T than that given by the N -th partial sum of (1.1), it is sufficient to multiply the coefficients C_{nm} in the latter by constants $a_n^{(N)}$. In other words, the new approximant of T is

$$\widetilde{T}^{(N)} = \sum_{n=2}^{N} a_n^{(N)} R^n \sum_{m=-n}^{n} C_{nm} \Phi_{nm}(r, \varphi, \lambda) , \quad N = 2, 3, \ldots$$

Another interpretation of the above result is possible. Assume that a certain accuracy of approximation δ of the potential T is prescribed and, to attain it, one should

take into account N terms of the series (1.1). Then the number of terms in the approximant can be reduced from N to $N^* < N$, by means of factors $d_n^{(N)}$, without increasing the error δ of approximation. This method is illustrated by a numerical experiment. We consider, as an initial expansion, a series majorizing (1.11), according to the estimate (1.14) (disregarding the constant factor) :

$$A = \sum_{n=1}^{\infty} \frac{1}{n^{3/2}} \quad , \quad A_N \equiv \sum_{n=1}^{N} \frac{1}{n^{3/2}} \quad , \quad \delta_N \equiv \frac{A - A_N}{A} .$$

We have : $A = \zeta(3/2)$ where $\zeta(x)$ is the Riemann zeta function. By virtue of (2.19), the new expansion of the potential (2.15) is majorized by the series (neglecting the constant factor) :

$$B = \sum_{n=1}^{\infty} \frac{1}{n(n+1)} = 1 \quad , B_N \equiv \sum_{n=1}^{N} \frac{1}{n(n+1)} = \frac{N}{N+1} \quad , \varepsilon_N \equiv \frac{B - B_N}{B} = \frac{1}{N+1} .$$

Approximating properties of functions A_N (which will be called further as "initial" ones) and B_N ("new"approximants) are compared. They characterize, to some extent, approximating qualities of the initial and new polynomials, defined by (1.17) and (2.26).

For each N = 25,50,75,100,150,200,250,300,500,1000 we evaluate the relative errors δ_N and ε_N (per cent). Their ratio δ_N / ε_N shows how many times the accuracy of B_N exceeds that of A_N, for the same N. Besides, the number of terms N^* in B_{N^*} is evaluated from the condition $\varepsilon_{N^*} = \delta_N$, for each N and corresponding δ_N.

The difference $N - N^*$ reveals to what extent the standard polynomial of degree N can be "contracted", with the aid of $a_n^{(N)}$, allowing the same tolerance δ_N. The number N / N^* is evaluated, as well.
The results obtained are presented in the tables 1 and 2 in the end of the paper.

3. Application of the method of economization of power series

The basic idea of the method of economization is as follows. Suppose that a function $f(z)$ can be expanded over the interval $-1 \le z \le 1$ in power series

$$f(z) = \sum_{n=0}^{\infty} a_n z^n ,$$

and

$$f^{(N)}(z) = \sum_{n=0}^{N} a_n z^n$$

is its partial sum. Let the power N of $f^{(N)}$ be large enough for providing a given accuracy of approximation :

$$\max \left| f - f^{(N)} \right| \le \varepsilon , \quad -1 \le z \le 1 .$$

Convergence of the initial power series can be improved with the aid of Lanczos' method of telescopic shifting /5/ or, by another terminology, economization of power series /17/. It is reduced to representing the function $f^{(N)}(z)$ in terms

in terms of Chebyshev polynomials $T_m(z)$:

$$f^{(N)}(z) = \sum_{m=0}^{N} e_m^{(N)} T_m(z).$$

Herewith, the coefficients of $T_m(z)$ in the last terms appear to be much smaller than the other ones. Taking into account that $|T_m| \leq 1$, the last terms may be omitted, practically without loss of precision. After converting the remaining sum into a power polynomial, we have an approximating polynomial of degree $N_0 < N$:

$$f^{(N)}(z) \approx \bar{f}^{(N_0)}(z) \equiv \sum_{m=0}^{N_0} c_n^{(N)} z^n,$$

in which the number of terms is by $(N - N_0)$ less than in the initial polynomial $f^{(N)}$. The additional error due to such "contraction" of $f^{(N)}$ turns out to be insignificant as compared to the error ε of this polynomial, if N is large enough.

When approximating the earth's potential, the most convenient for applications are expansions in Legendre polynomials $P_n(z)$. That is why we suggest a modification of economization procedure based on the use of the Legendre polynomials rather than the Chebyshev ones. After presentation of $f^{(N)}$ as a linear combination of Legendre polynomials, the coefficients of $P_n(z)$ in the last terms are somewhat greater than those of $T_n(z)$. Nevertheless, they are negligible, in comparison with the other coefficients, for large values of N.

We proceed again from the expression (2.1) for the potential

T at the boundary surface σ . The function f , entering the integrand, is defined by (2.6)-(2.8). Let us present f_1 and f_2 as

$$f_1 = -\frac{1}{2} \ln\left[1 - \frac{1+z}{2}\right] ,$$

$$f_2 = -\ln\left[1 + \sqrt{\frac{1-z}{2}}\right] , \quad z = \cos\psi .$$

Consider the power expansions of these functions /11/, which we denote $\bar{f}_1$ and $\bar{f}_2$:

$$\bar{f}_1 = \frac{1}{2} \sum_{n=1}^{\infty} \frac{1}{n} \left(\frac{1+z}{2}\right)^n , \quad -1 < z \leq 1 , \tag{3.1}$$

$$\bar{f}_2 = \frac{1}{2} \sum_{n=1}^{\infty} \frac{(\frac{1}{2})_n}{n\,(1)_n} \left(\frac{1+z}{2}\right)^n - \ln 2 , \quad -1 \leq z \leq 1 . \tag{3.2}$$

The function (2.6) becomes

$$\bar{f} = \bar{f}_1 + \bar{f}_2 \tag{3.3}$$

and the potential (2.1) will be presented, correspondingly, as

$$\bar{T}\big|_{\sigma} = \sum_{n=2}^{\infty} \bar{T}_n\big|_{\sigma} \tag{3.4}$$

where

$$\frac{1}{R}\overline{T}_n|_\sigma = \frac{2^{-n-1}}{4\pi n}\left[1+\frac{(\frac{1}{2})_n}{(1)_n}\right]\int_0^{2\pi}\int_0^{\pi} M(1+\cos\psi)^n \sin\theta_1\, d\theta_1\, d\lambda_1 .$$

After making use of (1.12) and estimating the resulting integral with the help of the generalized mean value theorem, we yield

$$\left|\frac{1}{R}\overline{T}_n|_\sigma\right| < \frac{M_{max}}{n(n+1)}, \qquad n=2,3,\ldots \qquad (3.5)$$

Comparing this estimate with (1.14). it can be seen that the general term of (3.4) decreases $\sqrt{n}$ times faster than the general term of the initial expansion (1.11).
The estimate (1.15) is better than (3.5) by the order of decreasing with respect to n . Nevertheless, as noted in Section 2, the right-hand side of (1.14), and consequently (3.5), may exceed the right-hand side of (1.15) only for very large values of n , at least for n greater than the number of terms in (1.1) taken currently into account.
Consider the partial sum $(\overline{f})_N$ of $\overline{f}$, represented by (3.1)-(3.3) :

$$(\overline{f})_N = \sum_{n=1}^{N} \frac{2^{-n-1}}{n}\left[1+\frac{(\frac{1}{2})_n}{(1)_n}\right](1+\cos\psi)^n - \ln 2, \qquad 0\le\psi\le\pi. \qquad (3.6)$$

This polynomial can be expressed in terms of Legendre polynomials

$$(\overline{f})_N = \sum_{n=2}^{N} \frac{1}{n}\beta_n^{(N)} P_n(\cos\psi) + \beta_0^{(N)} + \beta_1^{(N)}\cos\psi . \qquad (3.7)$$

Substituting this expression into (2.1), in place of f gives a certain polynomial $\overline{T}^{(N)}|_\sigma$ approximating $T|_\sigma$:

$$\overline{T}^{(N)}|_\sigma = \frac{R_*}{4\pi}\int_0^{2\pi}\int_0^{\pi} \rho \bar{f}^{(N)} \sin\theta_1 \, d\theta_1 \, d\lambda_1 , \qquad (3.8)$$

where

$$\bar{f}^{(N)} = \sum_{n=2}^{N} \frac{1}{n} \beta_n^{(N)} P_n(\cos\psi). \qquad (3.9)$$

Two last expressions, after comparing them with (2.3)-(2.5), give

$$\overline{T}^{(N)}|_\sigma = \sum_{n=2}^{N} \beta_n^{(N)} T_n|_\sigma \quad , \quad N = 2, 3, \ldots \qquad (3.10)$$

Evaluation of the coefficients of Legendre series (3.7) for (3.6) yields

$$\beta_n^{(N)} = \nu_n^{(N)} + \lambda_n^{(N)} \quad , \quad n = 2, 3, \ldots \qquad (3.11)$$

where

$$\nu_n^{(N)} \equiv \frac{n+\frac{1}{2}}{n+1} \sum_{p=0}^{N-n} \frac{(n)_p \, (1)_{n+p}}{(1)_p \, (n+2)_{n+p}} ,$$

$$\lambda_n^{(N)} \equiv \frac{n+\frac{1}{2}}{n+1} \sum_{p=0}^{N-n} \frac{(n)_p \, (\frac{1}{2})_{n+p}}{(1)_p \, (n+2)_{n+p}} . \qquad (3.12)$$

The constants $\nu_n^{(N)}$ and $\lambda_n^{(N)}$ can be represented as

$$\nu_n^{(N)} = 2^{-2n-1} \frac{(1)_n}{(\frac{1}{2})_n} \sum_{p=0}^{N-n} \frac{(n)_p\,(n+1)_p}{(1)_p\,(2n+2)_p}\,, \quad n=2,3,\ldots \quad (3.13)$$

$$\lambda_n^{(N)} = 2^{-2n-1} \sum_{p=0}^{N-n} \frac{(n)_p\,(n+\frac{1}{2})_p}{(1)_p\,(2n+2)_p}\,, \quad n=2,3,\ldots \quad (3.14)$$

The sum in (3.13) (and (3.14) too) can be treated as a truncated hypergeometric Gauss' series ${}_2F_1$. After transforming it into an infinite series and application of the summation formula for a hypergeometric series with unit argument /16/, we finally obtain

$$\nu_n^{(N)} = (-1)^n \frac{(n+\frac{1}{2})\,(-N)_n}{(n+1)(N+2)_n}\,, \quad n=2,3,\ldots \quad (3.15)$$

For large values of n it is advisable to present (3.12) as

$$\lambda_n^{(N)} = \frac{n+\frac{1}{2}}{n+1} \sum_{p=0}^{N-n} \frac{(n)_p\,(\frac{1}{2})_p\,(p+\frac{1}{2})_n}{(n+2)_p\,(1)_p\,(n+2+p)_n}\,. \quad (3.16)$$

From (3.13) and (3.14) it can be established that

$$\nu_N^{(N)} = O(\sqrt{N}\,2^{-2N-1})\,, \quad \lambda_N^{(N)} = O(2^{-2N-1})\,.$$

Therefore, for large N the coefficient $\beta_n^{(N)} = \nu_n^{(N)} + \lambda_n^{(N)}$ in (3.9) is very small and, in general, some number of the last terms are small and can be omitted without a noticeable loss of accuracy. As a result, the polynomial (3.9) "contracts" :

$$\bar{\zeta}^{(N)} \approx \sum_{n=2}^{N_0} \frac{1}{n} \beta_n^{(N)} P_n(\cos\psi) \quad , \quad N_0 < N \, , \; N = 2,3,\ldots \qquad (3.17)$$

which entails economization of the polynomial (3.10) :

$$\bar{T}^{(N)}\big|_\sigma \approx \sum_{n=2}^{N_0} \beta_n^{(N)} T_n\big|_\sigma \quad , \quad N = 2,3,\ldots \qquad (3.18)$$

In order to test the formulas (3.8)-(3.14), we tend N to infinity in them. It gives

$$\beta_n^{(\infty)} = 2^{-2n-1} \frac{(1)_n}{(\frac{1}{2})_n} F(n, n+1, 2n+2; 1) +$$

$$+ 2^{-2n-1} F(n, n+\tfrac{1}{2}, 2n+2; 1) \quad , \quad n = 2,3,\ldots$$

from where follows /16/ that $\beta_n^{(\infty)} = 1$, for all $n = 2,3,\ldots$ Comparing the limit of the sequence (3.8)-(3.9) for $N \to \infty$ with the series (2.1)-(2.2), we conclude that this limit is presented by the series (1.11), which confirms the correctness of the formulas obtained.

The solution of the exterior Dirichlet boundary value problem, corresponding to the boundary condition(3.10) on the sphere σ , can be constructed basing on the relation (1.16). As a result, the linear combinations of spherical functions $\bar{T}^{(N)}$ ($N = 2,3,\ldots$) have been provided which approximate the potential T in the domain $\bar{\Sigma}$:

$$\bar{T}^{(N)} = \sum_{n=2}^{N} \beta_n^{(N)} T_n \quad , \quad N = 2,3,\ldots \quad , \quad x \in \bar{\Sigma} \qquad (3.19)$$

or, with regard to (3.18),

$$\overline{T}^{(N)} \approx \sum_{n=2}^{N_0} \beta_n^{(N)} T_n \quad , \quad n=2,3,\dots , \; N_0 < N , \; x \in \overline{\Sigma} . \tag{3.20}$$

Since the additional error due to the transfer from (3.10) to (3.18) is small, then, according to the maximum principle of harmonic functions, the transition (3.19) $\to$ (3.20) implies an error which is also small, comparing to the one of $\overline{T}^{(N)}$.

As follows from the above estimates, the convergence of (3.4) (or (3.10)) is stronger than that of (2.5). As a result, the sequence (3.19) (and (3.20), as well) must tend to T more rapidly than the partial sums (1.17) of the original series (1.1). In other words, multiplication of T_n in (1.17) by $\beta_n^{(N)}$ leads to decreasing the error of approximation. At the same time, in the new approximant (3.19) the number of terms may be economized with a negligible additional error. Thus, the "contracted" polynomial (3.20) of degree $N_0 < N$ provides better approximation of T than the N-th partial sum of (1.1). By virtue of (1.1), we can present (3.20) as

$$\overline{T}^{(N)} \approx \sum_{n=2}^{N_0} \beta_n^{(N)} R^n \sum_{m=-n}^{n} C_{nm} \Phi_{nm}(r,\varphi,\lambda) \; , \; N_0 < N , \; N=2,3,\dots$$

This approximant of T differs from the N-th partial sum of (1.1) by lesser number of terms N_0 and by the factors $\beta_n^{(N)}$.

To give an idea of the efficiency of the economization proce-

dure, a numerical experiment has been carried out. The results are presented in the tables 1 and 2.

As an initial one, is used the same series A, as in Section 2, which majorizes the standard series (1.1), disregarding the constant factor. Comparing the estimates (2.19) and (3.5) for two kinds of the new series, (2.15) and (3.4), we conclude that for (3.4) there is the same majorizing series B, as before, neglecting the constant factor. The relative errors of A_N and B_N are also designated by δ_N and ε_N. Convergence of the new sequence of approximants is characterized by the same quantities : δ_N / ε_N, N^*, $N - N^*$ and N / N^*. It should be noted, however, that the former designations should be treated now as referring to the characteristics of the new series (3.4). The method of economization enables further improvement of results, and, besides the above quantities, we estimate also some additional ones. Thus, the number N_0 is determined which characterizes degree of the "contracted" polynomial (3.17), resulting from (3.9) after rejecting the "tail", "longways" $N - N_0$. Practically, the number N_0 is found from the condition

$$\sum_{n=N_0+1}^{N} \frac{1}{n} \beta_n^{(N)} < 0.01\, \varepsilon_N . \qquad (3.21)$$

Since the additional error due to "contraction" attains only $0.01\, \varepsilon_N$, it may be neglected. Consequently, the total error of the "contracted" function is, approximately, ε_N.

We compare the errors of two approximants having

N_0 terms - the initial and the new "contracted" ones - by evaluating $\delta_{N_0} / \varepsilon_N$. Let us recall that N^* means the number of terms in the new approximant B_{N^*} which provides the same accuracy of approximation, as the initial one A_N , i.e. N^* is defined by the equality $\varepsilon_{N^*} = \delta_N$. Now, replacing in (3.21) N by N^* and N_0 by N_0^* , we estimate, from the resulting relation, the number of terms N_0^* which remain in B_N^* after economization. The error of such "contracted" function is still, approximately, $\varepsilon_{N^*} = \delta_N$. Then the quantities $N - N_0^*$ and N / N_0^* characterize the total effect of the new series application as well as its economization, for a fixed error of approximation.

It should be especially emphasized that the obtained numerical results are valid for majorizing series. The actual efficiency of both proposed methods can be estimated only on the basis of the real data, referring to the global earth's gravitational field. Only in this way one can estimate which of the two methods is preferable.

Thus, the described procedures of improving the convergence of the earth's potential expansion may serve for two purposes. On one hand, the accuracy of approximation of the global earth's gravitational field can be increased, for a given number of terms in an approximating polynomial. On the other hand, the possibility arises for reducing the number of terms in the polynomial, without decreasing the given accuracy of approximation. The basic set of harmonic coefficients is represented by Stokes' constants c_{nm} ($n \leq N$,

$|m| \leq n$) which can be determined from observations by means of the integral formulas, depending upon the gravity anomaly Δg on the earth's surface /3/, /13/, /14/.

Consideration of non-sphericity and topography of this surface can be made, in particular, by the formulas, derived in /9/ and /10/.

The constants C_{nm} can be also interpreted as the coefficients of the best mean square approximants of the potential on the sphere σ . In this case, the reduction of Δg from the earth's surface to σ should be performed.

References

/1/ Brovar, V.V.: On the solution of Molodensky's problem; Izv. vyssh. uchebn. zaved. Geodeziya i aerofotos'emka, vyp. 4, 129-137, 1963 (in Russian).

/2/ Brovar, V.V.: Fundamental harmonic functions with a singularity on the segment and the solution of the external boundary value problems; Izv. vyssh. uchebn. zaved. Geodeziya i aerofotos'emka, vyp. 3, 51-52, 56-59, 1964 (in Russian).

/3/ Colombo, O.: Numerical methods for harmonic analysis on the sphere ; Reports of the Dept. of Geodetic Science, n. 310, The Ohio State University, 1981.

/4/ Kellogg, O.D.: Foundations of potential theory; 223, 248, 249, Verlag Springer, Berlin, 1929.

/5/ Lanczos, C.: Applied analysis; Prentice Hall, Inc., 1956.

/6/ Molodensky, M.S., Yeremeyev, V.F., Yourkina, M.I.: Methods for study of the external gravitational field and figure of the earth; Transl. from Russian. Jerusalem, Israel program for scientific translations, 1960.

/7/ Moritz, H.: Linear solutions of the geodetic boundary-value problem; Deutch. Geodät. Komission, Bayerischen Akad. Wiss., Reihe A: Höhere Geodäsie, 58, 44, 1968.

/8/ Pellinen, L.P.: Higher geodesy (Theoretical geodesy); "Nedra", Moscow, 1978 (in Russian).

/9/ Petrovskaya, M.S.: Solution of the geodetic boundary value problem; Bull. Geód., vol. 53, 21-36, 1979.

/10/ Petrovskaya, M.S., Lobkova, N.I.: On refinement of relations between Stokes' constants and surface gravitational data; Manuscripta Geodaetica, vol. 7, 45-76, 1982.

/11/ Prudnikov, A.P., Brychkov, Y.A., Marichev, O.I.: Integrals and series. Elementary functions; 698, 712, 726, "Nauka", Moscow, 1981 (in Russian).

/12/ Prudnikov, A.P., Brychkov, Y.A., Marichev, O.I.: Integrals and series. Special functions; 700, "Nauka", Moscow, 1983 (in Russian).

/13/ Rapp, R.H.: The use of gravity anomalies on a bounding sphere to improve potential coefficient determinations; Reports of the Dept. of Geodetic Science, n. 254, The Ohio State University, 1977.

/14/ Rapp, R.H.: The Earth's gravity field to degree and order 180 using seasat altimeter data, terrestrial gravity data and other data; Scientific Report n. 12, The Ohio State University Research Foundation, Dec. 1981.

/15/ Sansone, G.: Orthogonal functions; 202-203, Interscience publishers, Inc., New York, 1959.

/16/ Slater, L.J.: Generalized hypergeometric functions; Cambridge Univ. Press, 1966.

/17/ Snyder, M.A.: Chebyshev methods in numerical approximation; Prentice Hall, Inc., Inglewood Cliffs, N.J., 1966.

Table 1. Reducing the error of approximation for a given number of terms

N	δ_N (%)	ε_N (%)	δ_N/ε_N	N_0	δ_{N_0} (%)	$\delta_{N_0}/\varepsilon_N$
25	15.2	3.9	4	11	22.6	6
50	10.8	2.0	5	16	18.8	9
75	8.8	1.3	7	21	16.5	13
100	7.6	1.0	8	25	15.2	15
150	6.2	0.7	9	32	13.6	19
200	5.4	0.5	11	37	12.5	25
250	4.8	0.4	12	42	11.7	29
300	4.4	0.3	15	47	11.1	37
500	3.4	0.2	17	63	9.6	48
1000	2.4	0.1	24	92	8.0	80

N = given number of terms

δ_N = error of the initial approximation

ε_N = error of the new approximation

N_0 = number of terms in the new approximant after economization

Table 2. Reducing the number of terms in a polynomial for a given accuracy of approximation

N	N^*	N_o^*	$N-N^*$	N/N^*	$N-N_o^*$	N/N_o^*
25	6	5	19	4	20	5
50	8	6	42	6	44	8
75	10	6	65	8	69	13
100	12	7	88	8	93	14
150	15	8	135	10	142	19
200	18	9	182	11	191	22
250	20	10	230	13	240	25
300	22	10	278	14	290	30
500	28	12	472	18	488	42
1000	41	15	959	24	985	67

N = number of terms in the initial approximant providing the given accuracy

N^* = number of terms in the new approximant providing the same accuracy

N_o^* = number of terms in the latter after economization

FOIBE-TAOSARINTANIN' MADAGASIKARA
F.T.M.

BUREAU GRAVIMETRIQUE INTERNATIONAL
B.G.I.

GEOIDE GRAVIMETRIQUE SUR MADAGASCAR

PAR RAPPORT AU SYSTEME GEODESIQUE DE REFERENCE 1980

J. RAKOTOARY

Juin 1986

INTRODUCTION

Le géoide qui est une surface de référence particulière, peut être calculé à partir des données gravimétriques (anomalies à l'air libre) et d'un modèle en harmoniques sphériques en utilisant un champ de référence (développement en harmoniques sphériques) et l'intégrale de Stokes.

Cette surface de référence a une grande importance pour des fins géodésiques et géophysiques.

Un premier géoide sur Madagascar a été calculé sur des grilles de 15' x 15' à partir des données gravimétriques, des anomalies à l'air libre terrestres localisées dans une zone s'étendant jusqu'à 25° de part et d'autre de la grande île et complétées par des données marines obtenues par inversion des données altimétriques du satellite Seasat ; le modèle en harmoniques sphériques utilisé était celui de Rapp. 79 donné jusqu'au degré L = 180.

Nous présentons dans ce rapport en premier chapitre un rappel des définitions et quelques relations importantes et nous recommandons aux lecteurs qui veulent avoir plus de détails de se référer à l'ouvrage d'Heiskanen et Moritz (référence n° 2) ; dans le chapitre 2 nous parlons des données et de leur traitement puis nous exposons le principe de calcul et dans le dernier chapitre nous montrons les résultats obtenus.

I. RAPPEL DES DEFINITIONS ET QUELQUES RELATIONS IMPORTANTES

I.1. Définition du Géoide

Le géoide (G) est une surface équipotentielle particulière du champ de pesanteur de la Terre réelle, $W = V + \Phi$, voisin de la surface moyenne des océans, et que l'on peut définir par :

$$W = W_0 \qquad (1)$$

I.2. Potentiel Gravitationnel Terrestre, Potentiel Gravitationnel Normal

Le potentiel du champ de pesanteur de la Terre réelle est défini par :

$$W = V + \Phi \qquad (2)$$

où Φ est le potentiel dont dérive la force centrifuge

V est le potentiel de gravité de la Terre.

En tout point extérieur, de coordonnées sphériques (r,φ,λ) lié au repère terrestre, V est développé en harmoniques sphériques sous la forme [Heiskanen, Moritz, 1967] :

$$V = W - \phi = \frac{GM}{r}\left[1 - \sum_{n=2}^{\infty}\sum_{m=o}^{n}\left(\frac{R}{r}\right)^n (J_{nm}\cos m\lambda + K_{nm}\sin m\lambda)\, P_{nm}(\sin\varphi)\right] \quad (3)$$

Cela en supposant que le centre de gravité de la Terre est à l'origine du système de coordonnées et que l'axe z de ce système est un axe principal d'inertie.

L'expression (3) peut encore s'écrire :

$$V = \frac{GM}{r}\left[1 + \sum_{n=2}^{\infty}\sum_{m=o}^{n}\left(\frac{R}{r}\right)^n (\bar{C}_{nm}\cos m\lambda + \bar{S}_{nm}\sin m\lambda)\, \bar{P}_{nm}(\sin\varphi)\right] \quad (4)$$

où G est la constante de la gravitation universelle

M est la masse de la Terre

$\bar{P}_{nm}$ est la fonction de Legendre associée de deuxième espèce

$\bar{C}_{nm}, \bar{S}_{nm}$ sont des coefficients (sans dimension) normalisés, les harmoniques sphériques du champ de gravitation.

avec $\bar{C}_{no} = -J_{no}(2n+1)^{-1/2}$: les zonaux

et pour $m \neq o$ $\begin{bmatrix}\bar{C}_{nm}\\ \bar{S}_{nm}\end{bmatrix} = -\begin{bmatrix}J_{nm}\\ K_{nm}\end{bmatrix} \cdot \sqrt{\frac{(n+m)!}{2(2n+1)(n-m)!}}$: les tesseraux.

R est le rayon moyen de la Terre pris en général égal au demi-grand axe d'un ellipsoide (E) de référence, de révolution, dit "dynamique".

L'ellipsoide (E) a une masse égale à la masse M de la Terre, son centre de gravité est le même que celui de la Terre, il a la même vitesse de rotation que la Terre, et sa surface est équipotentielle du champ de pesanteur qu'il crée.

Le potentiel dont dérive la pesanteur d'un ellipsoide est égal à :

$$U = U_E + \phi \quad (5)$$

Le potentiel normal U_E du champ de gravité peut s'écrire :

$$U_E = U - \phi = \frac{GM'}{r}\left[1 - \sum_{n=2}^{\infty}\sum_{m=o}^{n}\left(\frac{a}{r}\right)^n (J'_{nm}\cos m\lambda + K'_{nm}\sin m\lambda)\, P_{nm}(\sin\varphi)\right] \quad (3)$$

Avec un ellipsoide (E) comme celui qu'on vient de décrire, ce développement en harmoniques sphériques de U_E ne comporte que des zonaux pairs.

$$U_E = \frac{GM}{r} \sum_{n=1}^{\infty} \left(\frac{a}{r}\right)^{2n} J'_{2n} P_{2n} (\sin \varphi)$$

$$= \frac{GM}{r} \sum_{n=1}^{\infty} \left(\frac{a}{r}\right)^{2n} \bar{C}'_{2n} \bar{P}_{2n,o} (\sin \varphi) \qquad (7)$$

et si on pose $m = \frac{\omega^2 a^2 b}{GM}$ (ω : vitesse de rotation de la Terre, $b=a(1-f)$) (8)

$$\text{on a : } J'_2 = \frac{2}{3} f - \frac{1}{3} m - \frac{1}{3} f^2 + \frac{2}{21} f.m$$

$$\text{et : } J'_4 = -\frac{4}{5} f^2 + \frac{4}{7} f.m \qquad (9)$$

Les J'_{2n} de degré supérieur peuvent être négligés car ils sont tous d'ordre f^{2n}, où f est l'aplatissement de (E) ($\approx 3.10^{-3}$).

I.3. Pesanteur, Pesanteur Normale

Le gradient de W, $\bar{g} = \bar{\nabla}.W$ (10), est appelé la pesanteur, c'est la somme vectorielle du vecteur gravité (gradient du potentiel gravitationnel) et de l'accélération centrifuge (gradient de Φ).

Le gradient de U, $\bar{\gamma} = \bar{\nabla}.U$ (11), est appelé la pesanteur normale ou théorique.

En un point de latitude <u>géocentrique</u> φ, la pesanteur théorique s'écrit :

$$\gamma(\varphi) = \gamma_a (1 + f_2 \sin^2 \varphi + f_4 \sin^4 \varphi) \qquad (12)$$

où γ_a est la pesanteur normale à l'équateur de (E)

$$\gamma_a = \frac{GM}{a^2 (1-f)} \left[1 - \frac{3}{2} m \left(1 + \frac{2f - f^2}{7 (1-f)^2} \right) \right] \qquad (13)$$

$$f_2 = -f + \frac{5}{2} m + \frac{1}{2} f^2 - \frac{26}{7} f.m + \frac{15}{4} m^2$$

$$f_4 = -\frac{1}{2} f^2 + \frac{5}{2} f.m \qquad (14)$$

I.4. Relief du Géoide

Soient les surfaces de référence ci-après (fig. 1) :

(T) : la surface topographique

(H) : la surface hypsométrique définie par l'ensemble des points H et tel que W (T) = U (H)

(G) : le géoide W = W_o

(E) : l'ellipsoide de référence tel que $U = W_o$

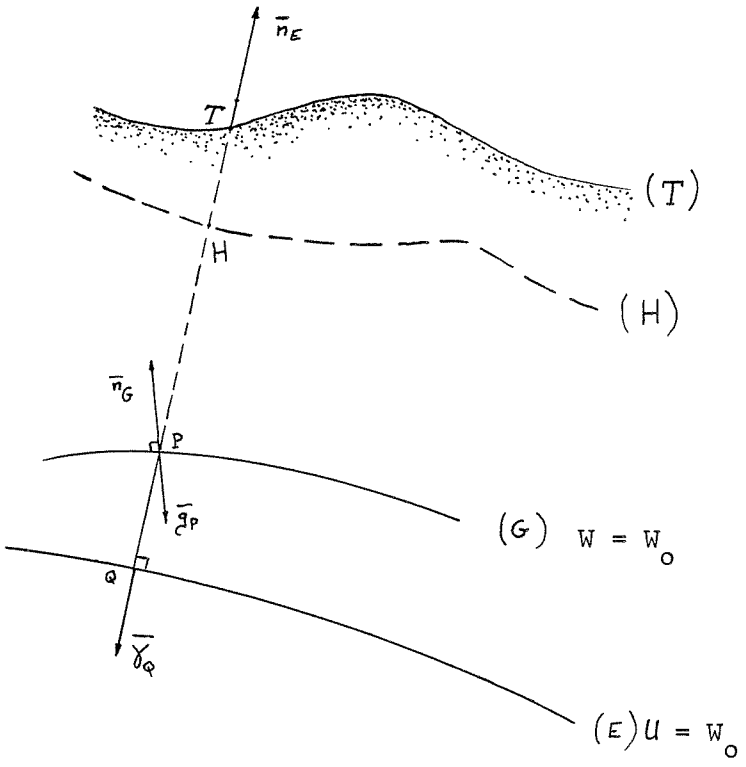

$\bar{n}_E$ = normale à l'ellipsoide

$\bar{n}_G$ = normale au géoide

Fig. 1. Surfaces de référence

Le relief du géoide est défini par $\overline{QP} = \overline{HT}$ où Q est la projection sur l'ellipsoide d'un point P de (G) suivant la normale (E) en Q.

Ce relief du géoide qu'on note N est donné par la formule de Bruns :

$$N = \overline{QP} = \frac{(W - U)_P}{\langle \gamma \rangle_{QP}} \qquad (15)$$

. $\langle \gamma \rangle_{QP}$ représente la valeur moyenne de γ sur QP,

. La différence (W - U), qu'on note d'habitude par T est appelée, potentiel perturbateur.

De cette formule de Bruns et en approximation sphérique, le relief N du géoide peut s'exprimer par la relation suivante :

$$N = \frac{GM}{r\gamma} \sum_{n=2}^{\infty} \left(\frac{a}{r}\right)^n \sum_{m=o}^{n} (\delta\bar{C}_{nm} \cos m\lambda + \delta\bar{S}_{nm} \sin m\lambda)\, \bar{P}_{nm} (\sin \varphi) \qquad (16)$$

avec $\delta\bar{C}_{2,0} = \bar{C}_{2,0} - \bar{C}'_{2,0}$, $\delta\bar{C}_{4,0} = \bar{C}_{4,0} - \bar{C}'_{4,0}$

$\delta\bar{C}_{nm} = \bar{C}_{nm}$ et $\delta\bar{S}_{nm} = \bar{S}_{nm}$ si $\{n,m\} \neq \{2,0\}$ et $\{4,0\}$.

Pratiquement, le développement (16) est tronqué à un certain degré L et s'écrit :

$$N \approx \frac{GM}{r\gamma} \sum_{n=2}^{L} \left(\frac{a}{r}\right)^n \sum_{m=o}^{n} (\delta\bar{C}_{nm} \cos m\lambda + \delta\bar{S}_{nm} \sin m\lambda)\, \bar{P}_{nm} (\sin \varphi) \qquad (17)$$

L est le degré maximum du développement en série de fonctions sphériques, modèle global, déterminé par analyses des perturbations orbitales de satellites artificiels, combinées aux informations à la surface (T) (gravimétrie terrestre - marine, altimétrie).

φ et λ sont respectivement la latitude géocentrique et la longitude au point de calcul.

I.5. Anomalie de Gravité, Déviation de la Verticale

Soit le vecteur $\Delta\bar{g} = \bar{g}_P - \bar{\gamma}_Q$,

$\bar{g}_P$ est la pesanteur en P

$\bar{\gamma}_Q$ la pesanteur en Q (voir fig. 1).

* L'intensité de ce vecteur $\Delta g = g_P - \gamma_Q$ (18) est appelée anomalie de gravité à l'air libre.

g_P est obtenue à partir de la valeur g_T mesurée sur la surface (T) par :

$$g_P = g_T \left[1 + \frac{2}{\bar{R}} \cdot \overline{PT} \right] \qquad (19)$$

avec $\bar{R}$: Rayon.moyen ; c'est le rayon d'une sphère de même volume que celui de l'ellipsoide de référence (E)

$$\bar{R} = a \left[1 - \frac{f}{3} \left[1 + \frac{f}{3} \left(1 + \frac{5}{3} \frac{f}{3} \right) \right] \right] \qquad (20)$$

$\overline{PT}$ est remplacée par l'altitude normale h en pratique :

$$h = \frac{1}{\langle \gamma \rangle_{QT}} \Sigma g \, dh \qquad (21)$$

* L'écart entre la direction de $\bar{g}_P$ et celle de $\bar{\gamma}_Q$ est appelé déviation de la verticale.

La déviation de la verticale a deux composantes, une composante Nord-Sud ξ et une composante Est-Ouest η.

avec [Heiskanen - Moritz] . $\xi = (\phi - \varphi)$

$$= - \frac{1}{R} \cdot \frac{\partial N}{\partial \varphi} \qquad (22)$$

$$\eta = (\Lambda - \lambda) \cos \varphi$$

$$= - \frac{1}{R \cos \varphi} \frac{\partial N}{\partial \lambda} \qquad (23)$$

(ϕ, Λ) sont les coordonnées astronomiques.

(φ, λ) sont les coordonnées géodésiques.

I.6. Formule de Stokes (géoide gravimétrique)

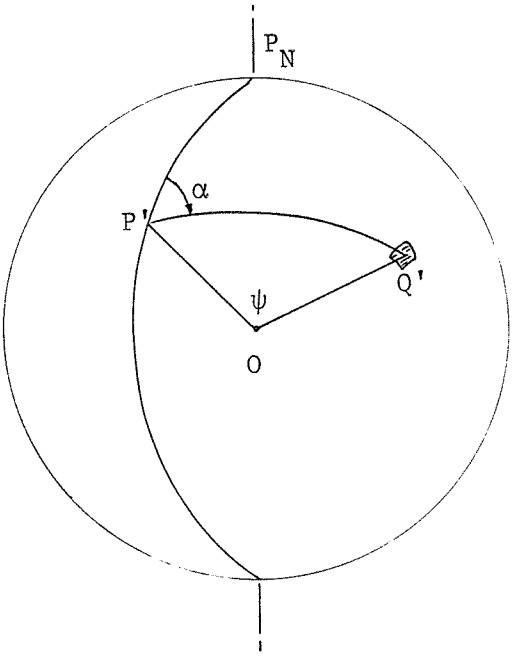

Fig. 2. Coordonnées polaires sur la sphère unité σ_1

En approximation sphérique, l'équation fondamentale de la géodésie physique s'écrit :

$$\Delta g = - \frac{\partial T}{\partial r} - \frac{2}{r} T \qquad (24)$$

Cette équation admet la solution analytique suivante :

$$T = \frac{\bar{R}}{4\pi} \iint_{\sigma_1} \Delta g \; S(\psi) \; d\sigma \qquad (25)$$

et de la formule de Bruns, on déduit la formule de Stokes qui donne le relief du géoide en un point donné :

$$N = \frac{\bar{R}}{4\pi\bar{\gamma}} \iint_{\sigma_1} \Delta g \; S(\psi) \; d\sigma \qquad (26)$$

où . $\bar{\gamma}$ est la valeur moyenne de la pesanteur sur (E)

$$\bar{\gamma} = \frac{1}{\pi} \int_{-\pi/2}^{\pi/2} \gamma(\varphi) \, d\varphi$$

$$= \gamma_a \left(1 + \frac{f_2}{2} + \frac{3}{8} f_4\right) \qquad (27)$$

. σ_1 : la sphère unité

. $\bar{R}$: le rayon moyen de la sphère $\bar{\sigma}(0,\bar{R})$

. Δg : l'anomalie de la pesanteur d'un élément de surface ds vu sous un élément d'angle solide $d\sigma$

. ψ : l'arc d'un grand cercle séparant le point considéré de l'élément de surface $d\sigma$ sur σ_1.

. $S(\psi)$: la fonction de Stokes donnée par :

$$S(\psi) = \frac{1}{\sin\left(\frac{\psi}{2}\right)} - 6 \sin\frac{\psi}{2} + 1 - 5\cos\psi - 3\cos\psi \ln\left[\sin\frac{\psi}{2} + \sin^2\frac{\psi}{2}\right] \qquad (28)$$

En utilisant les coordonnées polaires sphériques (ψ,α), α étant l'azimuth compté à partir d'une direction arbitraire, le point P considéré comme origine, on a $d\sigma = \sin\psi \, d\psi . d\alpha$, et la relation (26) s'écrit :

$$N = \frac{\bar{R}}{4\pi\bar{\gamma}} \int_{\alpha=0}^{2\pi} \int_{\psi=0}^{\pi} \Delta g \; (\psi,\alpha) \; S(\psi) \sin\psi \, d\psi \, d\alpha \qquad (29)$$

Sous cette forme la fonction $S(\psi) \sin\psi$ est parfaitement intégrable du point de vue numérique.

Par exemple, si l'on procède par intégration suivant des calottes et des zones sphériques centrées en chaque point P (et redécoupées en "templates"), l'équation de Stokes $\iint_{\sigma_1} S(\psi) \, \Delta g \, d\sigma'$ se calcule par :

$$\sum_k \bar{\Delta g}_k \int_{\alpha_1,k}^{\alpha_2,k} d\alpha \int_{\psi_1,k}^{\psi_2,k} S(\psi) \sin\psi \, d\psi$$

la deuxième intégrale est régulière même si $\psi_{1,k} = 0$.

II. CALCULS, DONNEES

II.1. Ellipsoides de Référence Utilisées

a) Système géodésique de référence 1967 (GRS 67)

Ellipsoide que nous désignons par E_o de constantes :

$a_o = 6378160$ m

$GM_o = 398603.10^9\ m^3\ s^{-2}$

$f_o = 1/298,2471$

$\omega = 7,2921151467.10^{-5}$ rad/s

b) GRS1980. Ellipsoide que nous désignons par E et de constantes :

$a = 6378137$ m

$GM = 398600,50\ 10^9\ m^3\ s^{-2}$

$f = 1/298,2572$

$\omega = 7,2921151467.10^{-5}$ rad/s

II.2. Calcul de l'Intégrale de Stokes

II.2.1. Géoide de référence

La formule (17) décrit un géoide que nous appelons géoide de référence. Les coefficients géopotentiels ($\overline{C}_{nm}$, $\overline{S}_{nm}$) que nous avons utilisés, sont ceux du modèle de Rapp 79. Ces harmoniques sphériques sont données jusqu'au degré L = 180 et sont associées au système de référence E (ellipsoide 80).

II.2.2. Géoide gravimétrique

La formule de Stokes (relation 26) permet de déterminer le géoide à partir des données gravimétriques d'où sa grande importance en géodésie physique. La résolution pratique de cette intégrale est développée dans la note technique n°4 du BGI (Balmino, 1982, référence n° 1).

Le principe consiste à introduire un champ de référence dans la quadrature $\iint_{\sigma_1} \ldots$ et ainsi réduire le domaine d'intégration D_P autour du point P à une distance géocentrique maximale ψ_{max}. En effet, à cause des limitations de temps

de calcul, d'encombrement mémoire ou d'organisation des programmes on ne peut pas étendre le calcul de cette quadrature à toute la sphère.

Disposant alors d'un champ de référence (relations 3 ou 4) jusqu'à un certain degré L, on peut écrire les développements suivants, analogues à 17, en tout point (r,φ,λ) de (E) :

$$\hat{N} = \frac{GM}{r\gamma} \sum_{n=2}^{L} \left(\frac{a}{r}\right)^n \sum_{m=o}^{n} (\delta\bar{C}_{nm} \cos m\lambda + \delta\bar{S}_{nm} \sin m\lambda) P_{nm} (\sin \varphi) \qquad (30)$$

$$\hat{\Delta g} = \frac{GM}{r^2} \sum_{n=2}^{L} (n-1) \left(\frac{a}{r}\right)^n \sum_{m=o}^{n} (\delta\bar{C}_{nm} \cos m\lambda + \delta\bar{S}_{nm} \sin m\lambda) P_{nm} (\sin \varphi) \qquad (31)$$

$\hat{N}$ et $\hat{\Delta g}$ vérifient l'équation intégrale . 26 ; en posant par conséquent : $\delta N = N - \hat{N}$ et $\delta\Delta g = \Delta g - \hat{\Delta g}$ on a :

$$\delta N_P = \frac{\bar{R}}{4\pi\gamma} \iint_{\sigma_1} S(\psi) \cdot \delta\Delta g_Q \, d\sigma_Q \qquad (32)$$

Q est ici le point courant sur $\bar{\sigma}$ $(0,\bar{R})$, $d\sigma_Q$ l'élément d'angle solide.

δN et $\delta\Delta g$ sont les valeurs résiduelles des fonctions N et Δg respectivement c.a.d. pour chacune d'elle, la valeur de la fonction (vraie) elle-même moins la valeur du développement en harmoniques sphériques.

On a donc à calculer le développement en harmoniques (30 et 31), à résoudre l'intégrale (32), et à en déduire la hauteur du géoide : $N = \hat{N} + \delta N$.

La résolution de l'intégrale (32) se fait par discrétisation. La Terre est supposée découpée en carrés curvilignes $\Delta\varphi \times \Delta\lambda$ et on est amené à calculer les sommations de type :

$$\delta N(p_o,q_o) = \sum_{p=1}^{2M} \sum_{q=1}^{N} \delta\bar{\Delta g}_{P_o-M+P-1/2,q-1/2} \int_{\delta\lambda=-\pi/2M}^{\pi/2M} \int_{\delta\varphi=-\pi/2N}^{\pi/2N} S[\psi(0,\varphi_{q_o},\Lambda_{p-1/2}+\delta\lambda,\varphi_{q-1/2}+\delta\varphi)] \cdot \cos(\varphi_{q-1/2}+\delta\varphi) \, d(\delta\varphi) \, d(\delta\lambda) \qquad (33)$$

La sphère est divisée en 2M secteurs et N zones et pour chaque carré curviligne les anomalies de gravité sont remplacées par leur valeur moyenne dans ce carré et $\delta\Delta g$ par $\delta\bar{\Delta g} = \bar{\Delta g} - \hat{\bar{\Delta g}}$ (pour avoir plus de détails voir la référence n° 1).

Pour les raisons sus-énoncées, l'intégrale (32) est calculée dans un domaine $D_{P,\psi_{max}} = \{Q \mid \psi_{PQ} \leqslant \psi_{max}\}$. Cette régionalisation à $D_{P,\psi_{max}}$ consiste à réduire les sommations sur p et q dans 33 à : $p_{min} \leqslant p \leqslant p_{max}$, $q_{min} \leqslant q \leqslant q_{max}$.

II.2.3. Erreur de Troncature

Hormis les approximations conceptuelles, à savoir l'approximation sphérique et l'assimilation de T (potentiel perturbateur) à une fonction harmonique à la surface de la Terre (alors que la présence de l'atmosphère fait de ces fonctions des solutions de l'équation de Poisson et non de Laplace), les sources d'erreur identifiées sont :

a) les incertitudes sur les mesures et donc les grilles de valeurs moyennes (ou ponctuelles) utilisées.
b) la couverture de ces mesures.
c) les erreurs numériques liées à la discrétisation.
d) les erreurs affectant les coefficients du modèle de référence utilisé.
e) l'erreur de troncature du fait que les intégrales ne sont évaluées que jusqu'à ψ_{max}.

La théorie sur les deux derniers types d'erreur d) et e) est largement développée dans la référence n° 1 (Balmino, 1982).

L'erreur de troncature sur l'intégrale 32 est égale à la quantité :

$$\delta N_P^{(2)} = \frac{\bar{R}}{4\pi\bar{\gamma}} \iint_{\sigma_1 - D_P} S(\psi).\delta\Delta g_Q \, d\sigma_Q \qquad (34)$$

qu'on ne calcule pas du fait de la régionalisation.

Cette erreur de troncature est d'autant plus petite que L est grand ou que $180° - \psi_{max}$ est petit.

Nous avons calculé les valeurs de cette erreur de troncature pour des valeurs données de ψ_{max}. Nous avons utilisé le noyau réduit :

$$\bar{S}^*(\psi) = \begin{cases} 0 \text{ pour } 0 \leqslant \psi \leqslant \psi_{max} \\ S^*(\psi) \text{ pour } \psi \geqslant \psi_{max} \end{cases}$$

avec $S^*(\psi) = S(\psi) - S(\psi_{max})$.

En effet, l'erreur de troncature peut se mettre sous la forme :

$$\eta(N_P) = \delta N_P^{(2)} = \frac{\bar{R}}{4\pi\bar{\gamma}} \iint_{\sigma_1} \bar{S}(\psi) \, \delta\Delta g_Q \, d\sigma_Q \qquad (35)$$

avec $\quad \bar{S}(\psi) = \begin{cases} 0 \text{ pour } 0 < \psi < \psi_{max} \\ S(\psi) \text{ pour } \psi_{max} \leqslant \psi \leqslant \pi \end{cases}$

Ce noyau $\bar{S}(\psi)$ est développable en fonction de Legendre sous la forme :

$$\bar{S}(\psi) = \sum_{n=o}^{\infty} \frac{2n+1}{2} \bar{S}_n P_n (\cos \psi) \qquad (36)$$

Mais à cause de la discontinuité en ψ_{max} de ce noyau, la convergence de cette série est très lente, c'est son inconvénient majeur, d'où l'introduction du nouveau noyau $\bar{S}^*(\psi)$ qui converge plus rapidement du fait de la suppression de la discontinuité.

En utilisant ce noyau réduit l'erreur au point P est de la forme :

$$\eta^* (N_P) = \frac{\bar{R}}{2\pi\bar{\gamma}} \left[\sum_{n=2}^{L} \bar{S}_n^* \eta (\delta\Delta g_n(P)) + \sum_{n=L+1}^{\infty} \bar{S}_n^* \delta\Delta g_n(P) \right] \qquad (37)$$

et l'erreur quadratique moyenne sur la sphère est égale à :

$$\sigma_N^* = \langle \eta^{*2} (N) \rangle = \frac{1}{4\pi} \iint_{\sigma_1} \eta^2 (N_P) \, d\sigma_P$$

$$= \frac{\bar{R}}{2\pi\bar{\gamma}} \left[\sum_{n=2}^{\infty} \bar{S}_n^* H_n' \right]^{1/2} \qquad (38)$$

- avec $\bar{S}_n^* = \int_o^{\pi} (S(\psi) - S(\psi_{max})) P_n (\cos \psi) \sin \psi \, d\psi$ et :

$$H_n' = \sum_{m=o}^{n} (\bar{h}_{C,nm}^2 + \bar{h}_{S,nm}^2),$$

$\bar{h}_{C,nm}$ et $\bar{h}_{S,nm}$ sont les coefficients normalisés du développement en série de fonctions sphériques de surface de $\delta\Delta g$.

Pour les développements de ces relations nous recommandons aux lecteurs de se reporter à la référence n° 1. Le tableau suivant résume les valeurs de l'erreur moyenne quadratique σ_N^* calculées pour des ψ_{max} donnés. Les deux modèles GRIM 3L1 et GEM 10B que nous avons pris pour calculer ces erreurs ont été donnés jusqu'au degré l = 36 et l'erreur du champ pour $36 < l \leqslant 180$ a été modélisée par une loi en $1/l^2$ (loi de Kaula).

ψ_{max} (en degré)	σ_N^* (en mètre)
5	1,02
7	0,75
9	0,56
11	0,42
13	0,33
15	0,27
17	0,24
19	0,23
21	0.21

Compte tenu de ces résultats de calcul sur les erreurs de troncature, nous avons fixé la distance géocentrique ψ_{max} à 20° correspondant à $\sigma_N^* \approx 0,20$ m.

II.3. Sources des Données

II.3.1. Anomalies à l'air libre

Des anomalies de gravité ponctuelles à l'air libre sur Terre et sur mer, s'étendant jusqu'à 25° de part et d'autre de la région $26° \leqslant \varphi \leqslant -12°$ et $42° \leqslant \lambda \leqslant 52°$ où se situe l'île de Madagascar nous ont été fort aimablement fournies par le B.G.I. Les points de mesure de ces anomalies, dont l'état est montré sur la figure n° 3, étaient donnés en coordonnées géodésiques (ϕ,λ).

Comme l'équation de Stokes donne la hauteur du géoide N en fonction des anomalies à l'air libre en faisant des approximations sphériques, toutes les latitudes doivent par conséquent être géocentriques.

Nous avons en premier lieu transformé les coordonnées de ces points de mesure, en coordonnées géocentriques par la relation :

$$\operatorname{tg} \varphi = (1 - e^2) \operatorname{tg} \phi \qquad (39)$$

où φ est la latitude géocentrique

ϕ la latitude géodésique

Fig. 3. Visualisation de la couverture des données gravimétriques dans le domaine :

$\varphi_1 = -51^\circ$, $\lambda_1 = 18^\circ$

$\varphi_2 = 13^\circ$, $\lambda_2 = 76^\circ$

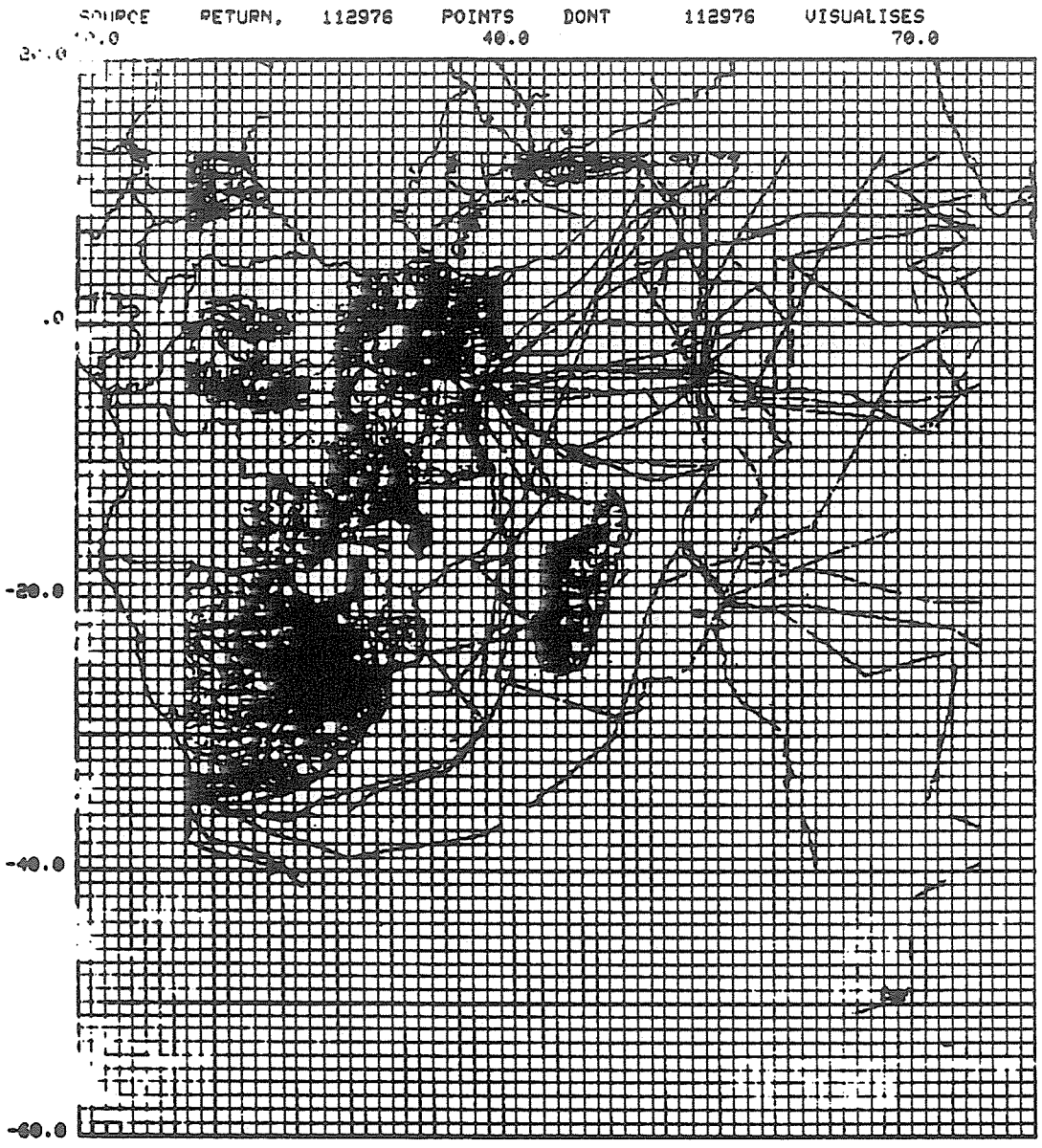

$e^2 = 2f - f^2$, e étant la première excentricité.

Ces anomalies à l'air libre étaient calculées dans le système de référence 1967 (E_o).

De ces données ponctuelles nous avons calculé (par interpolation) des valeurs également ponctuelles sur des grilles très fines de 0,125° x 0,125° (référence n° 3). Comme interpolateur nous avons pris la moyenne pondérée de toutes les données se trouvant dans le cercle de rayon r (r = 0°.5) et centré sur le point à interpoler. La fonction de poids que nous avons adoptée est égale à :

$$W = \frac{1}{1 + \left[\frac{d}{dc}\right]^2} \qquad (40)$$

où d est la distance du point de mesure au noeud (centre du cercle)

dc est la distance de corrélation (0°.25).

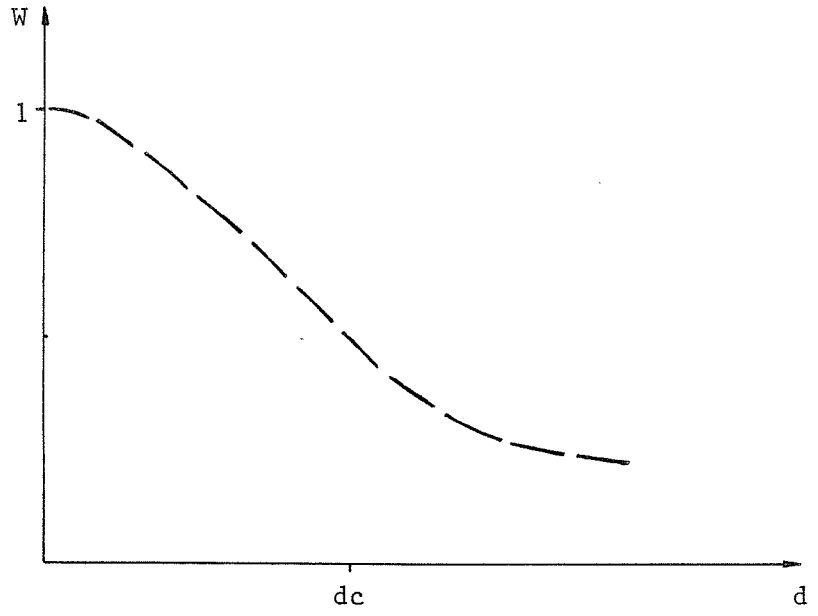

Fig. 4. Fonction de poids

A partir de ces anomalies de grilles (ponctuelles) nous avons calculé les anomalies moyennes dans les carrés curvilignes 0°.25 x 0°.25.

Le manque de données en mer - à part les quelques traces de bateaux comme on peut le visualiser sur l'état des points de données (fig. 3), nous a amené à remplacer les données marines par les anomalies à l'air libre obtenues à partir de l'inversion des données altimétriques du satellite Seasat, et couvrant toute la surface océanique. Ces anomalies, que nous appelons anomalies Seasat,

étaient disponibles dans le système de référence 80 ellipsoide E sur des grilles de 0°,25 x 0°,25 (valeurs ponctuelles).

Nous avons calculé des anomalies moyennes à l'air libre sur des grilles de 0°,25 x 0°,25 à partir de ces anomalies Seasat (fournies également par le B.G.I.).

Comme les anomalies dont nous avions disposé (anomalies moyennes à l'air libre terrestre et anomalies moyennes à l'air libre Seasat) n'étaient pas dans le même système de référence, nous avons transformé les anomalies terrestres dans le système GRS 1980 (E).

La transformation des anomalies à l'air libre pour passer d'un système de référence E_o à un autre système de référence E se fait comme suit :

Puisque $\Delta g_o = g - \gamma_o$

$\Delta g = g - \gamma$

γ_o et γ désignent respectivement les pesanteurs théoriques de E_o et E. On a :

$$\Delta g = (g - \gamma_o) + (\gamma_o - \gamma)$$
$$= \Delta g_o + (\gamma_o - \gamma) \qquad (41)$$

avec :

$$\gamma_o - \gamma = \gamma_a^o - \gamma_a \; (\gamma_a^o f_2^o - \gamma_a f_2) \sin^2 \varphi + (\gamma_a^o f_4^o - \gamma_a f_4) \sin^4 \varphi \qquad (42)$$

d'après la relation 12.

On écrit la relation 42 sous la forme :

$$\delta\gamma = \delta\gamma_a + \delta\gamma_2 \sin^2 \varphi + \delta\gamma_4 \sin^4 \varphi \qquad (43)$$

et s'il s'agit de transformer des valeurs moyennes de gravité, il faudra écrire :

$$\overline{\Delta g} = \overline{\Delta g_o} + \overline{\delta\gamma} \qquad (43)$$

$$\overline{\delta\gamma} = \delta\gamma_a + \delta\gamma_2 \langle \sin^2 \varphi \rangle + \delta\gamma_4 \langle \sin^4 \varphi \rangle \qquad (44)$$

$$\langle \sin^2 \varphi \rangle = \frac{1}{2} (1 - \cos 2\varphi \sin \Delta\varphi/\Delta\varphi) \qquad (45)$$

$$\langle \sin^4 \varphi \rangle = \frac{3}{8} - \frac{1}{2} \cos 2\varphi \sin \Delta\varphi/\Delta\varphi + \frac{1}{8} \cos 4\varphi \cos \Delta\varphi \sin \Delta\varphi/\Delta\varphi \qquad (46)$$

Dans ces deux dernières expressions. φ et λ désignent respectivement la latitude et la longitude du point central du "carré curviligne" défini par $[\varphi_1, \varphi_2] \times [\lambda_1, \lambda_2]$ avec $\varphi_2 = \varphi_1 + \Delta\varphi$ et $\lambda_2 = \lambda_1 + \Delta\lambda$.

Une carte de ces anomalies moyennes à l'air libre (anomalies 0°,25 x 0°,25) a été tracée (voir carte pliée jointe). On peut remarquer la mauvaise couverture dans le continent africain. Ces trous entrainent des erreurs, difficiles à estimer, pour le relief du géoide calculé. Les anomalies résiduelles dans ces trous sont remplacées par des zéros, c.a.d. on substitue aux anomalies à l'air libre les anomalies de référence (développement en harmoniques sphériques relation 31).

II.3.2. Anomalies de Bouguer

Pour le besoin des géophysiciens nous avons tracé une carte des anomalies de Bouguer sur l'île de Madagascar. Ces anomalies ont été extraites de la banque de données gravimétriques du B.G.I. puis interpolées sur des grilles de 0°,1 x 0°,1.

Nous rappelons que l'anomalie de Bouguer en un point est définie classiquement par la différence entre ce que serait la gravité, si on supprimait la topographie (altitude et relief) et remplaçait la station par sa projection au niveau de la mer et la valeur au point correspondant de la surface de l'ellipsoide. Elle est donnée par :

$$\Delta g_B = (g + C_P + C_T) - \gamma_o \qquad (47)$$

où g est la valeur observée de la pesanteur

C_P correction fonction de l'altitude de la station et de la densité des terrains

C_T Correction de relief qui tient compte des variations de la topographie autour de la station

γ_o valeur de la pesanteur théorique au point de l'ellipsoide de référence correspondant à la station.

Les anomalies de Bouguer que nous a fournies le B.G.I., ont été calculées dans le système de référence GRS 1967 (E_o) en prenant une densité d = 2,67 de la croûte. Les corrections de relief n'ont pas été faites.

Nous notons (pour une référence) qu'une carte des anomalies de Bouguer sur Madagascar a été publiée par l'O.R.S.T.O.M. en 1985 (Rechenmann, 1985).

Fig. 5. Anomalies de Bouguer

d = 2,67

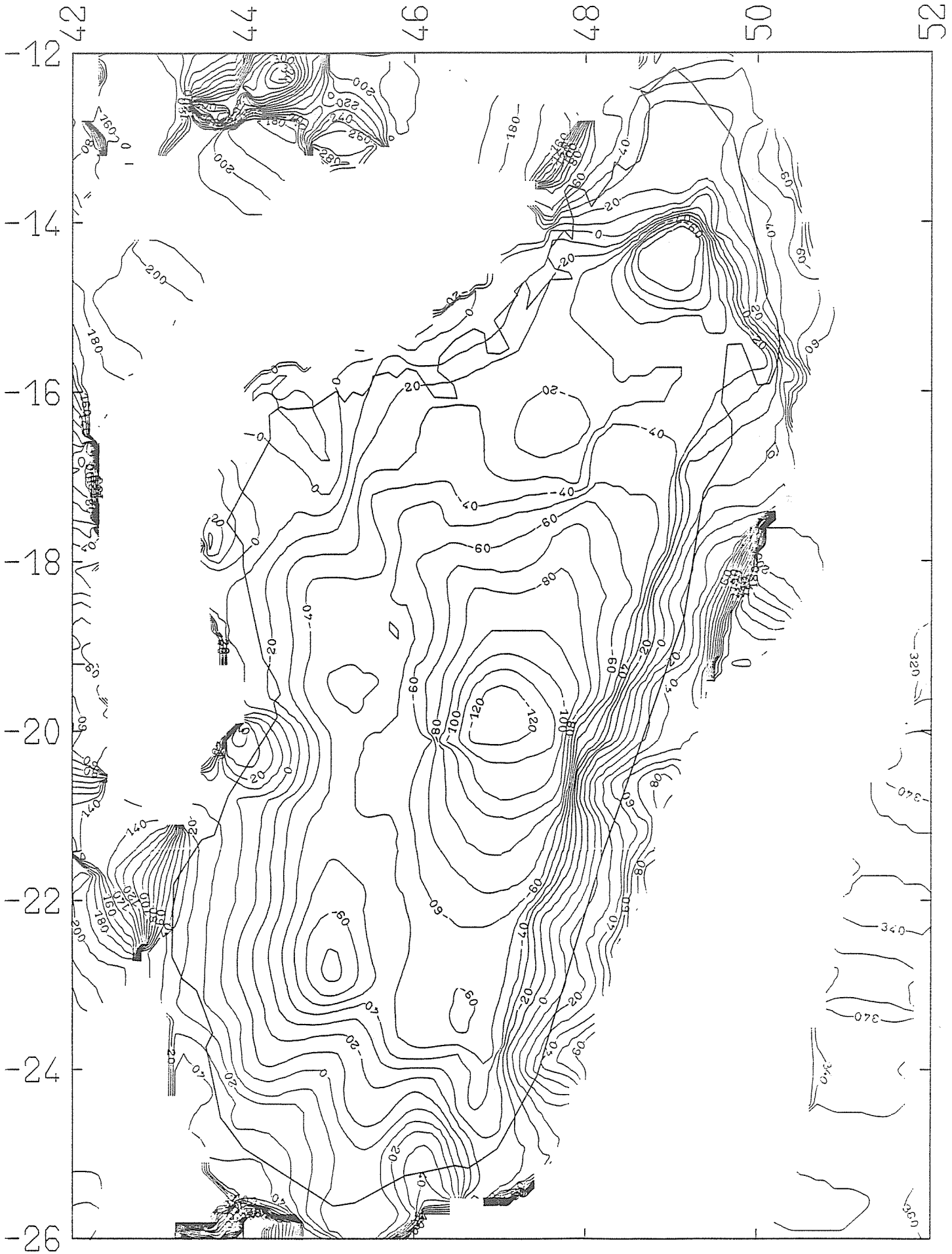

III. RESULTATS

III.1. Géoide de Référence $\hat{N}$ donné par la relation 30

La figure 6 montre les reliefs de ce géoide de référence sur Madagascar par rapport au système géodésique de référence 1980 (ellipsoide E). Ce géoide a été calculé sur des grilles de 15' x 15'. Le modèle en harmoniques sphériques (modèle de référence) que nous avons utilisé, était celui du Pr. Rapp (modèle Rapp 79) donné jsuqu'aux degré et ordre 180.

Fig. 6. Géoide Référence (Rapp 79)

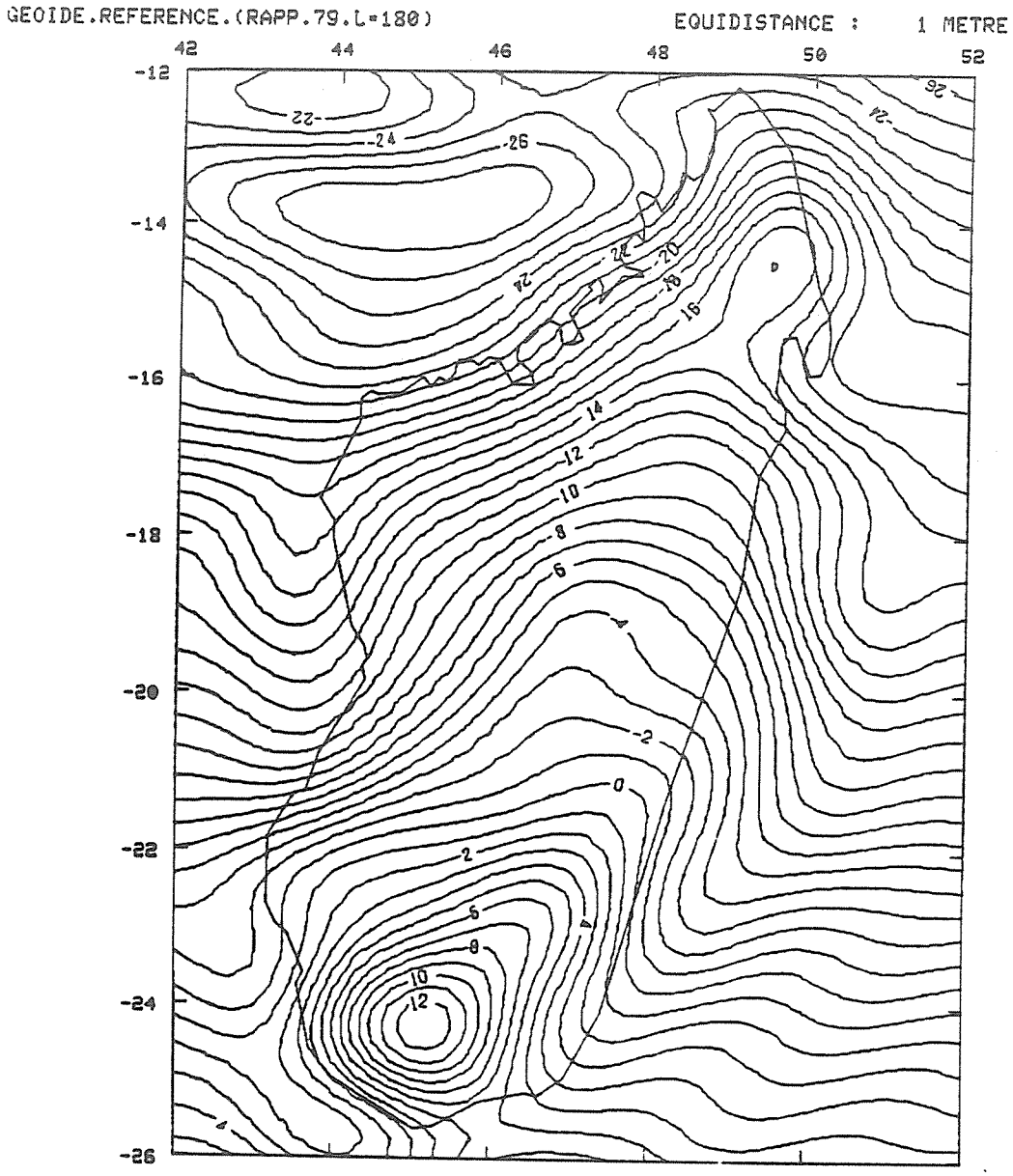

III.2. Géoide Gravimétrique

donné par $N = \bar{N} + \delta N$

δN est donné par la formule de Stokes tronquée et régularisée à l'origine :

$$\delta N = \frac{\bar{R}}{4\pi\bar{\gamma}} \iint_{\psi \leq \psi_{max}} \delta\Delta g_Q \, S^*(\psi) \, . \, d\sigma_Q$$

$S^*(\psi)$ est la fonction de Stokes régularisée.

Un géoide gravimétrique a été calculé sur des grilles de $0^{\circ}25 \times 0^{\circ}25$ par rapport au système géodésique de référence 1980 (ellipsoide E) sur l'île de Madagascar. L'intégrale de Stokes a été tronquée jusqu'à la distance géocentrique $\psi_{max} = 20^{\circ}$ autour du point de calcul. Les anomalies moyennes à l'air libre disponibles ont été calculées dans des grilles $15' \times 15'$ et par rapport à l'ellipsoide (E) 1980.

La figure 7 est la carte des courbes de niveau du géoide gravimétrique sur Madagascar, le modèle de référence utilisé était celui de Rapp 79.

Les tableaux 1 à 3 représentent les tables de valeurs des hauteurs de ce géoide. Les valeurs sont exprimées en mètre.

Fig. 7. Géoide gravimétrique (Modèle Rapp, 1979)

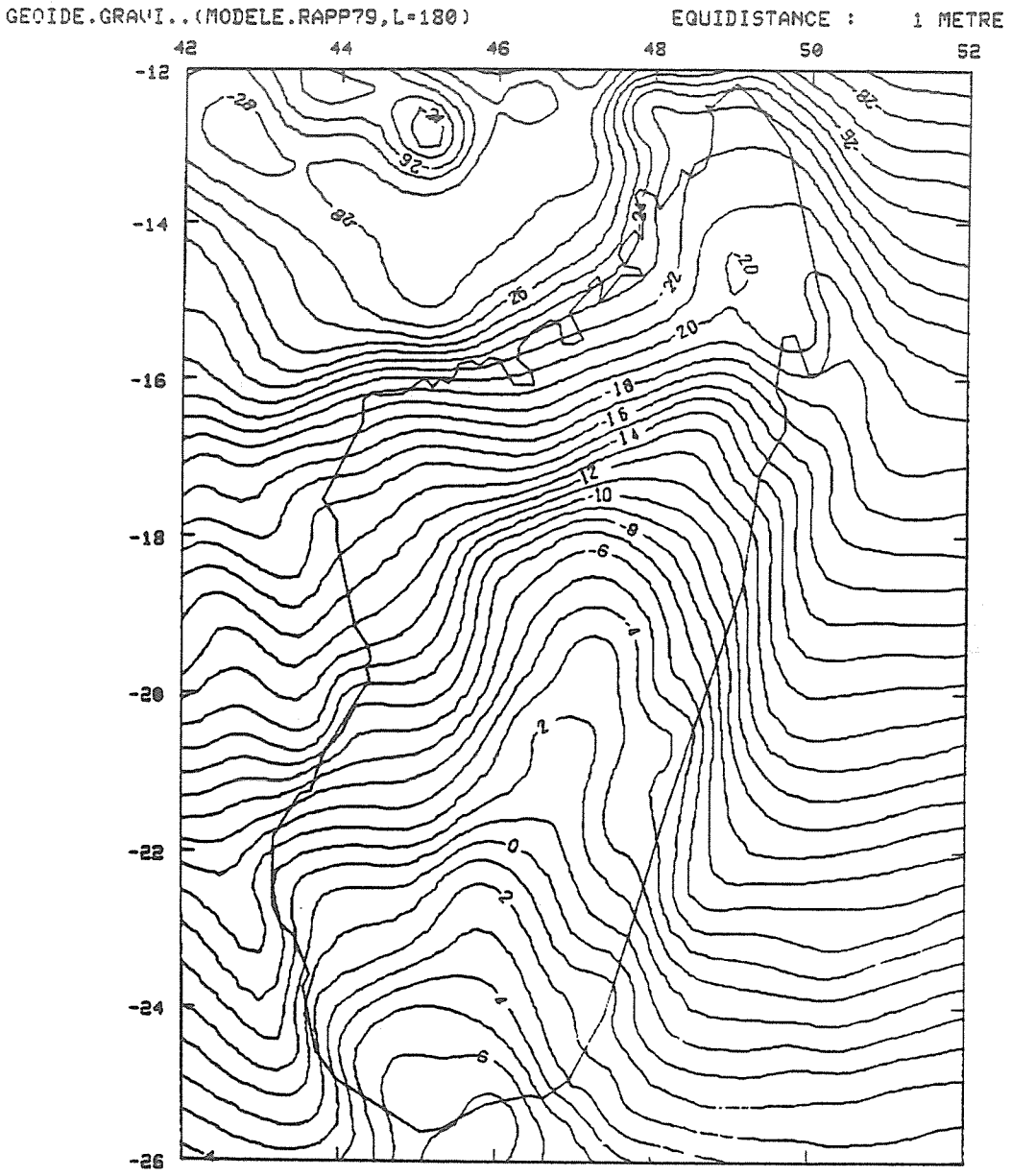

Tableau 1 : Hauteurs du géoide gravimétrique (Rapp 180)

FONCTION NGEO * 1.0E+00

	42	42	43	43	44	44	45
-12.00	-26.75 -27.06	-27.27 -27.05	-26.30 -25.46	-24.94 -24.90	-25.19 -25.40	-25.75 -26.52	-27.33
-12.25	-27.19 -27.55	-27.90 -27.68	-26.96 -25.89	-24.94 -24.51	-24.55 -24.72	-25.03 -25.30	-25.63
-12.50	-27.55 -27.97	-28.32 -28.25	-27.58 -26.46	-25.47 -25.11	-25.20 -25.41	-25.36 -24.58	-23.99
-12.75	-27.63 -28.11	-28.50 -28.51	-28.02 -27.19	-26.55 -26.44	-26.56 -26.59	-26.00 -24.54	-23.34
-13.00	-27.37 -27.88	-28.25 -28.39	-28.23 -27.84	-27.56 -27.58	-27.66 -27.48	-26.67 -25.23	-23.96
-13.25	-26.81 -27.33	-27.70 -28.02	-28.19 -28.10	-27.99 -28.06	-28.15 -28.00	-27.49 -26.60	-25.75
-13.50	-26.05 -26.59	-27.02 -27.49	-27.87 -27.93	-27.92 -28.08	-28.25 -28.28	-28.16 -27.84	-27.53
-13.75	-25.21 -25.76	-26.29 -26.79	-27.22 -27.47	-27.65 -27.92	-28.16 -28.28	-28.31 -28.27	-28.31
-14.00	-24.43 -24.95	-25.59 -26.11	-26.53 -26.92	-27.27 -27.62	-27.90 -28.05	-28.16 -28.32	-28.49
-14.25	-23.89 -24.31	-24.99 -25.54	-25.96 -26.39	-26.79 -27.21	-27.57 -27.80	-28.02 -28.30	-28.47
-14.50	-23.60 -23.85	-24.43 -25.05	-25.55 -25.99	-26.37 -26.77	-27.23 -27.63	-27.96 -28.24	-28.38
-14.75	-23.39 -23.47	-23.99 -24.71	-25.30 -25.76	-26.13 -26.43	-26.89 -27.47	-27.89 -28.14	-28.32
-15.00	-23.16 -23.16	-23.65 -24.40	-25.09 -25.62	-26.02 -26.23	-26.57 -27.19	-27.63 -27.90	-28.20
-15.25	-22.86 -22.92	-23.26 -23.95	-24.78 -25.42	-25.83 -26.04	-26.25 -26.65	-26.92 -27.22	-27.65
-15.50	-22.45 -22.62	-22.95 -23.56	-24.40 -25.08	-25.48 -25.64	-25.60 -25.50	-25.39 -25.53	-25.90
-15.75	-21.99 -22.23	-22.70 -23.31	-23.98 -24.53	-24.81 -24.67	-24.19 -23.55	-23.12 -23.11	-23.21
-16.00	-21.56 -21.73	-22.22 -22.84	-23.35 -23.63	-23.58 -22.97	-22.15 -21.43	-21.01 -20.91	-20.88
-16.25	-20.93 -20.97	-21.40 -21.99	-22.38 -22.32	-21.85 -21.04	-20.32 -19.86	-19.48 -19.24	-19.20
-16.50	-20.01 -19.90	-20.35 -20.87	-21.06 -20.74	-20.07 -19.50	-19.13 -18.74	-18.31 -17.92	-17.75
-16.75	-19.11 -18.76	-19.14 -19.56	-19.56 -19.14	-18.58 -18.36	-18.16 -17.75	-17.31 -16.79	-16.43
-17.00	-18.32 -17.82	-18.05 -18.36	-18.29 -17.85	-17.42 -17.24	-17.06 -16.76	-16.36 -15.78	-15.30
-17.25	-17.61 -17.16	-17.40 -17.68	-17.52 -17.00	-16.47 -16.12	-15.96 -15.80	-15.48 -14.96	-14.48
-17.50	-17.01 -16.67	-16.95 -17.21	-16.97 -16.42	-15.72 -15.23	-15.12 -15.02	-14.77 -14.35	-13.90
-17.75	-16.37 -16.06	-16.29 -16.57	-16.49 -16.08	-15.41 -14.85	-14.61 -14.47	-14.24 -13.87	-13.41
-18.00	-15.60 -15.25	-15.42 -15.84	-16.09 -15.93	-15.42 -14.79	-14.33 -14.08	-13.80 -13.42	-12.95
-18.25	-14.82 -14.43	-14.53 -15.04	-15.53 -15.67	-15.36 -14.65	-14.03 -13.69	-13.35 -12.96	-12.49
-18.50	-14.08 -13.64	-13.64 -14.17	-14.75 -15.11	-15.03 -14.33	-13.61 -13.25	-12.89 -12.50	-12.04
-18.75	-13.46 -13.04	-12.91 -13.30	-13.91 -14.40	-14.45 -13.88	-13.19 -12.78	-12.43 -12.05	-11.60
-19.00	-13.10 -12.68	-12.34 -12.52	-13.10 -13.65	-13.78 -13.31	-12.66 -12.25	-11.95 -11.60	-11.17
-19.25	-12.89 -12.36	-11.82 -11.86	-12.38 -12.94	-13.12 -12.66	-12.00 -11.64	-11.38 -11.08	-10.67
-19.50	-12.65 -12.06	-11.41 -11.33	-11.76 -12.30	-12.46 -11.97	-11.23 -10.79	-10.60 -10.39	-10.05
-19.75	-12.13 -11.57	-10.98 -10.85	-11.21 -11.70	-11.81 -11.28	-10.26 -9.60	-9.53 -9.50	-9.32
-20.00	-11.30 -10.89	-10.46 -10.34	-10.69 -11.13	-11.22 -10.76	-9.44 -8.44	-8.42 -8.53	-8.50
-20.25	-10.47 -10.29	-9.93 -9.76	-10.08 -10.51	-10.65 -10.33	-8.91 -7.65	-7.56 -7.67	-7.68
-20.50	-9.71 -9.69	-9.28 -9.02	-9.28 -9.76	-9.99 -9.68	-8.33 -7.08	-6.90 -6.93	-6.87
-20.75	-8.87 -8.87	-8.48 -8.19	-8.37 -8.79	-8.98 -8.37	-7.19 -6.42	-6.24 -6.18	-6.03
-21.00	-8.04 -7.99	-7.63 -7.33	-7.37 -7.58	-7.37 -6.52	-5.80 -5.54	-5.45 -5.38	-5.21
-21.25	-7.22 -7.13	-6.81 -6.42	-6.30 -6.34	-5.78 -5.02	-4.73 -4.62	-4.62 -4.62	-4.48
-21.50	-6.30 -6.26	-6.06 -5.63	-5.33 -5.05	-4.47 -3.96	-3.77 -3.73	-3.79 -3.85	-3.75
-21.75	-5.37 -5.43	-5.36 -5.00	-4.43 -3.78	-3.24 -2.93	-2.76 -2.73	-2.82 -2.89	-2.79
-22.00	-4.47 -4.65	-4.70 -4.34	-3.54 -2.73	-2.21 -1.88	-1.67 -1.62	-1.69 -1.75	-1.59
-22.25	-3.66 -3.98	-4.13 -3.77	-2.83 -1.90	-1.35 -.93	-.65 -.57	-.65 -.68	-.42
-22.50	-2.96 -3.40	-3.65 -3.49	-2.79 -1.70	-.80 -.26	.09 .20	.15 .16	.47
-22.75	-2.32 -2.82	-3.25 -3.45	-3.20 -1.94	-.56 .11	.54 .71	.72 .78	1.10
-23.00	-1.75 -2.24	-2.88 -3.35	-3.36 -2.40	-.81 .33	.84 1.06	1.15 1.30	1.65
-23.25	-1.25 -1.70	-2.41 -2.97	-3.09 -2.52	-.87 .63	1.17 1.44	1.64 1.93	2.36
-23.50	-.85 -1.26	-1.92 -2.48	-2.65 -2.13	-.45 1.11	1.66 2.01	2.40 2.84	3.30
-23.75	-.47 -.85	-1.40 -1.98	-2.34 -1.93	-.08 1.67	2.32 2.84	3.39 3.92	4.30
-24.00	.07 -.30	-.82 -1.40	-1.89 -1.63	.27 2.21	3.05 3.74	4.39 4.88	5.10
-24.25	.65 .28	-.27 -.81	-1.31 -1.27	.11 2.16	3.61 4.50	5.16 5.53	5.59
-24.50	1.17 .81	.25 -.28	-.77 -.91	-.14 1.90	3.91 4.95	5.60 5.89	5.90
-24.75	1.67 1.33	.84 .33	-.10 -.27	.13 1.56	3.63 5.13	5.82 6.11	6.17
-25.00	2.22 1.87	1.46 1.03	.70 .54	.68 1.40	3.03 4.88	5.90 6.27	6.38
-25.25	2.80 2.47	2.09 1.74	1.45 1.26	1.30 1.73	2.84 4.47	5.77 6.35	6.54
-25.50	3.38 3.08	2.71 2.42	2.15 1.91	1.88 2.16	2.95 4.18	5.36 6.24	6.70
-25.75	3.91 3.63	3.32 3.08	2.85 2.66	2.65 2.88	3.33 4.06	5.05 6.10	6.84
-26.00	4.41 4.19	4.04 3.82	3.59 3.49	3.52 3.68	3.91 4.31	5.12 6.13	6.90
	42 *****	*****	*****	*****	*****	*****	*****

Tableau 2 : Hauteurs du géoide grvimétrique (Rapp 180)

FONCTION NGEO * 1.0E+00

	45	45	46	46	47	47	48
-12.00	-27.33 -28.02 -28.65 -29.13 -29.27 -29.04 -28.82	-29.14 -29.74 -29.65 -28.47 -26.96 -26.40					
-12.25	-25.63 -26.47 -27.48 -28.25 -28.32 -27.68 -27.42	-28.15 -29.02 -28.80 -26.95 -24.70 -23.96					
-12.50	-23.99 -24.75 -25.28 -27.60 -27.98 -27.43 -27.27	-27.99 -28.57 -27.91 -25.78 -23.54 -22.84					
-12.75	-23.34 -23.70 -25.50 -27.35 -28.20 -28.17 -28.12	-28.49 -28.63 -27.71 -25.76 -23.86 -23.07					
-13.00	-23.96 -24.02 -25.76 -27.64 -28.48 -28.66 -28.66	-28.80 -28.77 -27.96 -26.45 -24.89 -23.72					
-13.25	-25.75 -25.77 -26.97 -28.23 -28.66 -28.65 -28.60	-28.67 -28.68 -28.08 -26.87 -25.35 -23.73					
-13.50	-27.53 -27.59 -27.99 -28.42 -28.57 -28.48 -28.33	-28.28 -28.27 -27.84 -26.67 -25.01 -23.29					
-13.75	-28.31 -28.42 -28.40 -28.35 -28.35 -28.28 -28.08	-27.84 -27.68 -27.30 -26.19 -24.51 -23.03					
-14.00	-28.49 -28.56 -28.47 -28.32 -28.23 -28.11 -27.85	-27.50 -27.21 -26.81 -25.86 -24.34 -23.04					
-14.25	-28.47 -28.45 -28.34 -28.21 -28.07 -27.89 -27.57	-27.18 -26.80 -26.30 -25.34 -24.16 -23.20					
-14.50	-28.38 -28.34 -28.20 -28.04 -27.83 -27.54 -27.12	-26.58 -26.07 -25.48 -24.56 -23.71 -23.09					
-14.75	-28.32 -28.28 -28.05 -27.74 -27.34 -26.91 -26.35	-25.59 -24.93 -24.35 -23.69 -23.16 -22.69					
-15.00	-28.20 -28.20 -27.80 -27.18 -26.46 -25.85 -25.22	-24.37 -23.68 -23.23 -22.82 -22.49 -22.09					
-15.25	-27.65 -27.65 -27.06 -26.18 -25.23 -24.46 -23.82	-23.12 -22.61 -22.29 -22.00 -21.70 -21.32					
-15.50	-25.90 -25.89 -25.38 -24.65 -23.75 -23.01 -22.49	-22.06 -21.72 -21.40 -21.08 -20.76 -20.38					
-15.75	-23.21 -23.19 -23.04 -22.77 -22.28 -21.82 -21.49	-21.17 -20.81 -20.40 -20.00 -19.65 -19.26					
-16.00	-20.88 -20.94 -21.02 -21.05 -20.99 -20.83 -20.58	-20.24 -19.78 -19.25 -18.76 -18.36 -17.93					
-16.25	-19.20 -19.33 -19.51 -19.64 -19.73 -19.73 -19.57	-19.19 -18.63 -18.00 -17.42 -16.93 -16.37					
-16.50	-17.75 -17.85 -18.05 -18.22 -18.38 -18.49 -18.40	-18.00 -17.37 -16.65 -15.95 -15.35 -14.66					
-16.75	-16.43 -16.43 -16.62 -16.81 -17.00 -17.17 -17.10	-16.66 -15.95 -15.10 -14.29 -13.67 -13.07					
-17.00	-15.30 -15.20 -15.36 -15.53 -15.70 -15.83 -15.68	-15.14 -14.33 -13.38 -12.59 -12.16 -11.88					
-17.25	-14.48 -14.30 -14.34 -14.41 -14.46 -14.42 -14.03	-13.33 -12.49 -11.64 -11.10 -10.99 -11.02					
-17.50	-13.90 -13.60 -13.43 -13.30 -13.12 -12.72 -12.01	-11.17 -10.40 -9.86 -9.75 -9.95 -10.17					
-17.75	-13.41 -12.95 -12.48 -12.01 -11.44 -10.71 -9.88	-9.02 -8.32 -8.02 -8.24 -8.74 -9.17					
-18.00	-12.95 -12.34 -11.49 -10.48 -9.57 -8.86 -8.18	-7.42 -6.76 -6.53 -6.82 -7.43 -8.06					
-18.25	-12.49 -11.80 -10.67 -9.22 -8.14 -7.52 -7.00	-6.39 -5.83 -5.61 -5.82 -6.37 -7.09					
-18.50	-12.04 -11.34 -10.15 -8.56 -7.32 -6.66 -6.16	-5.65 -5.19 -4.98 -5.13 -5.59 -6.33					
-18.75	-11.60 -10.94 -9.84 -8.26 -6.88 -6.10 -5.55	-5.01 -4.54 -4.33 -4.46 -4.93 -5.71					
-19.00	-11.17 -10.54 -9.57 -8.11 -6.67 -5.74 -5.05	-4.38 -3.84 -3.62 -3.78 -4.32 -5.21					
-19.25	-10.67 -10.08 -9.20 -7.89 -6.49 -5.45 -4.63	-3.83 -3.22 -2.98 -3.17 -3.80 -4.89					
-19.50	-10.05 -9.52 -8.71 -7.52 -6.19 -5.13 -4.25	-3.43 -2.84 -2.60 -2.77 -3.53 -4.84					
-19.75	-9.32 -8.91 -8.22 -7.15 -5.83 -4.68 -3.82	-3.12 -2.63 -2.45 -2.64 -3.56 -4.95					
-20.00	-8.50 -8.22 -7.64 -6.65 -5.27 -3.96 -3.15	-2.68 -2.39 -2.34 -2.64 -3.61 -4.75					
-20.25	-7.68 -7.44 -6.85 -5.82 -4.42 -3.14 -2.41	-2.12 -2.02 -2.12 -2.55 -3.38 -4.15					
-20.50	-6.87 -6.58 -5.93 -4.87 -3.62 -2.61 -2.01	-1.71 -1.64 -1.87 -2.44 -3.20 -3.69					
-20.75	-6.03 -5.68 -5.02 -4.09 -3.16 -2.46 -1.97	-1.60 -1.49 -1.83 -2.60 -3.38 -3.74					
-21.00	-5.21 -4.83 -4.20 -3.45 -2.81 -2.34 -1.93	-1.56 -1.52 -2.04 -2.94 -3.68 -3.95					
-21.25	-4.48 -4.10 -3.47 -2.76 -2.24 -1.90 -1.61	-1.38 -1.52 -2.25 -3.21 -3.82 -4.00					
-21.50	-3.75 -3.36 -2.65 -1.89 -1.42 -1.25 -1.14	-1.11 -1.48 -2.40 -3.35 -3.82 -3.95					
-21.75	-2.79 -2.31 -1.46 -.67 -.41 -.50 -.65	-.85 -1.41 -2.43 -3.26 -3.59 -3.78					
-22.00	-1.59 -.97 -.03 .64 .65 .28 -.13	-.57 -1.26 -2.21 -2.86 -3.13 -3.46					
-22.25	-.42 .26 1.14 1.65 1.53 1.02 .39	-.24 -1.01 -1.83 -2.34 -2.64 -3.37					
-22.50	.47 1.13 1.90 2.32 2.18 1.62 .88	.10 -.72 -1.45 -1.91 -2.25 -3.30					
-22.75	1.10 1.71 2.37 2.74 2.63 2.10 1.31	.43 -.39 -1.04 -1.44 -1.83 -2.91					
-23.00	1.65 2.21 2.76 3.04 2.95 2.50 1.70	.76 -.01 -.51 -.82 -1.23 -2.38					
-23.25	2.36 2.84 3.23 3.39 3.28 2.88 2.11	1.16 .49 .19 -.04 -.70 -1.96					
-23.50	3.30 3.65 3.83 3.84 3.66 3.23 2.49	1.63 1.11 .97 .78 -.19 -1.52					
-23.75	4.30 4.46 4.44 4.31 4.05 3.53 2.81	2.09 1.71 1.57 1.31 .28 -.99					
-24.00	5.10 5.07 4.93 4.76 4.45 3.86 3.11	2.45 2.02 1.74 1.20 .20 -.74					
-24.25	5.59 5.47 5.34 5.22 4.92 4.30 3.45	2.66 2.10 1.70 1.06 .21 -.52					
-24.50	5.90 5.81 5.76 5.76 5.54 4.88 3.87	2.89 2.20 1.78 1.40 .73 -.05					
-24.75	6.17 6.14 6.19 6.33 6.23 5.57 4.43	3.27 2.50 2.19 1.92 1.24 .53					
-25.00	6.38 6.41 6.54 6.80 6.84 6.26 5.08	3.84 3.01 2.67 2.26 1.58 1.07					
-25.25	6.54 6.63 6.79 7.10 7.31 6.89 5.69	4.65 4.02 3.26 2.47 1.87 1.54					
-25.50	6.70 6.85 6.99 7.31 7.57 7.24 6.26	5.47 4.91 3.96 2.98 2.39 2.16					
-25.75	6.84 7.10 7.26 7.54 7.59 7.13 6.40	5.76 5.21 4.52 3.75 3.23 3.01					
-26.00	6.90 7.25 7.49 7.65 7.38 6.76 6.19	5.83 5.52 5.10 4.56 4.08 3.76					
	45 *****	***** *****	*****	*****	*****	*****	*****

Tableau 3 : Hauteurs du géoide gravimétrique (Rapp. 180)

FONCTION NGLO * 1.0E+00

	48		48		49		49		50		50		51		51		52	
-12.00	-26.40	-26.58	-26.59	-26.29	-25.73	-25.41	-25.98	-27.01	-27.74	-28.17	-28.62	-29.12	-29.49	-29.63	-29.64	-29.65	-29.67	
-12.25	-23.96	-24.29	-24.45	-24.29	-23.91	-23.81	-24.55	-25.72	-26.68	-27.36	-27.93	-28.47	-28.84	-28.98	-29.03	-29.12	-29.17	
-12.50	-22.84	-23.05	-23.12	-23.02	-22.88	-22.93	-23.42	-24.35	-25.45	-26.45	-27.22	-27.82	-28.19	-28.33	-28.40	-28.48	-28.57	
-12.75	-23.07	-22.77	-22.55	-22.49	-22.38	-22.38	-22.59	-23.18	-24.20	-25.47	-26.54	-27.20	-27.54	-27.70	-27.76	-27.78	-27.90	
-13.00	-23.72	-22.74	-22.19	-22.11	-22.02	-21.99	-22.07	-22.37	-23.18	-24.56	-25.83	-26.54	-26.89	-27.07	-27.10	-27.09	-27.21	
-13.25	-23.73	-22.49	-21.96	-21.81	-21.70	-21.65	-21.63	-21.74	-22.42	-23.73	-25.02	-25.84	-26.25	-26.40	-26.41	-26.44	-26.59	
-13.50	-23.29	-22.21	-21.84	-21.61	-21.43	-21.37	-21.31	-21.29	-21.72	-22.83	-24.18	-25.12	-25.58	-25.72	-25.75	-25.83	-26.00	
-13.75	-23.03	-22.19	-21.75	-21.41	-21.11	-21.03	-21.02	-20.96	-21.13	-22.03	-23.37	-24.36	-24.90	-25.13	-25.20	-25.27	-25.42	
-14.00	-23.04	-22.24	-21.54	-20.96	-20.57	-20.56	-20.71	-20.67	-20.72	-21.40	-22.58	-23.58	-24.25	-24.62	-24.76	-24.80	-24.91	
-14.25	-23.20	-22.31	-21.29	-20.43	-20.06	-20.19	-20.47	-20.45	-20.36	-20.81	-21.83	-22.85	-23.62	-24.10	-24.32	-24.40	-24.49	
-14.50	-23.09	-22.27	-21.17	-20.23	-19.85	-20.02	-20.33	-20.29	-20.07	-20.33	-21.20	-22.21	-23.01	-23.55	-23.82	-23.95	-24.08	
-14.75	-22.69	-22.03	-21.13	-20.31	-19.90	-20.02	-20.33	-20.23	-19.87	-19.87	-20.57	-21.60	-22.43	-22.96	-23.24	-23.40	-23.55	
-15.00	-22.09	-21.54	-20.89	-20.32	-20.02	-20.21	-20.59	-20.47	-19.90	-19.53	-20.04	-21.10	-21.92	-22.39	-22.60	-22.75	-22.94	
-15.25	-21.32	-20.82	-20.31	-19.93	-19.81	-20.20	-20.72	-20.72	-20.17	-19.52	-19.78	-20.73	-21.42	-21.81	-21.99	-22.14	-22.32	
-15.50	-20.38	-19.88	-19.41	-19.10	-19.07	-19.55	-20.20	-20.44	-20.20	-19.56	-19.46	-20.15	-20.81	-21.22	-21.45	-21.60	-21.77	
-15.75	-19.26	-18.73	-18.22	-17.92	-17.92	-18.43	-19.19	-19.66	-19.68	-19.24	-18.95	-19.45	-20.24	-20.72	-20.99	-21.16	-21.30	
-16.00	-17.93	-17.26	-16.66	-16.45	-16.61	-17.25	-18.11	-18.70	-18.89	-18.62	-18.49	-19.11	-19.87	-20.33	-20.60	-20.78	-20.89	
-16.25	-16.37	-15.52	-14.89	-14.88	-15.33	-16.23	-17.20	-17.83	-18.14	-18.12	-18.34	-19.08	-19.70	-20.05	-20.23	-20.37	-20.46	
-16.50	-14.66	-13.85	-13.42	-13.57	-14.31	-15.48	-16.49	-17.10	-17.50	-17.74	-18.27	-19.06	-19.58	-19.84	-19.90	-19.93	-19.98	
-16.75	-13.07	-12.56	-12.42	-12.75	-13.70	-14.94	-15.84	-16.43	-16.92	-17.34	-18.05	-18.89	-19.40	-19.60	-19.59	-19.53	-19.54	
-17.00	-11.88	-11.69	-11.79	-12.32	-13.33	-14.39	-15.13	-15.74	-16.28	-16.91	-17.83	-18.68	-19.15	-19.30	-19.26	-19.16	-19.14	
-17.25	-11.02	-11.06	-11.31	-11.94	-12.88	-13.72	-14.31	-14.94	-15.76	-16.78	-17.79	-18.50	-18.85	-18.94	-18.90	-18.82	-18.75	
-17.50	-10.17	-10.37	-10.71	-11.36	-12.21	-12.95	-13.57	-14.44	-15.72	-16.94	-17.74	-18.21	-18.45	-18.52	-18.50	-18.44	-18.32	
-17.75	-9.17	-9.51	-9.96	-10.63	-11.44	-12.20	-13.13	-14.45	-15.89	-16.93	-17.44	-17.74	-17.92	-18.01	-18.00	-17.94	-17.83	
-18.00	-8.06	-8.63	-9.24	-10.01	-10.83	-11.66	-12.92	-14.55	-15.91	-16.72	-17.09	-17.26	-17.37	-17.44	-17.43	-17.42	-17.41	
-18.25	-7.09	-7.88	-8.75	-9.66	-10.48	-11.37	-12.83	-14.56	-15.76	-16.42	-16.71	-16.79	-16.83	-16.88	-16.85	-16.89	-16.98	
-18.50	-6.33	-7.28	-8.36	-9.39	-10.26	-11.35	-12.93	-14.48	-15.49	-16.01	-16.24	-16.30	-16.31	-16.34	-16.31	-16.31	-16.35	
-18.75	-5.71	-6.76	-7.92	-9.00	-9.96	-11.29	-12.98	-14.35	-15.18	-15.57	-15.71	-15.75	-15.78	-15.81	-15.81	-15.77	-15.70	
-19.00	-5.21	-6.33	-7.47	-8.48	-9.50	-11.06	-12.91	-14.20	-14.90	-15.16	-15.19	-15.16	-15.18	-15.22	-15.25	-15.23	-15.16	
-19.25	-4.89	-6.12	-7.11	-7.97	-9.26	-11.12	-12.87	-13.98	-14.52	-14.71	-14.69	-14.60	-14.56	-14.58	-14.62	-14.65	-14.60	
-19.50	-4.84	-6.06	-6.82	-7.57	-9.15	-11.19	-12.70	-13.63	-14.02	-14.13	-14.11	-14.00	-13.94	-13.94	-13.96	-14.00	-13.94	
-19.75	-4.95	-5.91	-6.48	-7.24	-8.94	-11.01	-12.41	-13.18	-13.49	-13.55	-13.52	-13.45	-13.36	-13.29	-13.31	-13.34	-13.23	
-20.00	-4.75	-5.38	-5.91	-7.06	-9.01	-10.93	-12.14	-12.78	-13.05	-13.04	-12.97	-12.93	-12.84	-12.73	-12.73	-12.72	-12.59	
-20.25	-4.15	-4.56	-5.14	-6.81	-9.09	-10.81	-11.90	-12.45	-12.67	-12.62	-12.47	-12.39	-12.33	-12.27	-12.22	-12.12	-11.99	
-20.50	-3.69	-3.97	-4.58	-6.49	-8.90	-10.49	-11.46	-11.98	-12.19	-12.16	-12.06	-11.95	-11.82	-11.74	-11.68	-11.52	-11.34	
-20.75	-3.74	-3.94	-4.79	-6.67	-8.66	-9.99	-10.82	-11.29	-11.51	-11.54	-11.54	-11.46	-11.25	-11.10	-11.03	-10.84	-10.60	
-21.00	-3.95	-4.14	-5.22	-6.95	-8.40	-9.48	-10.18	-10.61	-10.82	-10.85	-10.84	-10.77	-10.61	-10.43	-10.28	-10.09	-9.89	
-21.25	-4.00	-4.21	-5.32	-6.97	-8.18	-9.01	-9.59	-9.99	-10.21	-10.23	-10.16	-10.07	-9.91	-9.68	-9.44	-9.33	-9.24	
-21.50	-3.95	-4.37	-5.59	-7.04	-8.04	-8.64	-9.04	-9.36	-9.57	-9.58	-9.47	-9.33	-9.13	-8.86	-8.64	-8.55	-8.50	
-21.75	-3.78	-4.54	-5.86	-7.04	-7.86	-8.34	-8.59	-8.75	-8.85	-8.83	-8.69	-8.54	-8.37	-8.14	-7.94	-7.80	-7.72	
-22.00	-3.46	-4.53	-5.97	-6.98	-7.64	-7.97	-8.10	-8.13	-8.13	-8.07	-7.93	-7.80	-7.65	-7.45	-7.28	-7.14	-7.04	
-22.25	-3.37	-4.77	-6.09	-6.93	-7.35	-7.42	-7.43	-7.43	-7.35	-7.27	-7.17	-7.07	-6.95	-6.79	-6.68	-6.54	-6.37	
-22.50	-3.30	-4.86	-6.02	-6.61	-6.71	-6.60	-6.58	-6.60	-6.54	-6.47	-6.43	-6.39	-6.34	-6.26	-6.11	-5.86	-5.58	
-22.75	-2.91	-4.47	-5.56	-5.92	-5.82	-5.72	-5.74	-5.82	-5.85	-5.83	-5.85	-5.85	-5.82	-5.72	-5.47	-5.13	-4.80	
-23.00	-2.38	-3.90	-4.83	-5.08	-5.02	-5.01	-5.08	-5.21	-5.32	-5.39	-5.43	-5.36	-5.22	-5.02	-4.72	-4.37	-4.09	
-23.25	-1.96	-3.21	-3.96	-4.22	-4.29	-4.36	-4.48	-4.66	-4.85	-4.98	-4.93	-4.68	-4.40	-4.15	-3.87	-3.57	-3.37	
-23.50	-1.52	-2.46	-3.10	-3.40	-3.54	-3.65	-3.80	-4.01	-4.24	-4.34	-4.18	-3.83	-3.52	-3.28	-3.04	-2.80	-2.64	
-23.75	-.99	-1.83	-2.46	-2.74	-2.85	-2.96	-3.09	-3.22	-3.37	-3.42	-3.29	-3.04	-2.79	-2.57	-2.32	-2.09	-1.91	
-24.00	-.74	-1.44	-1.98	-2.19	-2.23	-2.31	-2.41	-2.46	-2.50	-2.56	-2.54	-2.37	-2.14	-1.93	-1.67	-1.41	-1.23	
-24.25	-.52	-1.10	-1.51	-1.67	-1.69	-1.72	-1.70	-1.67	-1.78	-1.91	-1.87	-1.67	-1.43	-1.22	-1.01	-.78	-.59	
-24.50	-.05	-.58	-.90	-1.01	-1.06	-1.10	-.96	-.83	-.97	-1.15	-1.07	-.86	-.62	-.41	-.28	-.12	.04	
-24.75	.53	.10	-.16	-.25	-.31	-.37	-.25	-.10	-.12	-.21	-.21	-.05	.20	.38	.44	.54	.65	
-25.00	1.07	.77	.54	.38	.31	.31	.39	.47	.55	.57	.52	.63	.86	.97	1.04	1.13	1.16	
-25.25	1.54	1.36	1.13	.95	.92	.95	.98	1.00	1.05	1.09	1.10	1.18	1.31	1.38	1.50	1.59	1.60	
-25.50	2.16	2.02	1.80	1.63	1.59	1.57	1.56	1.58	1.56	1.52	1.55	1.62	1.66	1.73	1.85	1.94	2.00	
-25.75	3.01	2.81	2.59	2.42	2.28	2.18	2.16	2.16	2.08	1.97	1.96	2.01	2.02	2.09	2.19	2.27	2.35	
-26.00	3.76	3.55	3.38	3.22	3.03	2.86	2.78	2.70	2.56	2.44	2.42	2.45	2.46	2.53	2.63	2.68	2.70	
	48	*****		*****		*****		*****		*****		*****		*****		*****		

La différence entre ce géoide gravimétrique et le géoide de référence, c.a.d. le géoide résiduel, est représentée sous forme de carte sur la figure 8. La figure 9 montre l'histogramme des fréquences de ce géoide résiduel.

Fig. 8.

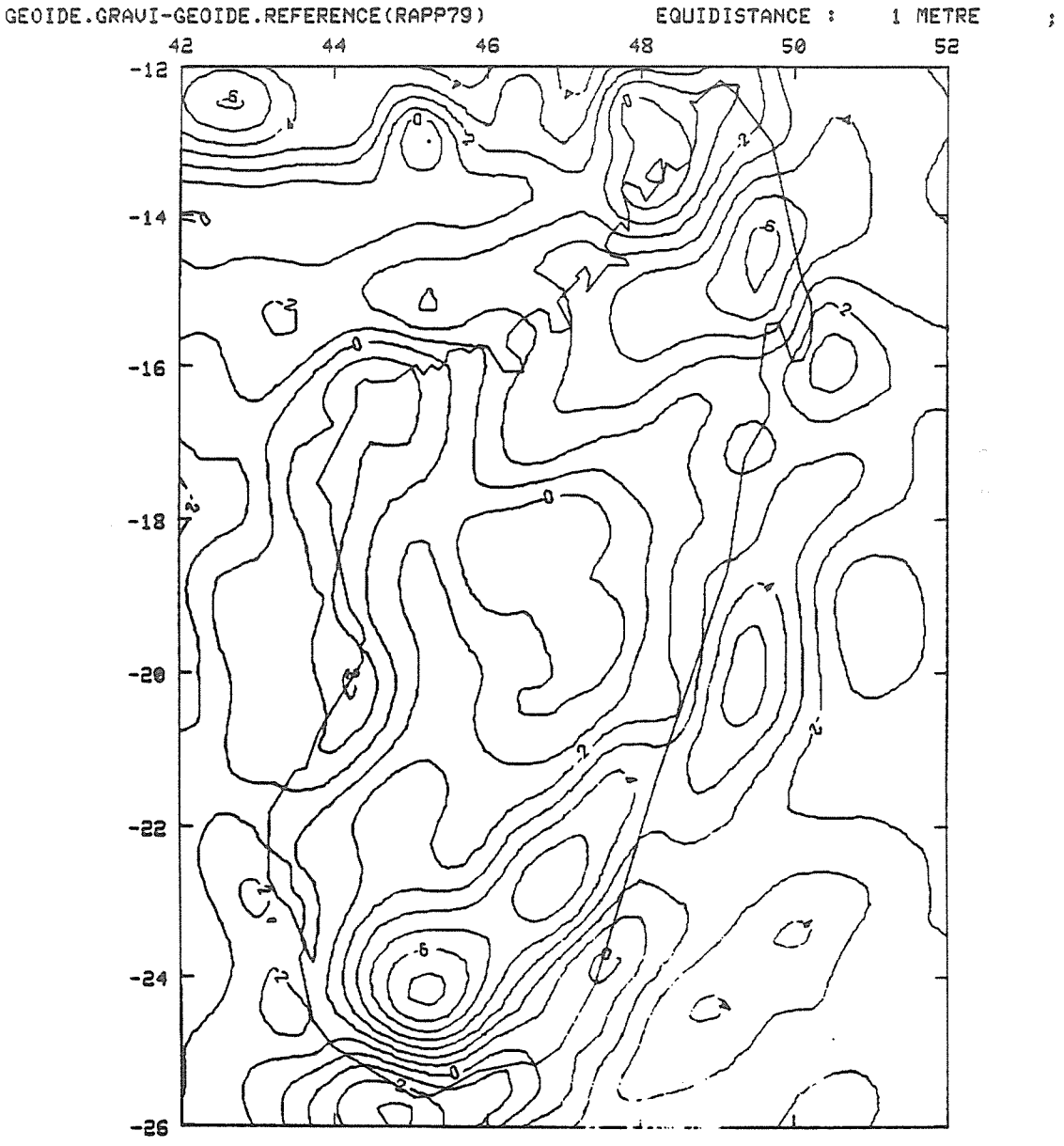

Fig. 9. Géoide gravimétrique - géoide de référence (Rapp 79)

Val. Min. = - 7.376 mètres
Val. Max. = 3.224 mètres
Moy. = - 1.892 mètres
RMS = 2.529 mètres

HISTOGRAMME DES FREQUENCES 2337 POINTS 30 CLASSES

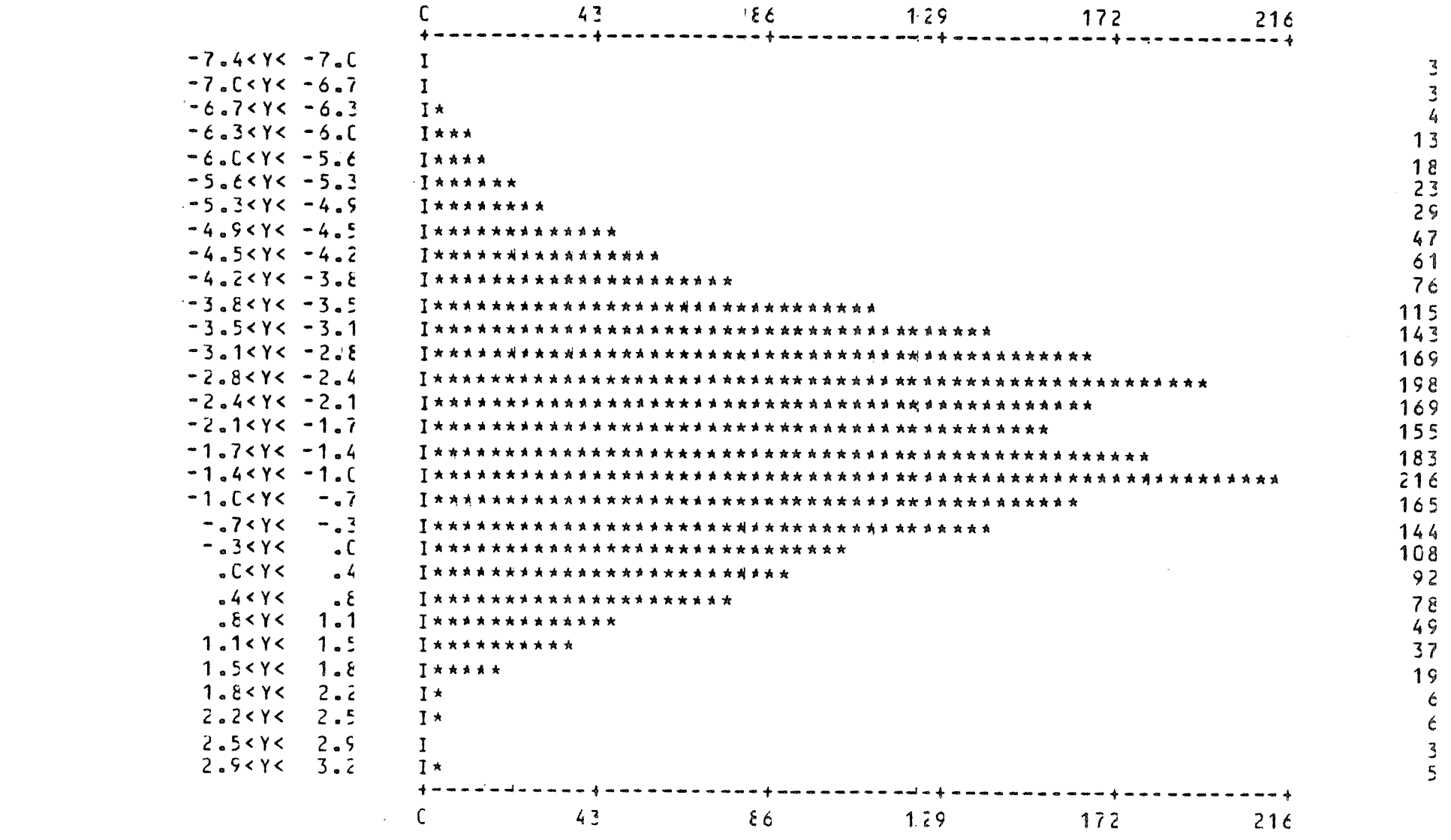

III.3. Déviation de la Verticale

Les composantes ξ et η de la déviation de la verticale sont données par les relations 22 et 23.

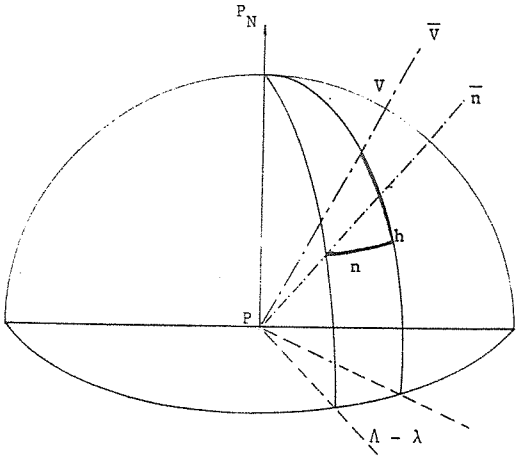

Ces composantes ξ et η ont été calculées, sur les noeuds des grilles 15' x 15', en transformant les hauteurs du géoide gravimétrique (§ III.2), qu'on a obtenues, par des dérivations numériques après ajustement d'une fonction polynomiale de degré n (ici n = 3 ou 5) le long d'un profil en utilisant les formules de Lagrange.

Fig. 10. Déviation de la verticale représentée sur la sphère unité centrale au point P

Les valeurs calculées en chaque point du noeud des grilles 15' x 15' de ξ et η sont résumées dans les tableaux 4 à 9. Ces valeurs sont exprimées en seconde d'arc.

Les contours par seconde d'arc de ces composantes sont représentées sur la figure 12 et 13.

La figure 14 représente la déviation de la verticale (arc nv) en chaque point et projetée sur chaque plan tangent à chaque sphère locale unité en n (fig. 11). En effet, il est plus simple de voir la déviation de la verticale en considérant une sphère de rayon unité centrée en P (fig. 10). La normale en P la coupe en n et la verticale en P la coupe en v, et on a :

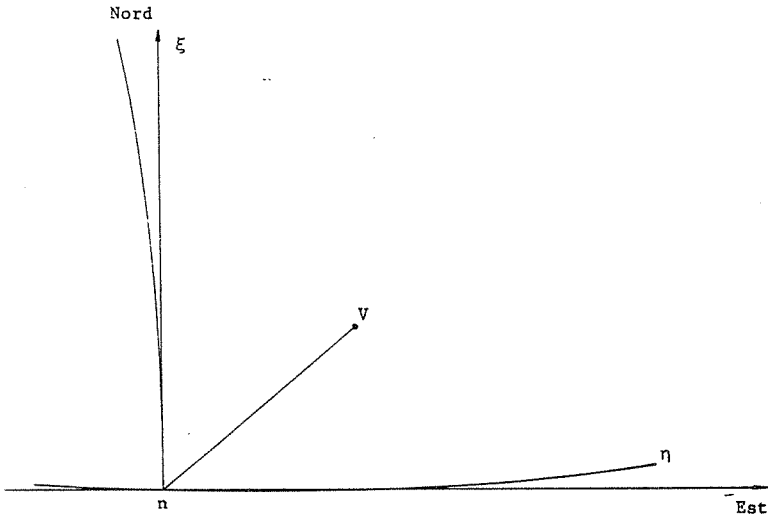

$\xi = vh$

$\eta = nh$

h étant l'intersection du parallèle de n avec le plan méridien astronomique en P

Fig. 11. Déviation de la verticale dans le plan tangent en n à la sphère locale unité.

Tableau 4 : Composante ξ (en seconde d'arc)

FONCTION VKSI * 1.0E+00

	42		42		43		43		44		44		45
-12.00	-3.50	-3.83	-4.04	-4.83	-5.02	-2.63	2.03	6.62	9.51	10.15	9.26	10.87	12.81
-12.25	-2.96	-3.36	-3.88	-4.47	-4.74	-3.70	-1.96	-.80	-.03	-.05	1.43	7.19	12.42
-12.50	-1.66	-2.10	-2.59	-3.09	-3.93	-4.82	-5.98	-7.18	-7.46	-6.94	-3.60	2.81	8.53
-12.75	.67	.34	.23	-.50	-2.39	-5.13	-7.74	-9.14	-9.12	-7.66	-4.85	-2.40	.10
-13.00	3.06	2.92	2.98	1.81	-.64	-3.38	-5.35	-6.00	-5.89	-5.23	-5.52	-7.61	-8.94
-13.25	4.89	4.77	4.59	3.34	1.31	-.31	-1.36	-1.88	-2.19	-2.98	-5.53	-9.69	-13.25
-13.50	5.95	5.81	5.22	4.57	3.61	2.36	1.24	.51	-.03	-1.03	-3.06	-6.22	-9.52
-13.75	6.00	6.10	5.30	5.11	4.98	3.73	2.44	1.74	1.28	.86	.00	-1.78	-3.54
-14.00	4.88	5.37	4.82	4.63	4.66	3.98	3.19	2.66	2.17	1.77	1.08	-.09	-.56
-14.25	3.10	4.08	4.28	3.92	3.64	3.46	3.34	3.14	2.50	1.56	.76	.32	.40
-14.50	1.84	3.12	3.70	3.08	2.46	2.33	2.44	2.86	2.54	1.23	.48	.57	.55
-14.75	1.64	2.54	2.92	2.43	1.71	1.36	1.30	2.00	2.46	1.64	1.22	1.24	.67
-15.00	1.98	2.05	2.70	2.82	1.93	1.27	1.11	1.48	2.35	3.05	3.59	3.43	2.49
-15.25	2.62	2.02	2.60	3.09	2.57	2.02	1.99	2.21	3.60	6.26	8.30	8.82	8.52
-15.50	3.25	2.54	2.09	2.39	2.98	3.32	3.81	5.08	7.64	11.51	14.12	15.26	16.44
-15.75	3.29	3.29	2.71	2.70	3.88	5.36	7.04	9.90	12.79	15.10	16.26	17.12	18.62
-16.00	3.90	4.67	4.85	4.90	5.93	8.17	10.97	13.46	14.38	13.70	13.49	14.34	14.90
-16.25	5.77	6.80	6.91	7.29	8.50	10.72	13.03	12.85	11.22	10.00	10.02	11.08	11.62
-16.50	6.77	8.23	8.37	8.99	10.46	11.82	12.13	9.93	7.99	7.81	8.07	9.09	10.27
-16.75	6.25	7.74	8.54	9.30	10.26	10.72	9.83	8.39	7.67	7.34	7.24	7.95	9.11
-17.00	5.56	5.92	6.45	6.98	7.57	7.93	7.86	8.34	8.18	7.23	6.78	6.80	7.24
-17.25	4.89	4.24	4.09	4.29	4.91	5.30	6.33	7.46	7.18	6.46	5.90	5.33	5.18
-17.50	4.60	4.07	4.13	4.13	3.80	3.42	3.90	4.68	5.00	4.93	4.59	4.04	3.95
-17.75	5.21	5.29	5.66	5.06	3.26	1.82	1.09	1.63	2.94	3.47	3.60	3.44	3.54
-18.00	5.77	6.07	6.52	5.66	3.58	1.52	.22	.76	2.16	2.91	3.32	3.36	3.41
-18.25	5.66	5.96	6.60	6.23	4.96	3.03	1.44	1.73	2.66	3.10	3.38	3.42	3.37
-18.50	5.03	5.14	6.01	6.46	6.02	4.71	3.34	2.84	3.12	3.37	3.38	3.37	3.31
-18.75	3.64	3.58	4.83	6.09	6.14	5.42	4.64	3.76	3.53	3.69	3.47	3.32	3.23
-19.00	2.11	2.51	4.04	5.33	5.66	5.40	4.93	4.56	4.39	4.24	3.90	3.61	3.46
-19.25	1.66	2.30	3.46	4.43	4.98	5.04	4.91	4.99	5.31	5.42	5.02	4.49	4.14
-19.50	2.85	2.96	3.11	3.77	4.36	4.60	4.86	5.10	6.47	7.56	6.88	5.85	5.00
-19.75	5.02	4.33	3.51	3.67	3.98	4.33	4.61	4.48	6.63	8.74	8.07	6.89	5.75
-20.00	6.15	4.71	3.92	4.04	4.19	4.42	4.32	3.54	5.01	7.25	7.31	6.77	6.08
-20.25	5.90	4.46	4.41	4.89	5.20	5.08	4.57	4.00	4.15	5.04	5.66	5.94	6.04
-20.50	5.92	5.28	5.37	5.81	6.35	6.41	6.19	7.26	6.39	4.54	4.90	5.55	6.12
-20.75	6.17	6.30	6.09	6.28	7.12	8.08	9.69	11.74	9.36	5.70	5.38	5.75	6.18
-21.00	6.14	6.45	6.19	6.59	7.65	9.06	11.87	12.44	9.13	6.70	6.00	5.77	5.74
-21.25	6.46	6.40	5.86	6.30	7.55	9.40	10.76	9.48	7.56	6.73	6.14	5.69	5.42
-21.50	6.86	6.33	5.37	5.25	6.94	9.52	9.45	7.75	7.30	6.99	6.69	6.41	6.30
-21.75	6.78	5.97	5.03	4.78	6.63	8.62	8.40	7.74	7.80	7.84	7.78	7.77	8.02
-22.00	6.35	5.35	4.60	4.56	5.94	6.96	7.01	7.41	7.83	8.02	8.04	8.22	8.76
-22.25	5.63	4.65	3.88	3.16	2.81	3.82	5.25	6.00	6.52	6.74	6.84	7.12	7.61
-22.50	4.95	4.33	3.23	1.18	-1.35	-.15	2.91	3.87	4.40	4.74	5.07	5.42	5.67
-22.75	4.47	4.29	2.88	.51	-2.12	-2.62	-.04	2.20	2.76	3.19	3.72	4.21	4.41
-23.00	3.96	4.13	3.11	1.78	.39	-2.14	-1.15	1.93	2.35	2.70	3.43	4.26	4.65
-23.25	3.33	3.67	3.56	3.25	2.62	1.00	1.32	2.87	3.04	3.53	4.62	5.74	6.10
-23.50	2.90	3.17	3.75	3.69	2.81	2.20	2.95	3.85	4.25	5.19	6.47	7.37	7.23
-23.75	3.43	3.54	4.09	3.99	2.82	1.86	2.66	4.08	5.16	6.42	7.39	7.55	6.69
-24.00	4.18	4.18	4.19	4.33	3.91	2.41	.70	1.83	4.82	6.19	6.58	5.97	4.76
-24.25	4.07	4.12	3.96	4.15	4.18	2.69	-1.52	-1.15	3.22	4.46	4.48	3.74	2.98
-24.50	3.76	3.89	4.13	4.24	4.49	3.73	.08	-2.25	.07	2.31	2.43	2.17	2.15
-24.75	3.89	3.93	4.47	4.88	5.44	5.36	3.06	-1.85	-3.28	-.24	1.14	1.42	1.77
-25.00	4.19	4.22	4.64	5.25	5.75	5.69	4.33	.64	-2.96	-2.43	-.17	.86	1.39
-25.25	4.31	4.50	4.67	5.14	5.39	5.09	4.44	2.84	-.28	-2.60	-2.02	-.13	1.17
-25.50	4.13	4.31	4.56	4.95	5.19	5.19	5.00	4.27	1.93	-1.51	-2.67	-.92	1.09
-25.75	3.81	4.13	4.90	5.19	5.32	5.85	6.09	5.64	3.56	.48	-.89	-.40	.74
-26.00	3.51	4.27	5.71	5.78	5.60	6.42	6.85	6.23	5.11	3.20	1.90	.89	.11
	42	*****	*****		*****		*****		*****		*****		*****

Tableau 5 : Composante ξ (en seconde d'arc)

FONCTION VKSI * 1.0E+00

	45		45		46		46		47		47		48	
-12.00	12.81	10.90	8.58	7.46	9.24	14.13	15.01	10.47	6.22	6.16	12.55	20.80	22.99	
-12.25	12.42	12.13	8.81	5.67	4.77	5.96	5.74	4.30	4.33	6.48	9.99	12.69	13.17	
-12.50	8.53	10.26	7.33	3.31	.45	-1.82	-2.60	-1.25	1.46	4.04	4.43	3.12	3.31	
-12.75	.10	2.70	1.92	-.15	-1.85	-4.54	-5.17	-3.02	-.77	-.19	-2.49	-5.00	-3.26	
-13.00	-8.94	-7.68	-5.43	-3.27	-1.71	-1.76	-1.78	-.70	-.19	-1.37	-4.13	-5.52	-2.45	
-13.25	-13.25	-13.23	-8.28	-2.87	-.34	.66	1.25	1.93	1.86	.44	-.83	-.45	1.62	
-13.50	-9.52	-9.83	-5.33	-.43	1.15	1.37	1.93	3.09	3.73	2.90	2.52	3.12	2.59	
-13.75	-3.54	-3.60	-1.79	.35	1.28	1.35	1.75	2.91	3.96	3.82	3.02	2.48	.90	
-14.00	-.56	-.12	.22	.53	1.02	1.46	1.88	2.46	3.25	3.71	3.16	1.29	-.61	
-14.25	.40	.81	1.01	1.06	1.46	2.11	2.71	3.39	4.23	4.94	4.83	2.35	-.18	
-14.50	.55	.64	1.08	1.72	2.71	3.61	4.55	5.90	6.94	7.26	6.12	3.71	1.87	
-14.75	.67	.53	1.49	3.19	5.09	6.30	7.05	8.21	8.87	8.36	6.43	4.53	3.72	
-15.00	2.49	2.35	3.68	5.81	7.86	9.09	9.39	9.16	8.62	7.62	6.28	5.42	5.10	
-15.25	8.52	8.58	8.96	9.38	10.06	10.50	10.13	8.58	7.25	6.78	6.47	6.40	6.34	
-15.50	16.44	16.53	14.92	12.66	10.91	9.80	8.63	7.23	6.68	7.04	7.42	7.60	7.66	
-15.75	18.62	18.36	16.18	13.34	10.25	8.12	7.08	6.75	7.22	7.97	8.59	8.90	9.09	
-16.00	14.90	14.33	13.11	11.59	9.49	7.76	7.13	7.35	8.06	8.88	9.59	10.08	10.71	
-16.25	11.62	11.43	11.03	10.53	9.68	8.68	8.12	8.31	8.92	9.66	10.44	11.18	12.15	
-16.50	10.27	10.76	10.69	10.51	10.10	9.50	9.17	9.38	9.95	10.76	11.58	12.10	12.23	
-16.75	9.11	9.83	9.97	9.97	9.92	9.86	10.09	10.62	11.28	12.11	12.47	11.84	10.29	
-17.00	7.24	7.91	8.48	8.90	9.42	10.21	11.36	12.34	12.86	12.86	11.84	9.96	7.63	
-17.25	5.18	5.96	7.17	8.26	9.58	11.56	13.62	14.72	14.59	13.08	10.55	8.21	6.33	
-17.50	3.95	5.03	6.89	8.90	11.22	13.74	15.41	16.00	15.45	13.40	10.61	8.35	6.87	
-17.75	3.54	4.68	7.20	10.49	13.16	14.31	14.18	13.91	13.51	12.35	10.86	9.32	7.83	
-18.00	3.41	4.23	6.73	10.33	12.26	11.85	10.69	9.75	9.22	8.94	8.98	8.78	7.70	
-18.25	3.37	3.68	4.95	7.09	8.36	8.17	7.50	6.55	5.82	5.74	6.27	6.83	6.43	
-18.50	3.31	3.22	3.09	3.57	4.65	5.26	5.37	5.14	4.81	4.76	5.04	5.34	5.10	
-18.75	3.23	2.98	2.18	1.68	2.42	3.42	4.12	4.72	5.01	5.06	4.98	4.74	4.17	
-19.00	3.46	3.17	2.37	1.38	1.45	2.42	3.44	4.37	4.90	5.00	4.81	4.21	3.07	
-19.25	4.14	3.78	3.17	2.19	1.75	2.26	2.97	3.51	3.70	3.77	3.74	2.93	1.36	
-19.50	5.00	4.34	3.62	2.73	2.44	2.87	2.97	2.62	2.18	1.97	1.94	.87	-.23	
-19.75	5.75	4.82	3.98	3.23	3.42	4.32	4.09	2.80	1.66	.97	.51	-.29	.33	
-20.00	6.08	5.46	5.09	4.96	5.22	5.72	5.26	3.72	2.28	1.23	.37	.67	2.98	
-20.25	6.04	6.09	6.33	6.62	6.13	5.01	4.22	3.61	2.78	1.76	.73	1.53	3.95	
-20.50	6.12	6.53	6.77	6.41	4.71	2.49	1.61	1.93	1.97	1.07	-.19	.00	1.50	
-20.75	6.18	6.52	6.42	5.25	2.99	.99	.30	.53	.46	-.63	-1.87	-1.80	-.96	
-21.00	5.74	5.86	5.77	4.91	3.40	2.09	1.35	.81	-.14	-1.55	-2.27	-1.62	-.98	
-21.25	5.42	5.46	5.77	5.83	5.16	4.07	2.93	1.69	.15	-1.33	-1.50	-.50	-.02	
-21.50	6.30	6.63	7.46	7.76	6.78	5.18	3.56	1.97	.41	-.66	-.21	.87	.84	
-21.75	8.02	8.84	9.73	9.36	7.69	5.68	3.72	2.00	.80	.70	1.82	2.56	1.81	
-22.00	8.76	9.55	9.64	8.61	7.22	5.64	3.86	2.25	1.49	2.24	3.43	3.50	1.49	
-22.25	7.61	7.80	7.13	6.21	5.69	4.97	3.76	2.49	2.02	2.82	3.53	3.23	.62	
-22.50	5.67	5.38	4.57	4.02	4.06	4.03	3.39	2.51	2.29	2.91	3.33	3.04	1.74	
-22.75	4.41	4.01	3.20	2.70	2.86	3.25	3.03	2.46	2.61	3.47	4.01	3.80	3.40	
-23.00	4.65	4.18	3.18	2.44	2.42	2.88	2.97	2.68	3.26	4.56	5.22	4.17	3.51	
-23.25	6.10	5.34	3.97	2.94	2.61	2.72	2.95	3.19	4.17	5.51	5.94	3.86	3.21	
-23.50	7.23	6.02	4.47	3.40	2.84	2.44	2.59	3.48	4.54	5.13	5.00	3.64	3.60	
-23.75	6.69	5.27	4.08	3.42	2.93	2.33	2.29	3.04	3.36	2.86	1.59	1.45	2.87	
-24.00	4.76	3.74	3.36	3.38	3.26	2.83	2.39	2.11	1.46	.47	-.92	-.27	1.74	
-24.25	2.98	2.75	3.09	3.71	4.07	3.79	2.82	1.64	.68	.14	.74	1.98	2.58	
-24.50	2.15	2.49	3.16	4.11	4.85	4.71	3.62	2.26	1.47	1.83	3.18	3.85	3.90	
-24.75	1.77	2.23	2.90	3.86	4.82	5.11	4.48	3.52	2.99	3.30	3.20	3.13	4.14	
-25.00	1.39	1.84	2.21	2.84	4.00	4.89	4.68	5.11	5.66	3.98	2.04	2.32	3.75	
-25.25	1.17	1.63	1.67	1.89	2.70	3.64	4.40	6.07	7.06	4.80	2.67	3.01	4.06	
-25.50	1.09	1.73	1.75	1.66	1.03	.90	2.66	4.13	4.42	4.67	4.73	5.05	5.46	
-25.75	.74	1.50	1.84	1.25	-.72	-1.77	-.27	1.32	2.28	4.21	5.85	6.26	5.94	
-26.00	.11	.80	1.55	.26	-2.40	-3.66	-2.87	-.33	2.33	4.34	6.20	6.31	5.19	
	45	*****	*****	*****	*****	*****	*****	*****						

Tableau 6 : Composante ξ en seconde d'arc

FONCTION VKSI * 1.0E+00

	48		48		49		49		50		50		51		51		52
-12.00	22.99	20.90	18.95	17.62	16.39	14.48	11.64	9.24	7.29	5.58	4.99	4.80	4.83	4.80	4.36	3.59	3.32
-12.25	13.17	13.06	12.90	12.13	10.57	9.20	9.48	9.88	8.51	6.35	5.20	4.83	4.81	4.84	4.59	4.35	4.09
-12.50	3.31	5.62	7.04	6.67	5.66	5.33	7.27	9.42	9.18	7.03	5.18	4.73	4.81	4.75	4.73	4.96	4.73
-12.75	-3.26	1.16	3.44	3.38	3.17	3.49	5.01	7.35	8.41	7.03	5.14	4.74	4.83	4.67	4.81	5.17	5.05
-13.00	-2.45	1.05	2.17	2.52	2.54	2.72	3.56	5.34	6.62	6.44	5.62	5.02	4.81	4.83	4.99	4.98	4.87
-13.25	1.62	1.97	1.31	1.86	2.18	2.32	2.83	3.97	5.43	6.40	6.11	5.28	4.87	4.99	5.02	4.67	4.48
-13.50	2.59	1.10	.81	1.50	2.17	2.27	2.26	2.91	4.76	6.31	6.13	5.52	5.00	4.70	4.51	4.34	4.33
-13.75	.90	-.12	1.09	2.42	3.20	2.97	2.22	2.32	3.70	5.33	5.96	5.69	4.94	4.10	3.66	3.80	4.05
-14.00	-.61	-.43	1.69	3.61	3.93	3.13	2.05	1.88	2.87	4.53	5.73	5.57	4.75	3.82	3.26	3.24	3.44
-14.25	-.18	-.10	1.37	2.70	2.69	2.03	1.40	1.41	2.39	3.97	5.11	5.11	4.58	3.98	3.50	3.15	3.09
-14.50	1.87	1.05	.60	.47	.57	.62	.53	.81	1.83	3.50	4.66	4.65	4.39	4.22	4.02	3.70	3.49
-14.75	3.72	2.69	1.04	-.35	-.66	-.73	-.97	-.67	.66	2.96	4.28	4.11	4.07	4.30	4.52	4.47	4.22
-15.00	5.10	4.47	3.04	1.37	.32	-.64	-1.47	-1.81	-1.14	1.28	2.93	3.23	3.77	4.29	4.60	4.68	4.56
-15.25	6.34	6.15	5.50	4.52	3.56	2.46	1.47	.10	-1.14	-.12	2.16	3.53	4.10	4.31	4.25	4.25	4.31
-15.50	7.66	7.76	7.75	7.47	7.03	6.55	5.66	3.94	1.83	1.03	3.09	4.73	4.38	4.05	3.73	3.64	3.79
-15.75	9.09	9.72	10.20	9.84	9.10	8.51	7.74	6.46	4.87	3.51	3.59	3.86	3.48	3.33	3.17	3.06	3.27
-16.00	10.71	11.91	12.34	11.29	9.61	8.15	7.41	6.78	5.70	4.18	2.24	1.40	2.01	2.49	2.81	2.93	3.11
-16.25	12.15	12.67	12.03	10.70	8.56	6.57	6.02	5.96	5.17	3.26	.82	.18	1.07	1.81	2.57	3.15	3.39
-16.50	12.23	10.99	9.16	7.89	6.03	4.81	5.05	5.19	4.55	2.87	1.10	.67	1.09	1.64	2.37	3.09	3.42
-16.75	10.29	8.02	6.03	4.63	3.62	4.07	5.04	5.03	4.53	3.07	1.65	1.41	1.60	1.99	2.39	2.86	3.12
-17.00	7.63	5.57	4.15	2.98	3.05	4.51	5.68	5.54	4.28	2.10	.97	1.47	2.04	2.47	2.57	2.64	2.95
-17.25	6.33	4.90	4.02	3.54	4.15	5.31	5.80	4.85	2.05	-.11	.33	1.76	2.62	2.88	2.80	2.68	3.04
-17.50	6.87	5.73	5.01	4.88	5.33	5.63	4.35	1.82	-.48	-.57	1.27	2.81	3.45	3.44	3.34	3.29	3.41
-17.75	7.83	6.45	5.42	5.02	5.11	4.81	2.40	-.43	-.68	.81	2.41	3.52	4.00	4.04	4.00	3.76	3.38
-18.00	7.70	6.07	4.48	3.62	3.56	3.08	1.11	-.40	.50	1.92	2.74	3.53	4.05	4.20	4.28	3.88	3.14
-18.25	6.43	5.00	3.27	2.28	2.12	1.14	-.04	.25	1.56	2.66	3.16	3.57	3.93	4.08	4.14	4.14	3.95
-18.50	5.10	4.16	3.07	2.42	1.95	.30	-.55	.75	2.14	3.14	3.69	3.86	3.92	3.97	3.86	4.16	4.76
-18.75	4.17	3.51	3.33	3.38	2.84	1.07	.06	1.04	2.20	3.13	3.90	4.22	4.18	4.13	3.94	3.99	4.40
-19.00	3.07	2.37	3.01	3.83	2.59	.62	.42	1.39	2.43	3.20	3.79	4.27	4.53	4.55	4.40	4.16	4.07
-19.25	1.36	1.00	2.38	3.40	1.28	-.46	.78	2.14	3.26	3.84	3.99	4.29	4.62	4.76	4.77	4.56	4.51
-19.50	-.23	.76	2.36	2.72	1.21	.41	1.72	2.95	3.82	4.31	4.35	4.27	4.44	4.78	4.87	4.85	5.09
-19.75	.33	2.52	3.39	1.90	.53	.96	2.10	3.13	3.59	4.03	4.24	3.97	4.08	4.48	4.57	4.77	5.01
-20.00	2.98	5.02	4.94	1.57	-.55	.74	1.88	2.74	3.06	3.43	3.87	3.92	3.81	3.78	4.04	4.52	4.60
-20.25	3.95	5.25	4.94	2.09	.40	1.65	2.51	2.99	3.19	3.28	3.39	3.64	3.78	3.67	3.90	4.44	4.65
-20.50	1.50	2.32	1.30	.52	1.56	3.05	4.01	4.27	4.30	4.00	3.48	3.44	3.99	4.34	4.41	4.75	5.17
-20.75	-.96	-.64	-2.39	-1.69	1.85	3.72	4.74	5.08	5.09	4.85	4.52	4.36	4.50	4.85	5.19	5.30	5.37
-21.00	-.98	-1.01	-1.97	-1.12	1.81	3.63	4.56	4.84	4.81	4.87	5.09	5.17	5.00	5.29	5.91	5.61	5.04
-21.25	-.02	-.86	-1.34	-.36	1.34	3.11	4.23	4.61	4.62	4.73	5.07	5.35	5.48	5.83	6.07	5.71	5.18
-21.50	.84	-1.23	-1.99	-.25	1.16	2.51	3.72	4.62	5.06	5.20	5.47	5.66	5.70	5.69	5.56	5.68	5.66
-21.75	1.81	-.59	-1.41	.22	1.48	2.50	3.50	4.57	5.35	5.60	5.73	5.70	5.48	5.24	5.05	5.22	5.39
-22.00	1.49	-.83	-.86	.42	1.92	3.42	4.28	4.90	5.56	5.77	5.64	5.46	5.28	5.00	4.68	4.66	4.98
-22.25	.62	-1.22	-.22	1.37	3.46	5.10	5.65	5.67	5.87	5.94	5.58	5.23	4.88	4.40	4.34	4.76	5.43
-22.50	1.74	1.11	1.98	3.74	5.68	6.30	6.28	5.95	5.58	5.36	4.90	4.50	4.18	3.99	4.47	5.26	5.83
-22.75	3.40	3.56	4.45	5.69	6.26	5.90	5.57	5.19	4.54	4.00	3.70	3.82	4.15	4.63	5.16	5.53	5.53
-23.00	3.51	4.65	5.94	6.32	5.67	5.03	4.68	4.30	3.68	3.14	3.40	4.35	5.28	5.82	5.95	5.78	5.33
-23.25	3.21	5.36	6.40	6.22	5.48	5.02	4.74	4.44	4.00	3.89	4.65	5.67	6.30	6.43	6.23	5.81	5.39
-23.50	3.60	5.11	5.57	5.50	5.36	5.20	5.15	5.34	5.51	5.78	6.09	6.11	5.98	5.87	5.75	5.50	5.39
-23.75	2.87	3.77	4.16	4.49	4.86	5.00	5.16	5.75	6.44	6.61	6.08	5.43	5.11	5.03	5.07	5.16	5.24
-24.00	1.74	2.72	3.52	3.97	4.28	4.60	5.16	5.75	5.91	5.61	5.28	5.08	5.03	5.01	4.86	4.85	4.92
-24.25	2.58	3.20	4.00	4.37	4.34	4.48	5.37	6.04	5.67	5.24	5.44	5.59	5.66	5.64	5.17	4.79	4.72
-24.50	3.90	4.45	4.99	5.24	5.11	5.03	5.39	5.83	6.14	6.30	6.15	5.99	6.07	5.92	5.39	4.92	4.58
-24.75	4.14	5.02	5.36	5.17	5.09	5.24	4.99	4.82	5.65	6.37	5.91	5.54	5.49	5.11	4.90	4.64	4.14
-25.00	3.75	4.69	4.81	4.45	4.59	4.90	4.55	4.08	4.34	4.85	4.85	4.58	4.10	3.73	3.91	3.89	3.53
-25.25	4.06	4.64	4.68	4.65	4.76	4.66	4.36	4.13	3.74	3.54	3.82	3.66	2.98	2.82	2.98	3.01	3.10
-25.50	5.46	5.36	5.39	5.47	5.04	4.55	4.37	4.30	3.83	3.24	3.20	3.06	2.65	2.61	2.55	2.52	2.80
-25.75	5.94	5.67	5.85	5.90	5.32	4.78	4.51	4.16	3.73	3.42	3.22	3.06	2.96	2.97	2.92	2.73	2.61
-26.00	5.19	5.33	5.92	6.01	5.75	5.28	4.71	3.90	3.46	3.67	3.61	3.45	3.55	3.58	3.70	3.31	2.52
	48	*****		*****		*****		*****		*****		*****		*****		*****	

Tableau 7 : Composante η en seconde d'arc

FONCTION VETA * 1.0E+00

	42		42		43		43		44		44		45
-12.00	2.73	1.96	-.05	-3.66	-6.02	-5.17	-2.14	.96	1.91	2.11	4.24	6.01	5.68
-12.25	3.10	2.34	.49	-3.20	-6.78	-7.69	-5.25	-1.45	.81	1.81	2.21	2.30	4.42
-12.50	3.43	2.91	1.09	-2.79	-6.82	-8.03	-5.11	-1.02	1.14	.62	-3.16	-5.23	.63
-12.75	3.98	3.30	1.51	-1.83	-5.03	-5.61	-2.83	.07	.57	-2.15	-7.79	-10.13	-3.21
-13.00	4.36	3.37	1.95	-.11	-2.08	-2.55	-1.01	.40	-.38	-3.76	-8.56	-10.33	-4.61
-13.25	4.48	3.39	2.65	1.89	.30	-.79	-.15	.63	-.22	-2.53	-5.36	-6.63	-3.14
-13.50	4.56	3.69	3.41	3.26	1.68	.20	.60	1.24	.76	-.33	-1.69	-2.40	-.97
-13.75	4.31	4.14	3.93	3.56	2.58	1.64	1.75	1.93	1.37	.59	-.03	.00	.57
-14.00	3.44	4.41	4.44	3.60	3.10	2.81	2.66	2.44	1.66	.98	1.03	1.24	.91
-14.25	2.23	4.21	4.70	3.73	3.25	3.17	3.12	2.98	2.29	1.72	1.89	1.70	.60
-14.50	.63	3.20	4.62	4.27	3.58	3.13	3.00	3.31	3.30	2.78	2.31	1.61	.41
-14.75	-1.14	2.30	4.76	5.02	4.04	3.20	2.57	2.89	3.98	3.86	2.57	1.62	.53
-15.00	-1.78	1.89	4.74	5.54	4.70	3.56	2.35	2.12	3.68	4.07	2.73	2.19	1.14
-15.25	-.71	1.55	3.97	5.83	5.66	4.06	2.36	1.61	2.37	2.58	2.18	2.77	1.65
-15.50	.69	1.91	3.63	5.58	5.82	4.18	2.16	.45	-.51	-.79	.08	1.97	1.39
-15.75	1.04	2.76	4.14	4.91	4.70	3.21	.54	-2.37	-4.31	-4.15	-1.71	.37	.34
-16.00	.11	2.52	4.25	4.37	3.07	.90	-2.57	-5.53	-5.92	-4.41	-2.02	-.48	.10
-16.25	-1.17	1.78	3.91	3.79	1.31	-2.03	-4.97	-5.94	-4.56	-3.22	-2.39	-1.10	.36
-16.50	-3.01	1.33	3.76	2.73	-.50	-3.83	-4.79	-3.66	-2.96	-3.17	-3.15	-2.15	-.28
-16.75	-5.61	.12	3.13	1.62	-1.65	-3.77	-3.00	-1.63	-2.37	-3.32	-3.73	-3.40	-1.38
-17.00	-6.84	-1.06	2.13	.94	-1.99	-3.38	-2.36	-1.40	-1.88	-2.73	-3.79	-4.11	-2.24
-17.25	-6.20	-.82	2.02	.45	-2.64	-4.09	-3.44	-1.97	-1.21	-1.86	-3.29	-3.89	-2.55
-17.50	-4.95	-.22	2.08	.08	-3.07	-4.88	-4.62	-2.31	-.84	-1.39	-2.61	-3.37	-2.91
-17.75	-4.49	-.33	1.97	.81	-1.91	-4.21	-4.77	-3.13	-1.48	-1.44	-2.37	-3.23	-3.59
-18.00	-4.84	-.70	2.33	2.60	.33	-2.61	-4.44	-4.27	-2.77	-2.08	-2.59	-3.32	-4.22
-18.25	-4.99	-1.13	2.41	3.91	2.44	-.68	-3.98	-5.18	-3.75	-2.67	-2.85	-3.34	-4.51
-18.50	-5.12	-1.69	2.05	4.34	3.71	1.10	-3.08	-5.56	-4.22	-2.84	-2.94	-3.32	-4.50
-18.75	-4.44	-2.16	1.02	3.91	4.30	2.15	-2.01	-4.96	-4.33	-2.96	-2.86	-3.27	-4.37
-19.00	-3.63	-2.97	-.60	2.97	4.44	2.68	-1.34	-4.40	-4.16	-2.79	-2.56	-3.08	-4.15
-19.25	-4.10	-4.22	-1.97	2.20	4.24	2.92	-1.13	-4.40	-4.01	-2.44	-2.20	-2.81	-3.91
-19.50	-4.45	-4.88	-2.86	1.37	3.80	2.77	-1.29	-4.84	-4.64	-2.50	-1.58	-2.16	-3.41
-19.75	-4.33	-4.50	-2.83	.88	3.37	2.39	-1.66	-6.12	-6.63	-2.89	-.39	-.83	-2.31
-20.00	-3.16	-3.29	-2.16	.88	3.11	2.10	-1.46	-7.00	-9.18	-4.04	.38	.31	-1.21
-20.25	-.59	-2.14	-2.12	.60	2.98	2.26	-.73	-6.87	-10.61	-5.36	.12	.48	-.93
-20.50	1.38	-1.70	-2.62	.03	2.92	2.78	-.30	-6.57	-10.32	-5.66	-.58	-.10	-1.38
-20.75	1.55	-1.57	-2.69	-.45	2.35	2.44	-1.65	-7.11	-7.73	-3.78	-.97	-.82	-1.98
-21.00	.74	-1.63	-2.61	-1.06	1.00	.03	-4.22	-6.23	-3.89	-1.42	-.63	-.95	-2.21
-21.25	.27	-1.62	-2.85	-2.02	-.30	-2.08	-5.27	-4.19	-1.59	-.43	.01	-.55	-2.07
-21.50	.37	-.98	-2.52	-2.89	-2.32	-3.42	-4.33	-2.81	-.94	.09	.49	-.18	-1.97
-21.75	.93	-.02	-1.69	-3.72	-4.89	-4.79	-3.39	-1.90	-.78	.23	.64	-.12	-2.32
-22.00	2.00	.90	-1.25	-4.62	-6.47	-5.34	-3.40	-2.17	-1.04	.11	.56	-.44	-3.12
-22.25	3.38	1.88	-.85	-5.18	-7.50	-5.96	-3.88	-2.80	-1.44	.00	.42	-.90	-3.76
-22.50	4.33	2.80	.36	-3.47	-7.21	-8.00	-5.77	-3.56	-1.85	-.23	.15	-1.27	-3.88
-22.75	4.21	3.75	2.56	-.22	-6.08	-10.60	-8.26	-4.43	-2.39	-.73	-.31	-1.55	-3.73
-23.00	3.40	4.53	4.46	1.95	-3.82	-10.30	-11.02	-6.62	-2.94	-1.27	-.95	-2.02	-3.67
-23.25	2.56	4.69	5.13	2.74	-1.84	-8.97	-12.72	-8.24	-3.24	-1.91	-2.01	-2.88	-3.66
-23.50	2.19	4.30	4.94	2.98	-1.38	-8.92	-13.11	-8.51	-3.68	-3.00	-3.36	-3.64	-3.25
-23.75	2.32	3.77	4.59	3.78	-.22	-9.15	-14.58	-9.70	-4.72	-4.34	-4.39	-3.72	-2.20
-24.00	2.42	3.60	4.47	4.37	.94	-8.78	-15.59	-11.28	-6.25	-5.46	-4.61	-2.89	-.77
-24.25	2.33	3.77	4.44	4.21	1.88	-5.78	-13.99	-14.25	-9.52	-6.29	-4.17	-1.74	.25
-24.50	2.09	3.73	4.45	4.14	2.55	-2.54	-11.42	-16.53	-12.45	-6.87	-3.83	-1.25	.33
-24.75	2.16	3.38	4.08	3.84	2.45	-.95	-7.47	-14.30	-14.58	-8.92	-4.04	-1.44	-.09
-25.00	2.57	3.11	3.42	3.09	2.03	.08	-3.51	-9.61	-14.27	-11.77	-5.68	-1.95	-.57
-25.25	2.54	2.89	2.96	2.63	1.98	.62	-1.92	-6.30	-11.24	-12.04	-7.68	-3.17	-1.18
-25.50	2.14	2.73	2.72	2.31	2.09	1.12	-1.03	-4.42	-8.31	-9.88	-8.44	-5.50	-2.52
-25.75	2.23	2.44	2.26	1.94	1.72	.83	-.91	-2.81	-4.87	-7.09	-8.37	-7.36	-4.13
-26.00	1.96	1.52	1.55	1.86	1.36	.27	-.80	-1.63	-2.60	-4.97	-7.50	-7.33	-4.64
	42	*****		*****		*****		*****		*****		*****	

Tableau 8 : Composante η en seconde d'arc

FONCTION VETA * 1.0E+00

	45		45		46		46		47		47		48
-12.00	5.68	4.99	4.22	2.33	-.36	-1.70	.41	3.48	1.93	-4.79	-10.22	-7.88	-1.46
-12.25	4.42	7.00	6.75	3.20	-2.14	-3.42	1.77	6.09	2.48	-7.86	-15.56	-11.37	-1.58
-12.50	.63	9.69	10.85	6.48	-.65	-2.70	2.11	4.93	-.29	-10.60	-16.60	-11.15	-1.84
-12.75	-3.21	8.24	13.89	10.25	3.12	-.30	1.18	1.94	-2.93	-10.92	-14.65	-10.24	-4.14
-13.00	-4.61	6.85	13.80	10.36	3.85	.70	.55	.43	-3.20	-8.85	-11.70	-10.38	-8.16
-13.25	-3.14	4.66	9.38	6.44	1.59	-.22	.10	.31	-2.25	-6.90	-10.42	-11.99	-10.91
-13.50	-.97	1.75	3.17	2.22	.23	-.94	-.76	-.20	-1.67	-6.10	-10.81	-12.92	-10.67
-13.75	.57	.35	-.27	-.21	-.26	-1.02	-1.68	-1.54	-2.06	-5.66	-10.67	-12.08	-8.85
-14.00	.91	-.06	-.90	-.94	-.80	-1.43	-2.36	-2.48	-2.62	-5.15	-9.45	-10.76	-8.02
-14.25	.60	-.46	-.95	-1.03	-1.22	-1.91	-2.72	-2.96	-3.35	-5.57	-8.20	-8.22	-7.09
-14.50	.41	-.69	-1.17	-1.41	-1.89	-2.72	-3.69	-4.05	-4.22	-5.78	-6.80	-5.61	-5.51
-14.75	.53	-1.01	-2.07	-2.72	-3.18	-3.83	-5.10	-5.44	-4.75	-4.74	-4.55	-3.84	-4.35
-15.00	1.14	-1.54	-3.92	-5.14	-5.12	-4.76	-5.67	-5.94	-4.39	-3.27	-2.84	-2.82	-3.62
-15.25	1.65	-2.25	-5.66	-7.06	-6.59	-5.42	-5.18	-4.65	-3.17	-2.32	-2.29	-2.62	-3.37
-15.50	1.39	-2.00	-4.75	-6.29	-6.30	-4.84	-3.69	-2.96	-2.53	-2.47	-2.45	-2.69	-3.38
-15.75	.34	-.68	-1.65	-2.91	-3.64	-3.06	-2.51	-2.64	-2.98	-3.10	-2.88	-2.87	-3.54
-16.00	.10	.54	.46	-.14	-.88	-1.55	-2.28	-3.11	-3.80	-3.91	-3.42	-3.22	-4.24
-16.25	.36	1.19	1.19	.86	.34	-.62	-2.09	-3.61	-4.58	-4.70	-4.13	-4.04	-5.46
-16.50	-.28	1.15	1.40	1.27	1.05	.07	-1.90	-3.96	-5.23	-5.51	-5.02	-5.00	-5.80
-16.75	-1.38	.76	1.45	1.47	1.40	.35	-1.98	-4.43	-6.03	-6.42	-5.55	-4.73	-4.31
-17.00	-2.24	.25	1.26	1.33	1.17	-.10	-2.69	-5.22	-6.81	-6.77	-4.75	-2.74	-1.82
-17.25	-2.55	-.54	.41	.49	.04	-1.67	-4.21	-6.02	-6.58	-5.37	-2.53	-.34	.27
-17.50	-2.91	-1.84	-1.14	-1.20	-2.28	-4.33	-6.02	-6.25	-5.10	-2.54	.34	1.67	1.64
-17.75	-3.59	-3.62	-3.65	-4.06	-5.04	-6.07	-6.60	-6.08	-3.87	-.30	2.77	3.59	3.02
-18.00	-4.22	-5.69	-7.26	-7.47	-6.31	-5.42	-5.62	-5.57	-3.47	.24	3.53	4.86	4.65
-18.25	-4.51	-7.12	-10.08	-9.89	-6.66	-4.44	-4.41	-4.55	-3.04	-.04	2.95	4.95	5.88
-18.50	-4.50	-7.37	-10.88	-11.09	-7.46	-4.52	-3.92	-3.82	-2.62	-.24	2.40	4.72	6.60
-18.75	-4.37	-6.91	-10.48	-11.58	-8.45	-5.21	-4.30	-3.97	-2.64	-.29	2.35	4.90	7.15
-19.00	-4.15	-6.28	-9.53	-11.38	-9.33	-6.33	-5.32	-4.77	-2.99	-.20	2.75	5.59	7.91
-19.25	-3.91	-5.78	-8.61	-10.64	-9.59	-7.32	-6.38	-5.53	-3.32	-.20	3.20	6.76	9.12
-19.50	-3.41	-5.26	-7.88	-9.91	-9.43	-7.65	-6.66	-5.56	-3.27	-.25	3.65	8.14	9.98
-19.75	-2.31	-4.33	-6.93	-9.42	-9.76	-7.91	-6.14	-4.71	-2.63	.06	4.39	9.08	9.26
-20.00	-1.21	-3.40	-6.21	-9.34	-10.63	-8.39	-5.06	-2.99	-1.34	.97	5.01	8.36	7.01
-20.25	-.93	-3.29	-6.42	-9.59	-10.60	-7.98	-4.03	-1.55	.02	2.10	4.99	6.33	4.66
-20.50	-1.38	-3.72	-6.80	-9.16	-8.95	-6.38	-3.57	-1.47	.63	3.16	5.26	4.96	3.06
-20.75	-1.98	-3.99	-6.32	-7.41	-6.45	-4.69	-3.44	-1.93	.93	4.41	6.16	4.54	2.19
-21.00	-2.21	-3.99	-5.46	-5.52	-4.41	-3.52	-3.10	-1.64	1.88	5.67	6.53	3.99	1.83
-21.25	-2.07	-4.04	-5.33	-4.89	-3.43	-2.52	-2.08	-.34	3.47	6.71	6.25	3.17	1.55
-21.50	-1.97	-4.38	-5.88	-4.89	-2.53	-1.14	-.55	1.35	5.14	7.46	5.66	2.41	2.22
-21.75	-2.32	-5.31	-6.56	-4.17	-.66	.95	1.37	3.05	6.31	7.40	4.63	2.05	3.82
-22.00	-3.12	-6.24	-6.47	-2.71	1.44	3.14	3.41	4.51	6.56	6.38	3.67	2.43	5.63
-22.25	-3.76	-6.28	-5.57	-1.58	2.54	4.58	5.04	5.62	6.35	5.33	3.28	4.15	8.51
-22.50	-3.88	-5.74	-4.77	-1.16	2.79	5.24	6.10	6.40	6.22	4.78	3.24	5.60	10.47
-22.75	-3.73	-5.11	-4.12	-1.03	2.55	5.32	6.71	6.83	5.94	4.23	3.15	5.89	10.63
-23.00	-3.67	-4.45	-3.37	-.79	2.20	5.07	6.99	6.89	5.15	3.27	2.89	6.28	10.77
-23.25	-3.66	-3.53	-2.25	-.20	2.09	4.74	6.95	6.55	3.91	2.10	3.59	7.77	10.14
-23.50	-3.25	-2.15	-.77	.70	2.45	4.71	6.50	5.58	2.64	1.36	4.70	9.28	9.18
-23.75	-2.20	-.53	.60	1.58	3.15	5.03	5.84	4.45	2.12	1.61	5.23	9.33	8.57
-24.00	-.77	.70	1.25	1.96	3.65	5.42	5.74	4.43	2.85	3.31	6.26	7.90	6.68
-24.25	.25	1.00	1.00	1.70	3.76	6.01	6.65	5.49	3.93	4.21	6.07	6.45	5.32
-24.50	.33	.57	.20	.90	3.58	6.82	8.13	6.80	4.51	3.26	4.26	5.91	5.37
-24.75	-.09	-.10	-.79	-.16	3.12	7.38	9.37	7.88	4.42	2.35	3.87	5.69	4.68
-25.00	-.57	-.67	-1.60	-1.22	2.21	7.22	9.92	8.48	4.77	3.04	4.46	4.90	3.31
-25.25	-1.18	-1.01	-1.90	-2.14	.86	6.66	9.18	6.82	5.68	6.37	5.72	3.81	2.08
-25.50	-2.52	-1.23	-1.89	-2.37	.28	5.37	7.27	5.56	6.20	7.92	6.46	3.38	1.52
-25.75	-4.13	-1.75	-1.83	-1.34	1.71	4.88	5.64	4.89	5.11	6.04	5.32	3.03	1.74
-26.00	-4.64	-2.46	-1.62	.47	3.64	4.90	3.86	2.75	3.02	3.98	4.21	3.29	2.18
	45	*****	*****		*****		*****		*****		*****		*****

Tableau 9 : Composante η en seconde d'arc

FONCTION VETA * 1.0E+00

	48		48		49		49		50		50		51		51		52	
-12.00	-1.46	.75	-1.08	-3.29	-3.34	.95	6.07	6.69	4.38	3.33	3.62	3.30	1.94	.56	.08	.15	.19	
-12.25	-1.58	1.85	.00	-2.04	-1.80	2.44	7.24	8.06	6.23	4.77	4.21	3.44	1.94	.73	.52	.54	.34	
-12.50	-1.84	1.03	-.13	-.91	-.35	2.07	5.39	7.70	8.00	6.72	5.19	3.71	1.93	.78	.59	.66	.73	
-12.75	-4.14	-1.98	-1.08	-.63	-.42	.80	3.06	6.12	8.69	8.88	6.57	3.83	1.92	.81	.31	.54	1.26	
-13.00	-8.16	-5.84	-2.41	-.64	-.46	.18	1.43	4.23	8.35	10.09	7.55	4.04	2.01	.80	.07	.42	1.46	
-13.25	-10.91	-6.73	-2.58	-1.01	-.63	-.26	.36	2.98	7.58	9.94	8.05	4.66	2.12	.63	.15	.67	1.61	
-13.50	-10.67	-5.53	-2.30	-1.54	-.93	-.48	-.27	1.56	5.88	9.41	8.71	5.32	2.32	.65	.39	.97	1.69	
-13.75	-8.85	-4.91	-3.00	-2.41	-1.43	-.35	-.30	.42	4.10	8.54	8.88	5.84	2.96	1.15	.53	.86	1.48	
-14.00	-8.02	-5.74	-4.92	-3.72	-1.50	.53	.40	.04	2.79	7.10	8.36	6.39	3.95	1.97	.71	.57	1.05	
-14.25	-7.09	-7.29	-7.18	-4.73	-.93	1.59	.99	-.42	1.38	5.61	7.82	6.86	4.78	2.69	1.13	.66	.83	
-14.50	-5.51	-7.35	-7.82	-5.09	-.82	1.86	1.04	-.98	.16	4.31	7.20	6.95	5.13	3.08	1.56	.99	.88	
-14.75	-4.35	-6.00	-6.60	-4.71	-1.08	1.63	.80	-1.77	-1.40	2.70	6.65	7.15	5.23	3.08	1.67	1.22	1.15	
-15.00	-3.62	-4.60	-4.69	-3.34	-.42	2.18	.99	-2.67	-3.60	.56	6.02	7.19	4.94	2.62	1.40	1.31	1.59	
-15.25	-3.37	-3.89	-3.41	-1.90	1.00	3.48	2.01	-2.11	-4.61	-1.51	4.65	6.29	4.15	2.22	1.26	1.27	1.62	
-15.50	-3.38	-3.74	-3.01	-1.32	1.71	4.35	3.44	.03	-3.38	-2.85	2.25	5.19	4.14	2.47	1.46	1.24	1.40	
-15.75	-3.54	-4.00	-3.12	-1.16	1.97	4.92	4.73	1.87	-1.59	-2.82	.81	4.97	4.86	2.90	1.69	1.21	1.05	
-16.00	-4.24	-4.90	-3.14	-.18	3.09	5.78	5.59	3.01	-.33	-1.53	1.89	5.32	4.70	2.79	1.75	1.15	.63	
-16.25	-5.46	-5.71	-2.49	1.68	5.25	7.23	6.17	3.65	1.11	.78	3.71	5.22	3.75	2.07	1.23	.90	.62	
-16.50	-5.80	-4.80	-1.10	3.44	7.41	8.44	6.24	3.90	2.49	3.00	5.10	5.08	3.01	1.24	.36	.30	.49	
-16.75	-4.31	-2.52	.73	4.95	8.48	8.27	5.79	4.19	3.53	4.38	6.02	5.25	2.74	.74	-.27	-.20	.31	
-17.00	-1.82	-.35	2.44	5.97	8.03	6.98	5.26	4.46	4.55	6.02	6.86	5.14	2.40	.41	-.54	-.46	.14	
-17.25	.27	1.12	3.45	6.12	6.90	5.54	4.73	5.66	7.14	7.86	6.69	4.14	1.70	.19	-.45	-.60	-.56	
-17.50	1.64	2.07	3.87	5.86	6.19	5.26	5.76	8.40	9.75	7.84	4.92	2.75	1.23	.23	-.33	-.71	-1.11	
-17.75	3.02	3.08	4.35	5.80	6.13	6.59	8.74	10.75	9.67	6.04	3.15	1.86	1.05	.30	-.29	-.67	-1.00	
-18.00	4.65	4.60	5.39	6.20	6.44	8.13	11.28	11.66	8.48	4.60	2.09	1.09	.69	.23	-.05	-.06	-.14	
-18.25	5.88	6.48	6.95	6.79	6.71	9.18	12.44	11.42	7.26	3.70	1.46	.49	.35	.06	.05	.53	.91	
-18.50	6.60	7.94	8.27	7.43	7.65	10.43	12.25	10.01	5.96	2.93	1.13	.28	.16	.00	-.11	.14	.45	
-18.75	7.15	8.65	8.80	7.99	8.98	11.84	11.99	8.61	4.75	2.07	.70	.26	.24	.12	-.15	-.42	-.66	
-19.00	7.91	8.86	8.43	7.97	10.12	13.41	12.32	7.78	3.77	1.14	-.02	-.02	.25	.26	.03	-.35	-.81	
-19.25	9.12	8.74	7.27	8.45	12.40	14.18	11.22	6.50	2.85	.64	-.43	-.52	-.06	.26	.25	-.07	-.61	
-19.50	9.98	7.80	5.92	9.16	14.25	13.97	9.60	5.16	1.99	.38	-.50	-.69	-.25	.09	.24	-.07	-.85	
-19.75	9.26	6.02	5.21	9.70	14.89	13.68	8.56	4.29	1.42	.09	-.39	-.62	-.61	-.20	.18	-.30	-1.39	
-20.00	7.01	4.57	6.60	12.23	15.29	12.35	7.31	3.59	1.03	-.31	-.44	-.52	-.79	-.43	-.06	-.53	-1.41	
-20.25	4.66	3.95	8.91	15.59	15.82	11.12	6.45	3.05	.70	-.77	-.92	-.56	-.46	-.44	-.60	-.90	-1.15	
-20.50	3.06	3.53	9.99	17.12	15.81	10.14	5.90	2.87	.73	-.51	-.83	-.94	-.83	-.57	-.87	-1.34	-1.54	
-20.75	2.19	4.17	10.86	15.36	13.17	8.55	5.17	2.74	.98	.10	-.32	-1.12	-1.43	-.89	-1.03	-1.71	-2.13	
-21.00	1.83	5.08	11.15	12.62	10.08	7.08	4.46	2.51	.98	.09	-.31	-.92	-1.35	-1.31	-1.36	-1.53	-1.66	
-21.25	1.55	5.26	11.01	11.35	8.11	5.62	3.89	2.48	.95	-.19	-.64	-1.03	-1.56	-1.86	-1.37	-.79	-.63	
-21.50	2.22	6.52	10.65	9.78	6.39	4.01	2.87	2.09	.85	-.38	-.97	-1.37	-1.88	-1.95	-1.24	-.57	-.32	
-21.75	3.82	8.32	9.99	8.00	5.17	2.89	1.64	1.05	.32	-.64	-1.14	-1.27	-1.60	-1.72	-1.37	-.89	-.43	
-22.00	5.63	10.01	9.81	6.70	3.95	1.84	.65	.10	-.26	-.79	-1.09	-1.10	-1.39	-1.50	-1.22	-.94	-.65	
-22.25	8.51	10.89	8.67	5.03	1.95	.34	.04	-.33	-.62	-.73	-.81	-.89	-1.10	-1.08	-1.01	-1.22	-1.50	
-22.50	10.47	10.95	7.04	2.74	-.07	-.52	.03	-.14	-.55	-.47	-.32	-.35	-.50	-.91	-1.61	-2.12	-2.39	
-22.75	10.63	10.67	5.85	1.04	-.82	-.31	.42	.43	.03	.01	.11	-.11	-.54	-1.40	-2.39	-2.69	-2.51	
-23.00	10.77	9.85	4.74	.77	-.29	.23	.80	.97	.74	.45	-.12	-.85	-1.39	-2.01	-2.60	-2.53	-1.98	
-23.25	10.14	8.06	4.06	1.34	.59	.76	1.21	1.52	1.30	.32	-1.21	-2.15	-2.15	-2.14	-2.35	-2.03	-1.24	
-23.50	9.18	6.42	3.82	1.78	1.02	1.04	1.43	1.78	1.35	-.26	-2.07	-2.65	-2.22	-1.95	-1.93	-1.62	-1.06	
-23.75	8.57	5.94	3.66	1.58	.92	.99	1.06	1.13	.81	-.32	-1.58	-2.04	-1.90	-1.90	-1.95	-1.64	-1.16	
-24.00	6.68	5.04	3.04	1.01	.47	.72	.61	.39	.42	.13	-.80	-1.60	-1.79	-1.92	-2.08	-1.81	-1.22	
-24.25	5.32	4.01	2.30	.76	.22	.02	-.20	.32	.98	.38	-1.00	-1.77	-1.83	-1.73	-1.77	-1.72	-1.43	
-24.50	5.37	3.50	1.76	.64	.35	-.41	-1.10	.06	1.31	.40	-1.19	-1.84	-1.84	-1.39	-1.16	-1.31	-1.38	
-24.75	4.68	2.82	1.44	.63	.46	-.28	-1.09	-.51	.46	.36	-.66	-1.69	-1.76	-.99	-.67	-.82	-.84	
-25.00	3.31	2.16	1.60	.94	.28	-.32	-.64	-.66	-.40	.11	-.28	-1.39	-1.37	-.74	-.66	-.49	-.02	
-25.25	2.08	1.67	1.70	.87	-.03	-.24	-.19	-.27	-.38	-.21	-.36	-.86	-.83	-.79	-.85	-.41	.30	
-25.50	1.52	1.48	1.58	.86	.27	.13	-.05	.02	.25	.02	-.41	-.45	-.44	-.75	-.87	-.62	-.29	
-25.75	1.74	1.75	1.59	1.26	1.00	.51	.08	.33	.80	.48	-.17	-.25	-.33	-.68	-.75	-.69	-.70	
-26.00	2.18	1.58	1.34	1.46	1.51	1.03	.64	.89	1.07	.59	-.01	-.17	-.34	-.71	-.61	-.27	-.09	
	48	*****		*****		*****		*****		*****		*****		*****		*****		

Fig. 12. Composante ξ de la déviation de la verticale - contour : 1 sec. arc.

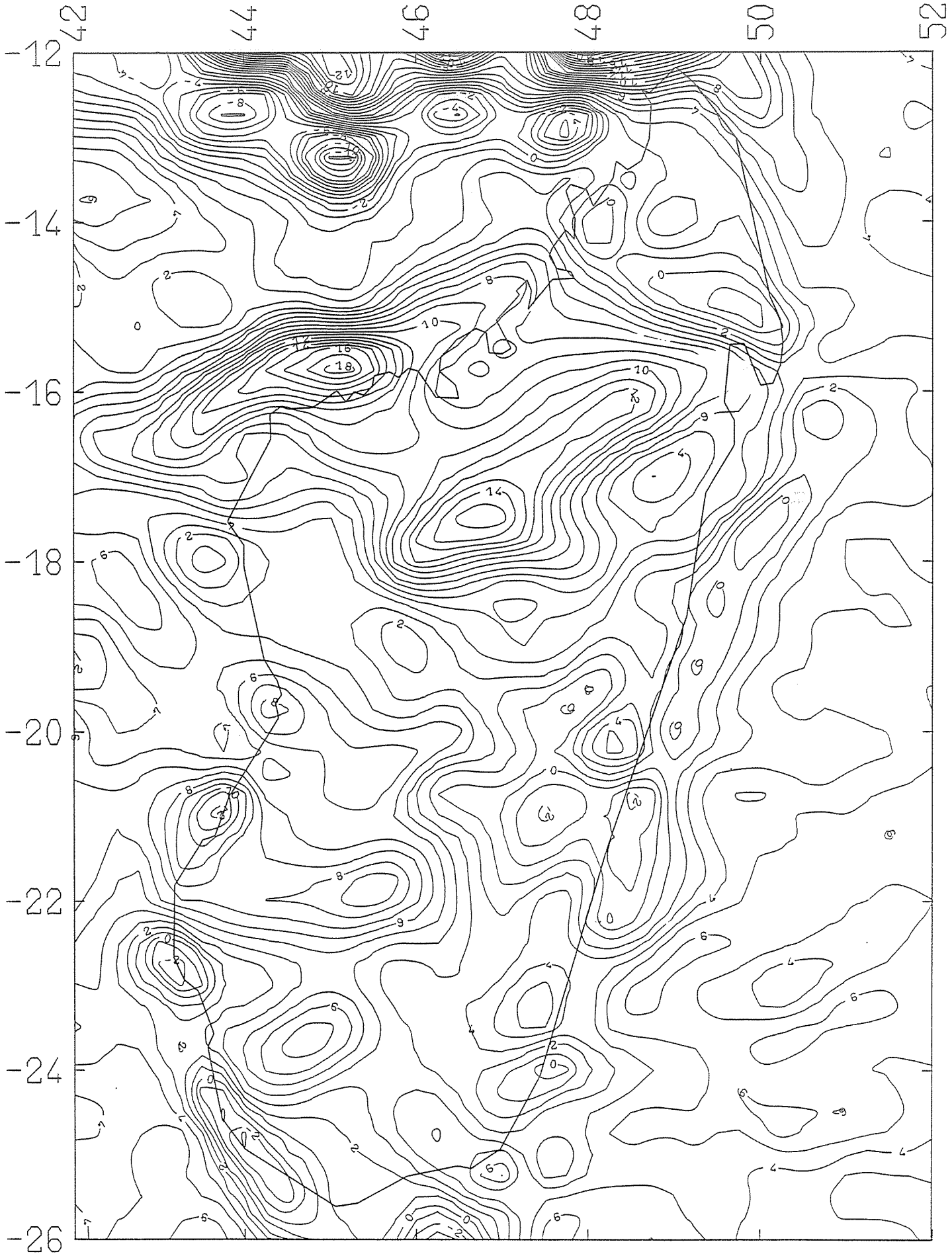

Fig. 13. Composante η de la déviation de la verticale - contour : 1 sec. arc.

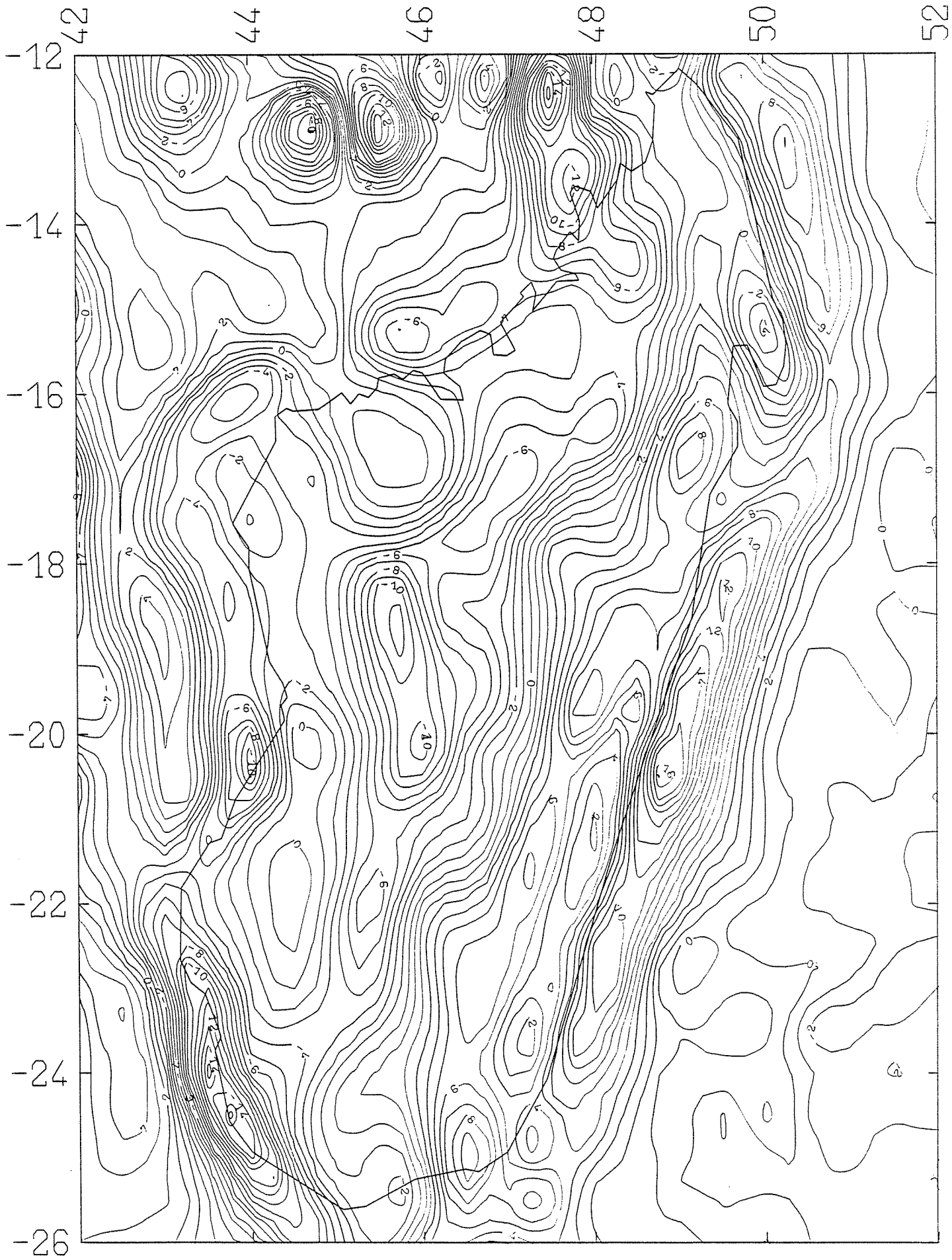

Fig. 14

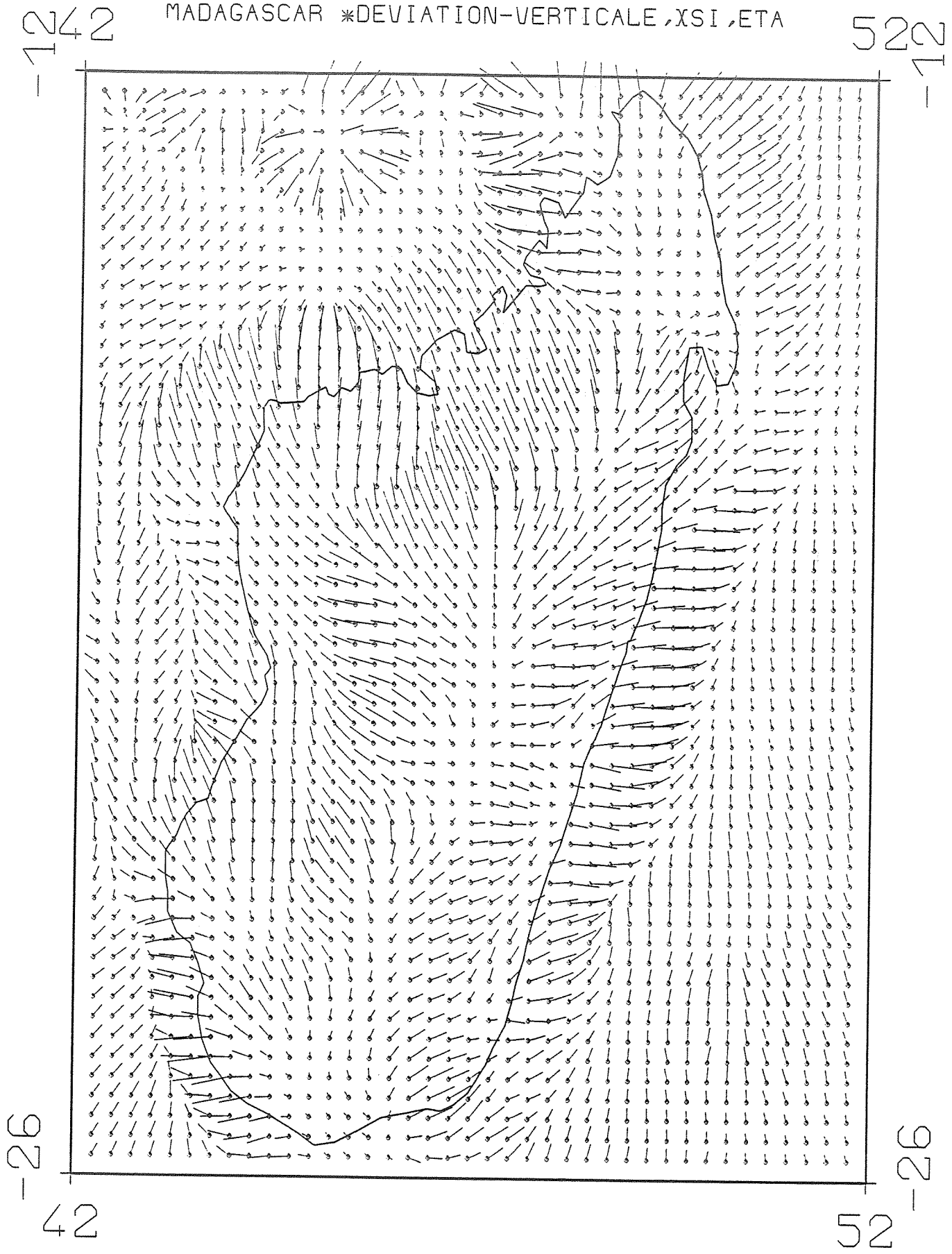
MADAGASCAR *DEVIATION-VERTICALE,XSI,ETA
-12 42
52 21
-26
42
52
-26
10 SEC. D ARC

III.4. Géoide Calculé à Partir du Modèle GRIM 3L1

Les mêmes calculs ont été faits avec un autre modèle (modèle GRIM 3L1) disponible jusqu'au degré L = 36 (dans le but de tester la précision des résultats obtenus).

Une comparaison entre le géoide gravimétrique calculé avec ce modèle GRIM 3L1 (L = 36) et celui calculé en utilisant le modèle Rapp 79 pris jusqu'au degré L = 180 a été faite. L'histogramme de fréquences des écarts (Rapp-GRIM 3L1) entre ces deux géoides est montré sur la figure 17. Ces écarts présentent une moyenne à - 0,26 mètre et une r.m.s. égale à 0,29 mètre comparable avec l'erreur de troncature calculée a priori.

Le géoide de référence calculé à partir de ce modèle est représenté sur la figure 15 et le géoide gravimétrique déduit de ce modèle est représenté sur la figure 16.

Finalement, nous montrons sur la figure 18 un extrait de carte (planche 26) tiré de l'Atlas global des hauteurs de la surface de la mer obtenue par ajustement des données altimétriques du satellite Seasat (R.H. Rapp, 1982). Visuellement les lignes caractéristiques des courbes de niveau en mer sont exactement retrouvées sur notre géoide fig. 7. La comparaison n'a pas pu être faite plus précisément car nous n'avions pas le fichier numérique de ces hauteurs de la surface de la mer calculées par le Pr. Rapp.

Fig. 15

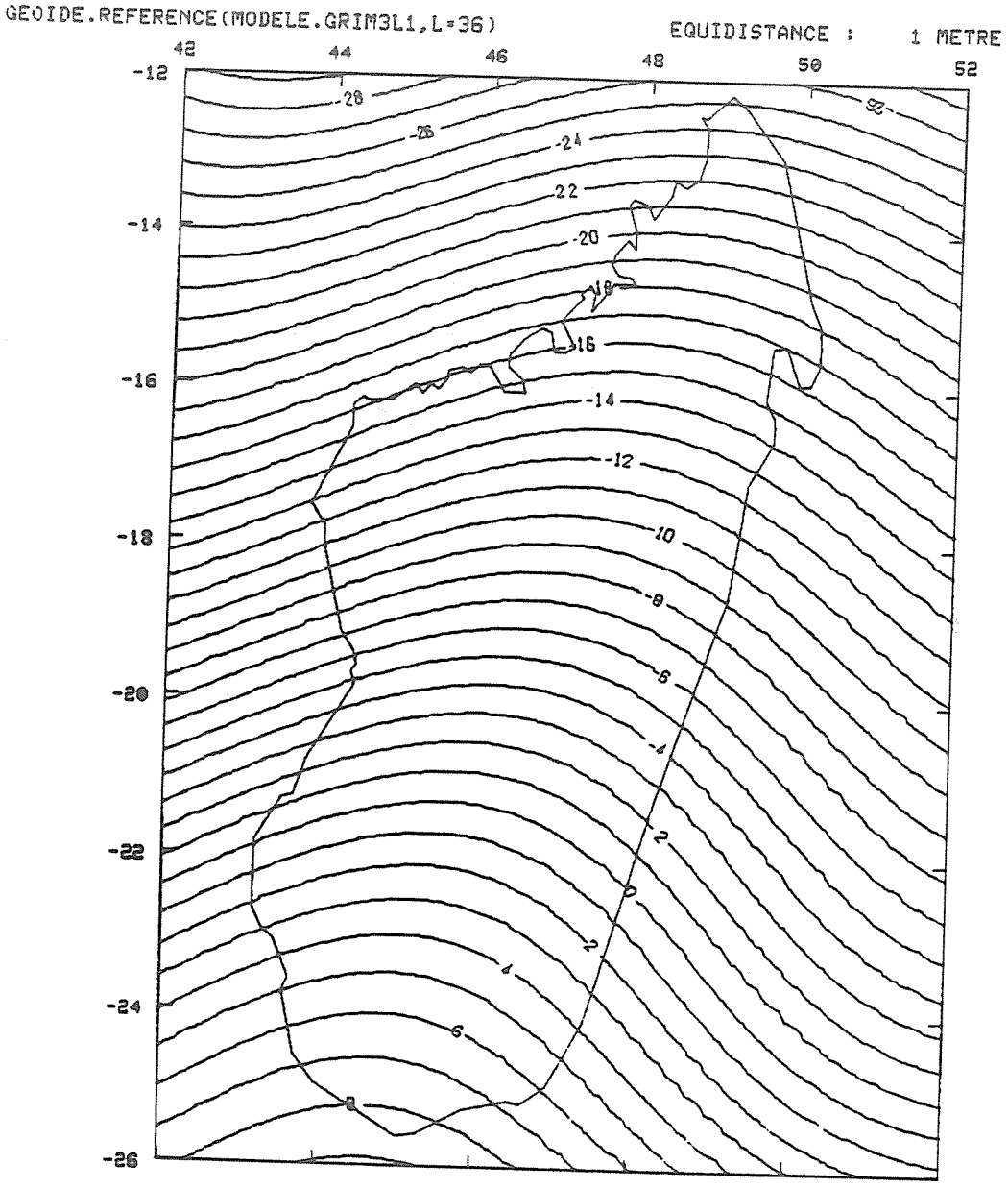
GEOIDE.REFERENCE(MODELE.GRIM3L1,L=36)
EQUIDISTANCE : 1 METRE
42
44
46
48
50
52
-12
-14
-16
-18
-20
-22
-24
-26

Fig. 16

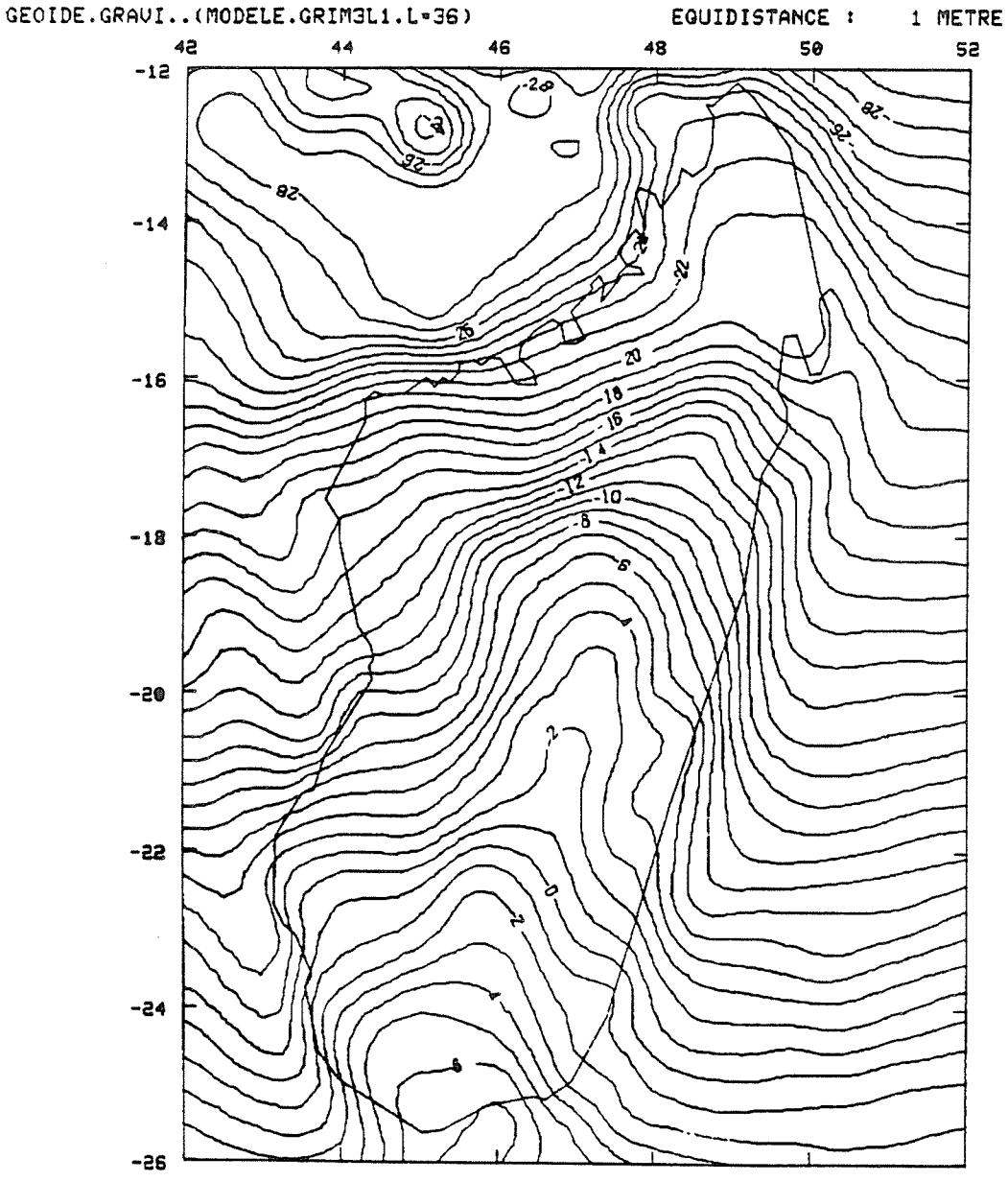
GEOIDE.GRAVI..(MODELE.GRIM3L1.L=36)
EQUIDISTANCE : 1 METRE
42
44
46
48
50
52
-12
-14
-16
-18
-20
-22
-24
-26

Fig. 17. Géoide gravimétrique Rapp-GRIM 3L1

Val. Min. = - .549
Val. Max. = .012
RMS = .287
MOY. = - .260

HISTOGRAMME DES FREQUENCES 2337 POINTS 30 CLASSES

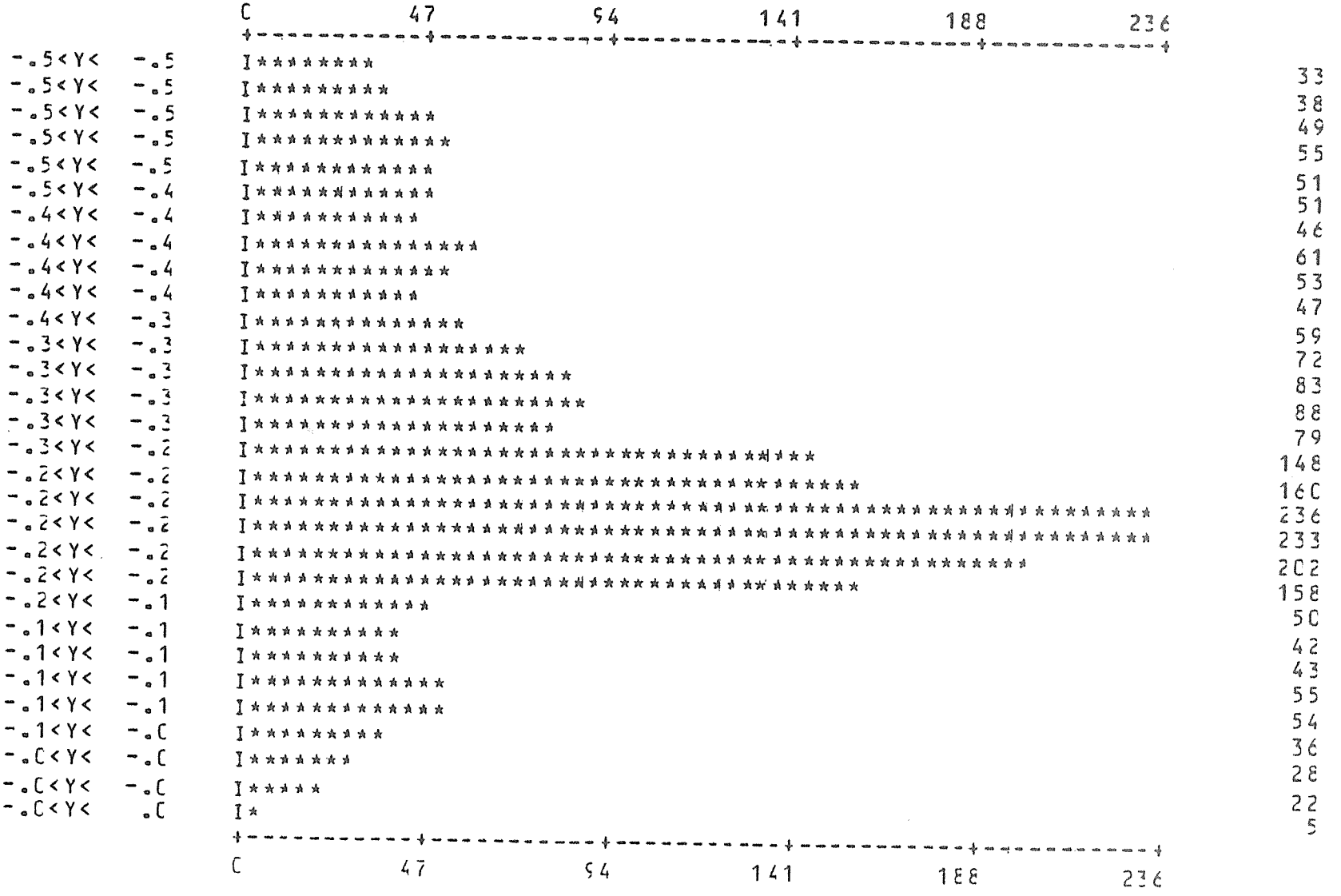

Fig. 18. Sea Surface Height Map 26

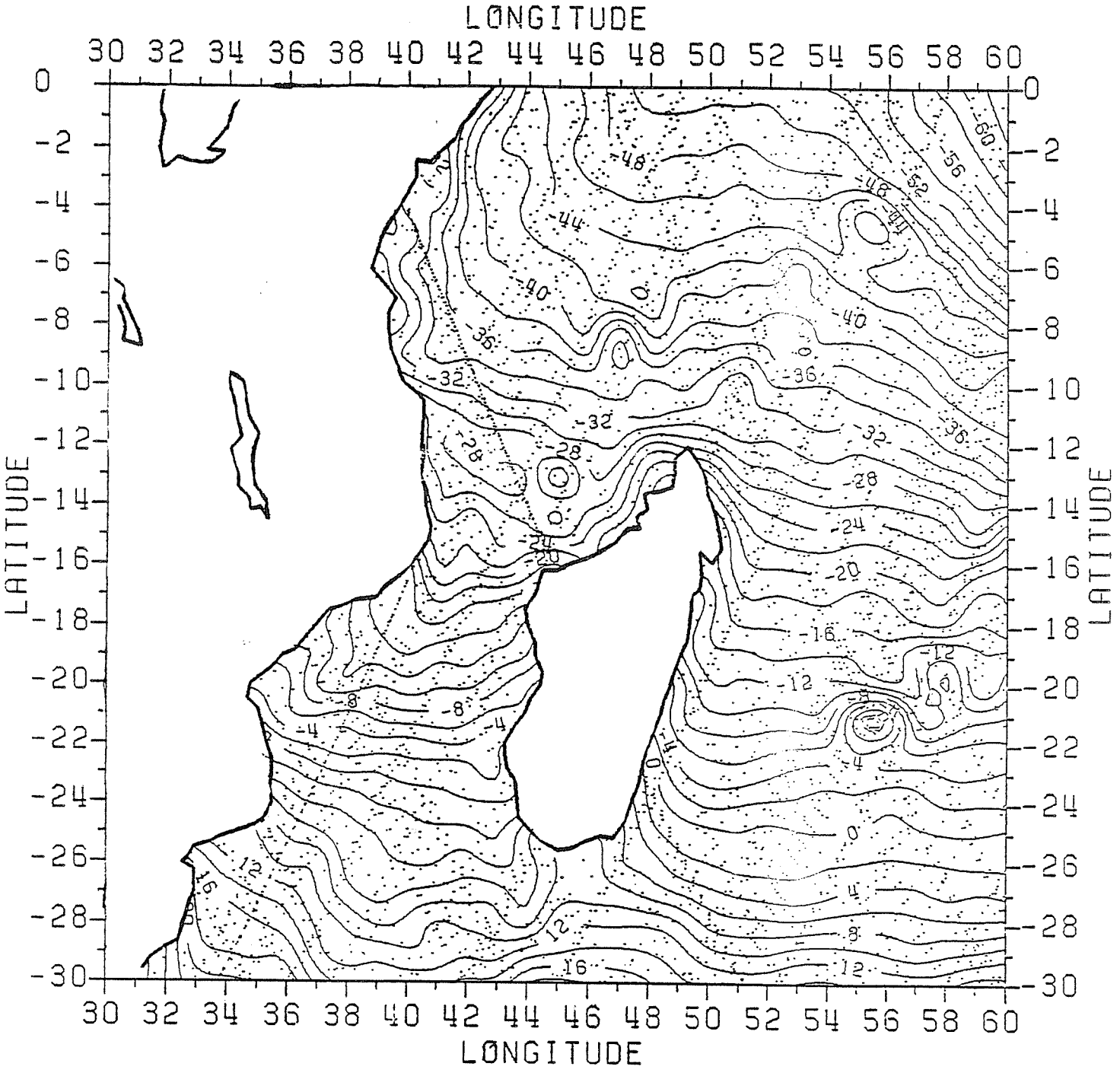

CONCLUSION

Au moment de l'écriture de ce rapport nous n'avons eu aucun moyen de contrôler notre géoide du fait de l'inexistence de données extérieures (par exemple : points Doppler) permettant de faire cette vérification sur Madagascar. Des futurs travaux comme la densification des stations astrogéodésiques pourraient être entrepris pour contrôler le géoide calculé.

REFERENCES

1 - G. Balmino, Algorithms and Software Package for the Resolution of Stokes and Inverse Stokes Equations. Technical note n° 4. B.G.I., April 1982.

2 - W.A. Heiskanen et H. Moritz, Physical Geodesy. Institute of PHysical Geodesy Technical University, Graz, Austria.

3 - J. Rakotoary, Optimisation de recherche de données pour l'interpolation. Note technique n° 7. B.G.I. (Mai, 1986).

4 - R.H. Rapp, A Global Atlas of Sea Surface Heights Based on the Adjusted Seasat Altimeter Data, Report n° 333, Dept. of Geodetic Sciences and Surveying, Aug. 1982.

5 - J. Rechenmann, Gravimétrie de Madagascar, Interprétation et relations géologiques. Géophysique 18, ORSTOM, 1982.

6 - Ch. Reigber et al., GRIM Gravity Model Improvement Using LAGEOS (GRIM 3-L1). Journal of Geophysical Research, Vol. 90, pp. 9285-9299, Sept. 1985.

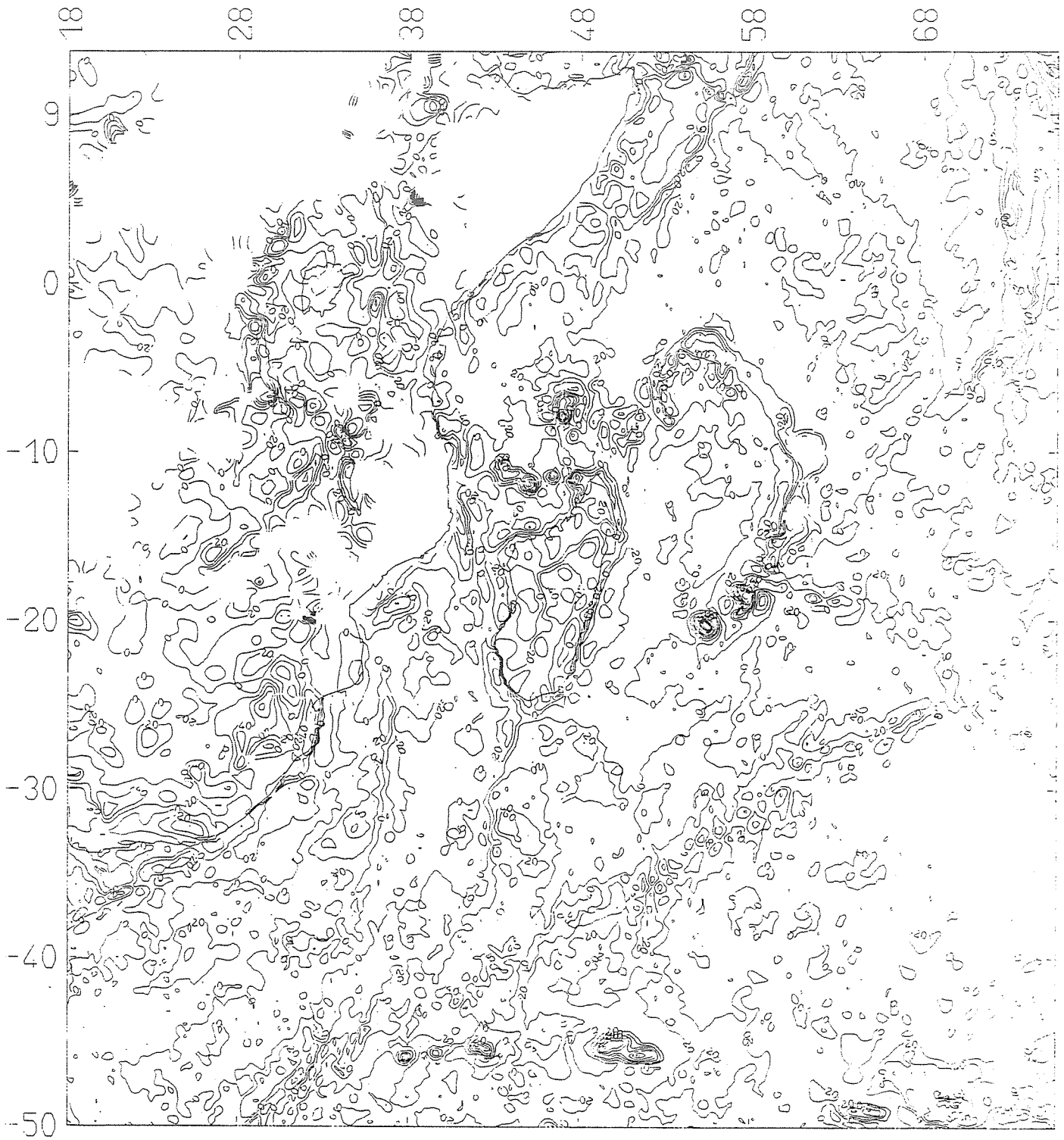

ANOMALIES A L AIR LIBRE 20 mgls